Secondary metabolism and development in the filamentous fungus *Aspergillus nidulans*

Activation of silent gene clusters

and characterization of the SAM synthetase SasA

Dissertation

zur Erlangung des Doktorgrades

der Mathematisch-Naturwissenschaftlichen Fakultäten

der Georg-August-Universität zu Göttingen

vorgelegt von

Jennifer Gerke

aus Göttingen

Göttingen 2011

Die vorliegende Arbeit wurde in der Arbeitsgruppe von Prof. Dr. Gerhard H. Braus in der Abteilung Molekulare Mikrobiologie und Genetik des Instituts für Mikrobiologie und Genetik der Georg-August-Universität Göttingen angefertigt.

Teile dieser Arbeit wurden veröffentlicht in:

Nahlik, K., Dumkow, M., Bayram, O., Helmstaedt, K., Busch, S., Valerius, O., Gerke, J., Hoppert, M., Schwier, E., Opitz, L., Westermann, M., Grond, S., Feussner, K., Goebel, C., Kaever, A., Meinicke, P., Feussner, I., Braus, G. H. (2010) The COP9 signalosome mediates transcriptional and metabolic response to hormones, oxidative stress protection and cell wall rearrangement during fungal development. *Mol Microbiol* **78:** 964-979.

Gerke, J., Bayram, O., Feussner, K., Landesfeind, M., Shelest, E., Feussner, I., Braus, G. H. (2012) Breaking the silence: protein stabilization uncovers silenced biosynthetic gene clusters in the fungus *Aspergillus nidulans*. *Appl Environ Microbiol* **78:** 8234-8244.

Gerke, J., Bayram, O., Braus, G. H. (2012) Fungal S-adenosylmethionine synthetase and the control of development and secondary metabolism in *Aspergillus nidulans*. *Fungal Genet Biol* **49:** 443-454.

Referent: Prof. Dr. G. H. Braus

Korreferent: Prof. Dr. A. Zeeck

Tag der Verteidigung: 26.01.2012

Table of content

Abbreviations

1D-SOM	.....	one-dimensional self-organizing-map
°C	.....	degree Celsius
Δ	.....	deletion
ΔCn	.....	relative difference between best and second best X^{corr} score
λ	.....	wavelength
λ_{max}	.....	peak wavelength
µ	.....	micro
A, asex.	.....	asexual
aa	.....	amino acid
ACP	.....	acyl carrier protein
AdoMet	.....	S-adenosylmethionine
AF	.....	aflatoxin
amu	.....	atomic mass unit
aRNA	.....	amplified ribonucleic acid
AT	.....	acyl transferase
ATP	.....	adenosine-5'-triphosphate
BPB-PPMS	.....	Bi-profile Bayes-Prediction of Protein Methylation Sites
BV	.....	Baeyer Villiger
c	.....	concentration
cAMP	.....	cyclic adenosine monophosphate
cm	.....	centimeter
CoA	.....	coenzyme A
COMPASS	.....	Complex Proteins Associated with Set1
COP9	.....	constitutively photomorphogenic
Cys	.....	cysteine
d	.....	doublet
DAD	.....	diode array detector
dATP	.....	deoxyadenosine triphosphate

dd	.....	doublet of doublet
DEPC	.....	diethylpyrocarbonate
Dev.	.....	development
DHMBA	.....	2,4-dihydroxy-3-methyl-6-(2-oxopropyl)benzaldehyde
DHPDI	.....	3,3-(2,3-dihydroxypropyl)diindole
DIC	.....	differential interference contrast
DMATS	.....	dimethylallyl tryptophan synthetase
DNA	.....	deoxyribonucleic acid
E	.....	expression
e.g.	.....	exempli gratia, for example
EDTA	.....	ethylenediaminetetraacetate
ESI	.....	electron spray ionization
et *al*.	.....	et alii, and others
FAD	.....	flavin adenine dinucleotide
FAS	.....	fatty acid synthase
Fig.	.....	figure
g	.....	gram
GABA	.....	γ-amino-N-butyrate
GFP	.....	green fluorescent protein
GTP	.....	guanosine-5'-triphosphate
h	.....	hour
H	.....	histone
His	.....	histidine
HPLC	.....	High Performance Liquid Chromatography
HRP	.....	horseradish peroxidase
ID	.....	identification
IgG	.....	immunoglobulin G
K	.....	lysine
kb	.....	kilo base pairs
kDa	.....	kilodalton

KS	.....	ketosynthase
l	.....	liter
LB	.....	Luria-Bertani
LC	.....	liquid chromatography
lg	.....	logarithm to the base 10
log_2	.....	logarithm to the base 2
M	.....	molar (mol/l)
m	.....	multiplet
M*	.....	oxidized methionine
m/z	.....	mass-to-charge ratio
Mb	.....	mega base pairs
mDa	.....	millidalton
MFS	.....	major facilitator superfamily
MHz	.....	megahertz
min	.....	minute
ml	.....	milliliter
mm	.....	millimeter
mM	.....	millimolar
MOS	.....	methylorcinaldehyde producing PKS
mRNA	.....	messenger ribonucleic acid
MS	.....	mass spectrometry
MT	.....	methyltransferase
NAD	.....	nicotinamide adenine dinucleotide
NLS	.....	nuclear localization signal
nm	.....	nanometer
NMR	.....	nuclear magnetic resonance
NRP	.....	nonribosomal peptide
NRPS	.....	nonribosomal peptide synthetase
NSAS	.....	norsolorinic acid synthase
OE	.....	overexpression

OSMAC	.....	one strain many compounds
PCR	.....	polymerase chain reaction
pH	.....	power of hydrogen
P_i	.....	phosphate
PKS	.....	polyketide synthase
PP_i	.....	pyrophosphate
PPTase	.....	phosphopantetheinyl transferase
PT	.....	product template
ptiA	.....	pryithiamine
R	.....	thioester reductase
RNA	.....	ribonucleic acid
rRNA	.....	ribosomal ribonucleic acid
s	.....	singlet
S, sex.	.....	sexual
SAM	.....	S-adenosylmethionine
SAT	.....	starter unit acyl transferase
SDS	.....	sodium dodecyl sulfate
sec.	.....	second
Ser	.....	serine
sgfp	.....	synthetic green fluorescent protein
ST	.....	sterigmatocystin
Tab.	.....	table
TAP	.....	tandem affinity purification
TEV	.....	tobacco etch virus
TF	.....	transcription factor
TLC	.....	thin layer chromatography
TOF	.....	time-of-flight
Tris	.....	tris(hydroxymethyl)aminomethane
tRNA	.....	transfer ribonucleic acid
U	.....	unit

Ub	.....	ubiquitin
UPLC	.....	Ultra Performance Liquid Chromatography
USA	.....	United States of America
UV	.....	ultraviolet
UV/VIS	.....	ultraviolet-visible spectrophotometry
V, veg.	.....	vegetative
v/v	.....	volume per volume
v/v/v/v	.....	volume per volume per volume per volume
wt	.....	wild type
w/v	.....	weight per volume
X_{corr}	.....	cross-correlation score

Summary

Antimicrobial resistance is spreading whereas the number of newly discovered antibiotics is declining. The genomes of filamentous fungi comprise numerous putative gene clusters coding for biosynthetic enzymes of structurally diverse secondary metabolites, which are rarely expressed under laboratory conditions. Previous approaches to activate these genes were primarily based on artificially targeting the cellular protein synthesis apparatus. In this work, an alternative approach of genetically impairing the protein degradation apparatus of the model fungus *Aspergillus nidulans* was applied, by utilizing the deletion mutant of the conserved eukaryotic *csnE/CSN5* deneddylase subunit of the COP9 signalosome. This defect in protein degradation results in transcriptional activation of a previously silenced biosynthetic gene cluster (*dba*), comprising an orphaned polyketide synthase (PKS) gene. The direct product of the PKS was isolated and identified as 2,4-dihydroxy-3-methyl-6-(2-oxopropyl)benzaldehyde (DHMBA), which to our knowledge had never been described in an *Aspergillus* species before and which showed antibiotic activity against *Micrococcus luteus*. Additionally, a second new *A. nidulans* compound was identified in wild type as 3,3-(2,3-dihydroxypropyl)diindole (DHPDI), which is lost in a strain overexpressing the specific transcription factor gene *dbaA* of the PKS gene cluster. This supports the idea of interplay between secondary metabolite pathways, resulting in mutually exclusive metabolite production. Genes for CSN are highly conserved and can easily be identified. Therefore, the construction and analysis of *csn* mutant strains of other fungi can be a highly promising approach to uncover hidden biosynthetic gene clusters.

Expression of biosynthetic gene clusters is regulated by heterochromatin formation, in which S-adenosylmethionine- (SAM-) dependent methylations play a crucial role. The biosynthesis of the ubiquitous methyl group donor SAM from methionine and ATP is catalyzed by the conserved SAM synthetase. The filamentous fungus *A. nidulans* carries a single gene coding for the SAM synthetase SasA. In this work, the *A. nidulans* SAM synthetase was comprehensively characterized by genetic, cell biological and biochemical analysis. Deletion of its encoding gene *sasA* is lethal, and overexpression leads to impaired secondary metabolism and development, including very small sterile fruiting bodies and unusually pigmented auxiliary Hülle cells. This suggests defects in coordination of development and secondary metabolite production, which is emphasized by a putative interaction of the predominantly cytoplasmic SasA with histone-2B, reflecting a putative epigenetic link to gene expression.

Zusammenfassung

Die Entdeckung neuer Sekundärmetabolite, welche zur Entwicklung neuer Antibiotika führen, gewinnt zunehmend an Bedeutung, da im Laufe der letzten Jahrzehnte die Ausbildung von mikrobiellen Resistenzen gegenüber etablierten Antibiotika stetig zunahm. Filamentöse Pilze weisen eine Vielzahl von Genclustern auf, die Enzyme für die Biosynthese von Sekundärmetaboliten kodieren. Allerdings sind große Teile dieser Gencluster unter Laborbedingungen reprimiert, was eine erfolgreiche Identifizierung der Sekundärmetabolite erschwert. Experimentelle Ansätze zur Aktivierung dieser Cluster basieren unter anderem auf Modifizierungen des zellulären Proteinsyntheseapparats. Im Rahmen dieser Arbeit wurde ein alternativer Ansatz angewandt, welcher den Proteindegradationsweg angreift. Die Deletion des hochkonservierten *csnE*/*CSN5*-Gens, welches eine Deneddylase-Untereinheit des COP9-Signalosoms kodiert, führt zu einer Fehlregulierung des Proteinabbaus, wodurch unter anderem Transkriptionsfaktoren für Gencluster stabilisiert werden, was folglich zu einer Aktivierung der Genexpression des gesamten Clusters führt. Mithilfe dieser Methode konnte ein neues Polyketidsynthase-Gencluster und sein Produkt als 2,4-dihydroxy-3-methyl-6-(2-oxopropyl)benzaldehyde (DHMBA) identifiziert werden. Unseres Wissens ist dies die erste Isolierung von DHMBA aus einer *Aspergillus*-Art und die erste Dokumentation seiner antibiotischen Aktivität gegen *Micrococcus luteus*. Zusätzlich konnte eine zweite neue *A. nidulans*-Verbindung, nämlich 3,3-(2,3-dihydroxypropyl)diindole (DHPDI), aus dem Wildtyp isoliert werden. Interessanterweise wird dieser Metabolit nicht in einer *dbaA*-Mutante produziert, welche den Transkriptionsfaktor des PKS-Clusters vermehrt produziert. Dies lässt auf ein regulatorisches Zusammenspiel zwischen dem DHMBA und dem DHPDI produzierenden Gencluster schließen. Da der CSN-Komplex in Eukaryoten hochkonserviert ist, stellt die Analyse der CSN-kodierenden Gene einen vielversprechenden neuen Ansatz zur erfolgreichen Identifizierung neuer Gencluster und deren Produkte in filamentösen Pilzen dar.

Die Expression von Sekundärmetaboliten-Genclustern wird unter anderem von der Heterochromatinbildung gesteuert, wobei S-Adenosylmethionin- (SAM-) abhängige Methylierungen eine bedeutende Rolle einnehmen. Der ubiquitäre Methylgruppendonor SAM wird biosynthetisch aus Methionin und ATP gewonnen, einer Reaktion, die von der SAM-synthetase katalysiert wird. Das Genom des filamentösen Pilzes *A. nidulans* kodiert eine SAM-synthetase SasA, welche im Rahmen dieser Arbeit mit genetischen, zellbiologischen und biochemischen Methoden charakterisiert wurde. Es konnte gezeigt werden, dass eine veränderte Expression des essentiellen *sasA*-Gens zu Defekten im Sekundärmetabolismus und

der sexuellen Entwicklung führt, welche sich in der Ausbildung von Mikrocleistothecien und ungewöhnlich pigmentierten Hülle-Zellen äußert. Dies lässt auf eine defekte Koordination zwischen Sekundärmetabolismus und Entwicklung schließen, was durch eine putative Proteininteraktion des hauptsächlich im Cytoplasma lokalisierten SasA mit Histon-2B gestützt wird. Diese Interaktion stellt eine mögliche epigenetische Verbindung zur Genexpression dar.

1 Introduction

1.1 Metabolism

Metabolism describes all reactions in an organism supporting the maintenance of life, like internal and external respiration, nutrition or interaction with the environment. It includes uptake, transport, chemical conversion, and disposal of chemical substances. Metabolism is divided into primary and secondary metabolism. Primary metabolism defines the sum of all biochemical reactions that are essential to maintain life of an organism. These reactions can be categorized by their energy balance. Energy consuming processes are assigned to anabolism and energy producing processes are assigned to catabolism. In contrary, secondary metabolism defines all reactions that are not directly needed for survival of an organism, but confer an advantage in response to the environment. This can be changing environmental or nutritional conditions or defense against competitors. Therefore, secondary metabolites are cellular dispensable and defined as nonessential.

The borders between primary and secondary metabolism are sometimes hard to define, because most secondary metabolites are built up from primary metabolite precursors. The correlation between them is represented in Fig. 1.

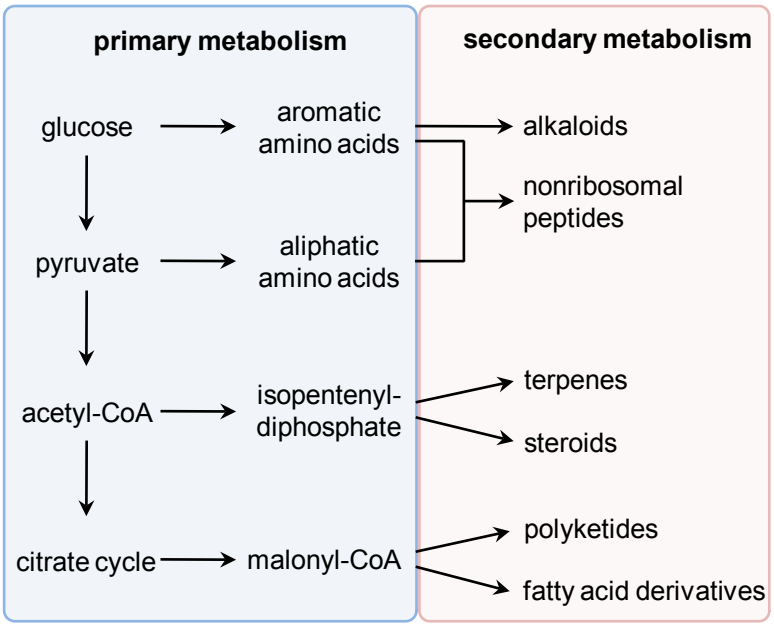

Fig. 1: Correlation between primary and secondary metabolism.

1.1.1 Secondary metabolism

Secondary metabolites are low molecular weight molecules produced by certain fungi, plants and bacteria. They span a wide field of structurally and chemically diverse products, although they are produced by only a few common biosynthetic pathways. Due to their occurrence, they are also called natural products. The reason for the existence of secondary metabolites is controversial and has been discussed over decades. The hypotheses range from waste molecules to chemical signaling and defense or protection (Bennett, 1995).

Many secondary metabolites show biological activities and therefore are pharmaceutically relevant. Since its discovery by Fleming in the 1920s, fungal penicillin has saved the lives of millions. Currently, the World Health Organization forecasts that the dramatic increase in antimicrobial resistance all over the world might lead to a disaster and that there is an imminent need for novel drugs (Cooper *et al.*, 2011). Natural products of the fungal kingdom members possess a great influence on human affairs on earth. With almost 1.5 million members (Pimm *et al.*, 1995), the fungal kingdom still has much greater potential considering that each species can produce a variety of different secondary chemicals. Bioactive fungal natural products range from antibiotics, such as penicillins or cyclosporins, to deleterious mycotoxins, such as liver damaging aflatoxins produced by various Aspergilli or food contaminant fumonisins secreted by *Fusarium* species (Keller *et al.*, 2005). Fungal natural products possess not only high potential against pathogenic microorganisms as anti-bacterial, -fungal, or -protozoan agents but also as drugs e.g. against cancer cells. Although many fungal natural products have been described and tested, their complete potential is by far not exploited.

Besides secondary metabolites with antibacterial or antifungal activity that are supposed to be a defense arsenal against competitors, also protective metabolites against environmental dangers exist. Pigments are ubiquitous, colored natural products that are often associated with developmental structures in fungi. The most common pigments are the dark brown, macromolecular melanins. Melanins are biosynthetically derived by oxidative polymerization of phenolic compounds that are deposited in the cell wall of fungal spores. They function by protecting the organism from environmental stress conditions as UV light, extreme temperatures, and chemical or biochemical stresses.

1.1.2 Classes of secondary metabolites

Secondary metabolites can be classified according to their different characteristics, like structure, occurrence, biosynthesis, or function. Especially for large and complex molecules it is difficult to ascribe them to only one class, because they can be synthesized by a combination of various biosynthetic pathways. Four of the biggest classes are described in the following sections: terpenes, alkaloids, nonribosomal peptides (NRPs), and polyketides.

1.1.2.1 Terpenes

Terpenes are built up from isoprene units (**1,** Fig. 2) and can be summarized by the general formula $(C_5H_8)_n$. They show a great variety of carbon skeletons and can be linear, cyclic, branched, saturated, or unsaturated and can be further modified in various ways. Oxidized terpenes are called terpenoids. In nature, terpenes are produced by plants, especially by conifers, and some insects, like termites. Its name is deduced from turpentine, a resin. Due to their occurrence in essential oils, they are commercially used in perfumery, food industry, and in traditional medicine, e.g. aroma therapy. Examples of familiar terpenes are the flavor limonen or vitamin A (**2**, Fig. 2).

1.1.2.2 Alkaloids

Alkaloids are a huge class of nitrogen containing secondary metabolites, which are structurally very diverse. They mostly contain basic nitrogen but no uniform classification exists. Earlier, it was assumed that alkaloids are only produced by plants, but with the discovery of alkaloids isolated from fungi or animals, the classification was further extended. Most alkaloids have in common that they exert a pharmacological effect on mammals. Due to the intoxicative effect of several alkaloids, they are used as drugs, like cocaine. Some prominent examples for alkaloids are nicotine, caffeine, strychnine, or morphine (**3**, Fig. 2). Alkaloids are divided into subcategories due to similarities of carbon skeletons. Indole alkaloids are usually derived from tryptophan and dimethylallyl pyrophosphate by prenylation. This reaction is catalyzed by dimethylallyl tryptophan synthetases (DMATSs).

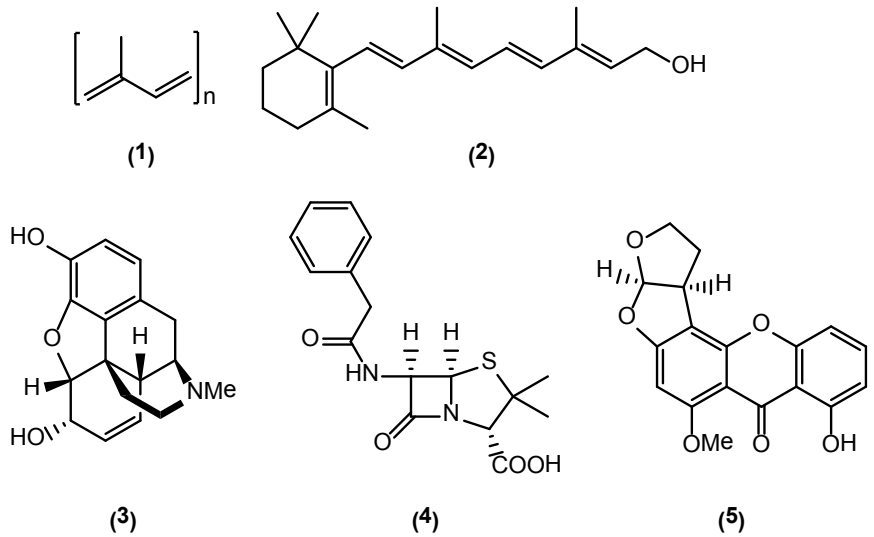

(1) (2) (3) (4) (5)

Fig. 2: Chemical structures of isoprene (**1**), the terpene vitamin A (**2**), the alkaloid morphine (**3**), the nonribosomal peptide penicillin G (**4**), and the polyketide sterigmatocystin (**5**).

1.1.2.3 Nonribosomal peptides (NRPs)

In contrast to ribosomal proteins, nonribosomal peptides can contain nonproteinogenic amino acids. They are mostly macrocyclic and among them we find antibiotics like the β-lactam penicillin (**4,** Fig. 2), pigments, or siderophores.

The biosynthesis of NRPs is catalyzed by multidomain, multimodular enzymes called nonribosomal peptide synthetases (NRPSs). Each module in an NRPS is specific for loading one amino acid. The modules are further divided into domains catalyzing each individual step. Amino acids are recognized by an adenylation domain and activated by a pantothenylation/peptidyl carrier domain. Peptide bonds are formed between the different amino acids by the condensation/peptide-bond formation domain and the resulting peptides are released by a thioesterase domain. The great variety of NRP structures is achieved by incorporation of different amounts of amino acids, subsequent cyclizations or modifications as acetylations or glycosylations.

1.1.2.4 Polyketides

Polyketides are classified by their biosynthesis rather than their structure. A well-studied fungal example is sterigmatocystin (**5**, Fig. 2), the biosynthetic precursor of the mycotoxin aflatoxin. Polyketides are built up by CoA-activated starter units (mostly acetyl-CoA or malonyl-CoA) and undergo a stepwise elongation similar to fatty acid biosynthesis. These

reactions are catalyzed by multidomain enzymes called polyketide synthases (PKSs). PKSs can be divided into three different types depending on domain composition. Type I PKSs are covalently linked multi-functional enzymes, whereas type II PKSs have free-standing subunits. Both types use malonyl-S-panthetheine for activation. Type III PKSs are homodimeric and utilize malonyl-CoA. Additionally, PKSs are classified as iterative or non-iterative depending on whether the substrate is used for one or more rounds of elongation. In fungi, all of the identified PKSs are iterative type I PKSs.

All PKSs at least contain a β-ketoacyl synthase (KS) domain, an acyl transferase (AT) domain and an acyl carrier protein (ACP) domain. Additionally, they can contain optional domains, like methyltransferases (MT), ketoreductases, dehydratases, or enoyl reductases. Recently, two new domains were identified: SAT (starter unit acyl transferase) and PT (product template) domains (Udwary *et al.*, 2002). The SAT domain is supposed to select the acyl starter unit and the PT domain is suggested to control the ketide chain length.

The general biosynthesis of polyketides is shown in Fig. 3. It starts with the addition of a phosphopantetheinyl group to the conserved serine of ACP by a phosphopantetheinyl transferase (PPTase). Then, the starter unit acetyl-CoA is loaded onto the conserved cysteine residue of the KS domain and the extender unit malonyl-CoA is loaded onto the PPTase arm of the ACP domain catalyzed by the AT domain. Under carbon dioxide release, the acetyl- and malonyl-units condensate in a Claisen condensation and form a diketide. Subsequent loadings of more malonyl-CoA extender units stepwise elongate the carbon chain and result in the formation of polyketides. The huge variety of polyketide structures results from the availability of optional domains, which process the ketides after Claisen condensation, before they are transferred back to the KS domain.

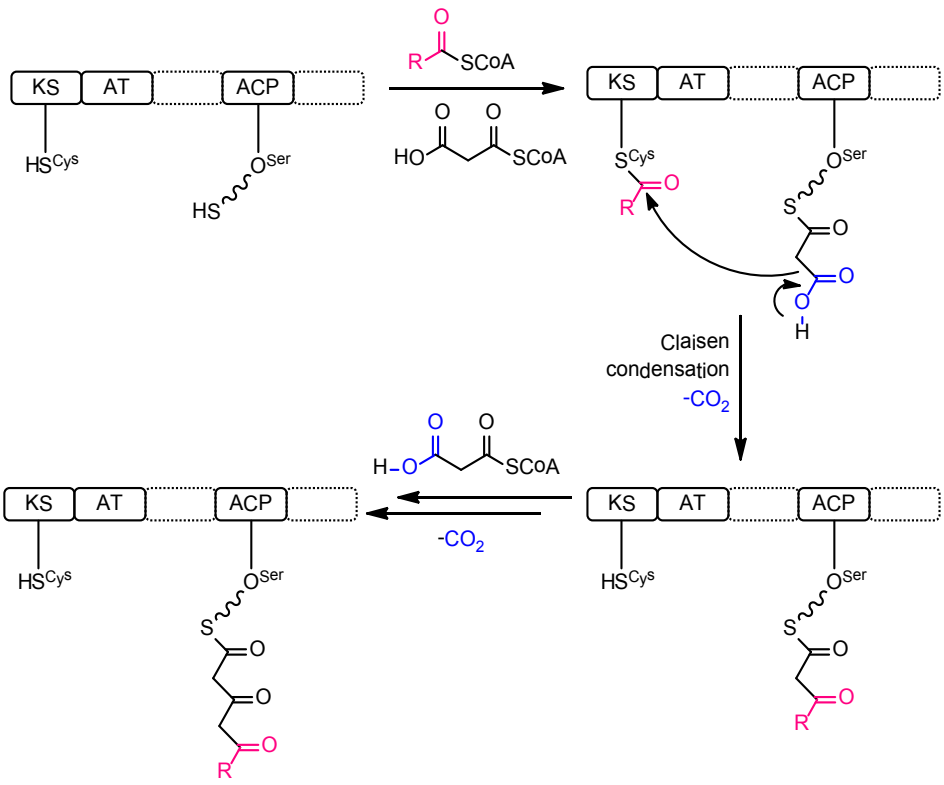

Fig. 3: General polyketide synthesis pathway. KS (β-ketoacyl synthase), AT (acyl transferase), ACP (acyl carrier protein).

1.2 Biosynthetic gene clusters

In contrast to primary metabolites, whose biosynthetic genes are widespread over the complete genome, the genes involved in biosynthesis of secondary metabolites in fungi are often clustered and located near telomeres (Keller *et al.*, 1997). One of the best studied gene clusters is the sterigmatocystin/aflatoxin (ST/AF) gene cluster. The carcinogenic and toxic AF and its penultimate precursor ST are produced by various *Aspergillus* spp. In *A. flavus* and *A. parasiticus*, the AF gene cluster spans more than 70 kb including 21 verified or predicted biosynthetic genes (Minto *et al.*, 1997, Yu *et al.*, 2004). In *A. nidulans*, the two genes catalyzing the last conversion from ST over *O*-methyl sterigmatocystin to AF are missing and therefore, no AF is produced. The *A. nidulans* ST gene cluster consists of 25 co-regulated genes spanning approximately 60 kb (Brown *et al.*, 1996). ST/AF is produced from acetyl-CoA and malonyl-CoA by consecutive acting fatty acid synthase (FAS) and polyketide synthase (PKS), resulting in the first stable intermediate norsolorinic acid. Subsequent oxidations, dehydratations, cyclations, and methylations result in the synthesis of ST or AF, respectively (Fig. 4).

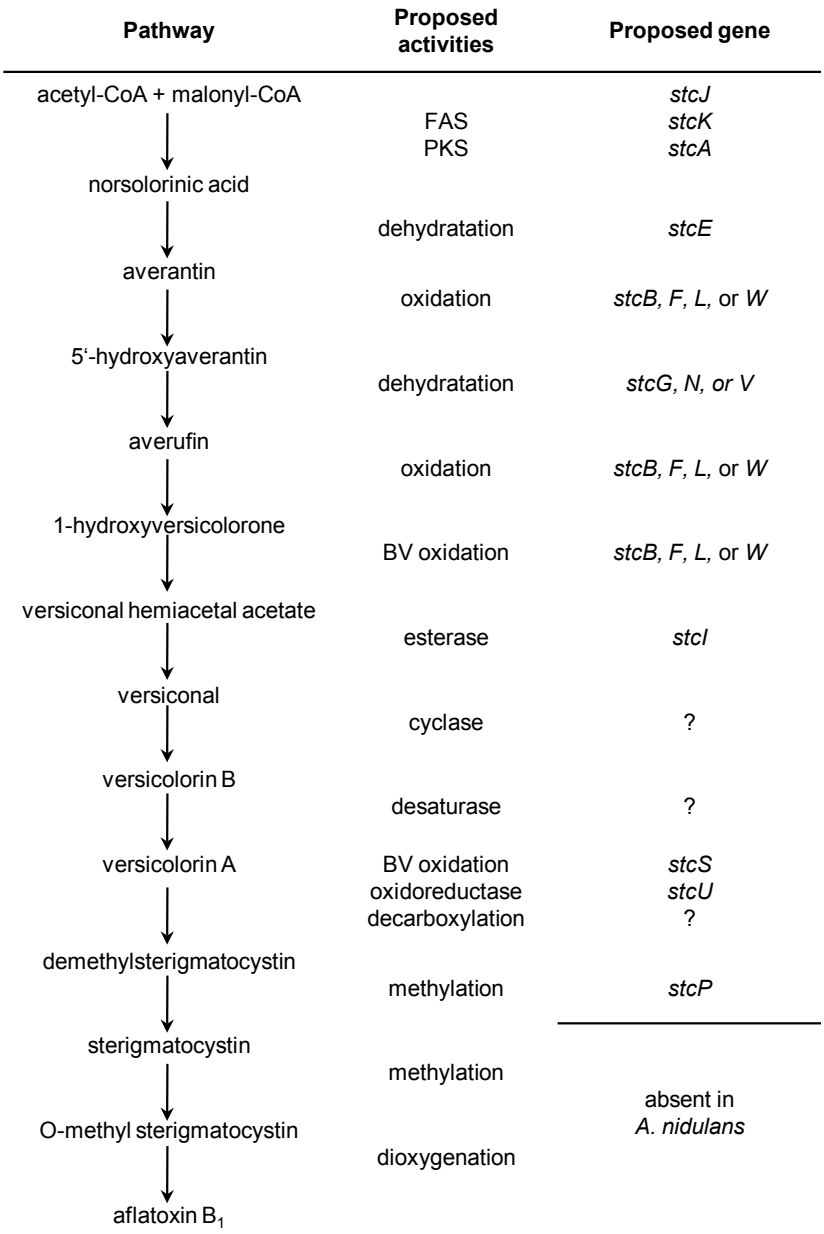

Fig. 4: Proposed biosynthetic pathway of sterigmatocystin and aflatoxin in *Aspergillus* spp., corresponding activities and proposed genes for each reaction step. BV = Baeyer-Villiger. Modified from Brown *et al.*, 1996.

Recently, a long-sought after polyketide, produced by many different organisms, and its corresponding PKS gene were identified in *Aspergillus nidulans* (Schroeckh *et al.*, 2009). Orsellinic acid (**6,** Fig. 5) represents the simplest acetate-derived non-reduced aromatic metabolite and is therefore regarded as archetypal phenolic polyketide. The gene cluster *orsA-orsE* (AN7909-AN7914) contains a PKS gene *orsA*, producing orsellinic acid as direct PKS product (Fig. 5). Genes *orsB* and *orsC* are involved in biosynthesis of the cathepsin K inhibitors F-9775A (**7,** Fig. 5) and F-9775B (**8,** Fig. 5), although the individual steps in its proposed biosynthesis from an orsellinic acid precursor were not yet identified. The function

of *orsD* and *orsE* is currently unknown. Besides orsellinic acid, F-9775A and F-9775B, eight additional metabolites, summarized in Fig. 5, have been linked to the *ors* gene cluster: lecanoric acid (**9**), gerfelin (**10**), C10-deoxy-gerfelin (**11**), orcinol (**12**), diorcinol (**13**), cordyol C (**14**), violaceol I (**15**) and violaceol II (**16**) (Nahlik *et al.*, 2010, Sanchez *et al.*, 2010). The typical lichen metabolite lecanoric acid is the dimerization product of orsellinic acid. By decarboxylation of orsellinic acid, orcinol and its dimerization product diorcinol can be synthesized. Moreover, oxidation and dimerization of orcinol result in production of violaceol I and II. The metabolites gerfelin, C10-deoxy-gerfelin and cordyol C are combinatory products of the metabolites mentioned before.

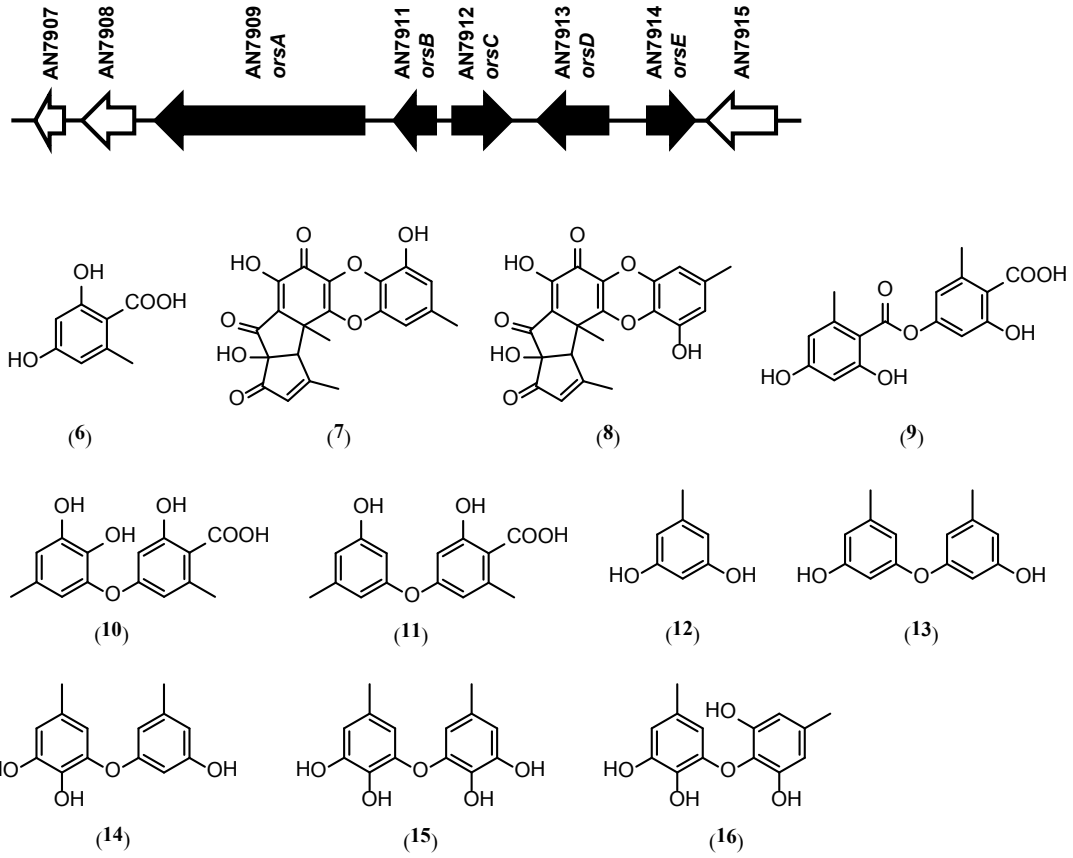

Fig. 5: Orsellinic acid gene cluster *orsA-orsE* (AN7909-AN7914) in *A. nidulans* and chemical structures of its products orsellinic acid (**6**), F-9775A (**7**), F-9775B (**8**), lecanoric acid (**9**), gerfelin (**10**), C10-deoxy-gerfelin (**11**), orcinol (**12**), diorcinol (**13**), cordyol C (**14**), violaceol I (**15**) and violaceol II (**16**).

1.2.1 Regulation of biosynthetic gene clusters

1.2.1.1 Transcription factors

Besides structural genes like polyketides synthases, oxygenases, or reductases, also regulatory genes are embedded in secondary metabolite gene clusters. The encoded regulators, which transcriptionally control the structural genes, are divided into two classes: pathway specific transcription factors (TFs), controlling one specific gene cluster, and general TFs, controlling several different gene clusters or mediating environmental signals. In total, twelve TF superfamilies have been identified in fungi, three of which are exclusively present in fungi (Shelest, 2008). The largest fungal-specific superfamily is the zinc-cluster superfamily $Zn(II)_2Cys_6$. Its DNA-binding domain consists of six cysteine residues binding two zinc ions. These TFs do not share a common function, but they are involved in a large number of different cellular processes, like sugar and amino acid metabolism, cell cycle, or stress response (MacPherson *et al.*, 2006). Many gene clusters contain one or more TFs. A prominent example of a pathway-specific TF is the $Zn(II)_2Cys_6$-domain containing TF AflR, that positively regulates expression of the ST/AF gene cluster in Aspergilli (see chapter 1.2). AflR binds to the palindromic sequence 5'-$TCGN_5CGA$-3' of the promoters of the AF/ST biosynthetic genes (Fernandes *et al.*, 1998). A second motif 5'-TTAGGCCTAA-3' was proposed to control autoregulation of *aflR* transcript (Chang *et al.*, 1995). Deletion of *aflR* disrupts, while a modified expression of *aflR* changes the expression of the complete gene cluster (Ehrlich *et al.*, 1998, Yu *et al.*, 1996a).

Recent studies revealed that in some cases a cross-talk between assumed pathway-specific TFs occurs. In this way, some TFs control not only the gene cluster they are embedded in, but also different gene clusters located on even different chromosomes (Bergmann *et al.*, 2010). ScpR is a C_2H_2-type zinc finger TF, embedded in a cryptic NRPS gene cluster in *A. nidulans,* containing two NRPS genes *inpA* and *inpB*. Besides activation of these two genes, ScpR additionally activates expression of the asperfuranone gene cluster, containing the two PKS genes *afoE* and *afoG*, by binding to the promoter region of the asperfuranone-specific TF gene *afoA*.

Global regulatory factors do not activate one specific pathway, but several independent pathways by e.g. mediating environmental cues. The response to external signals like light, pH, temperature, or carbon and nitrogen sources is triggered by global TFs, containing mostly conserved Cys_2His_2 zinc finger domains, like CreA in *A. nidulans*, mediating carbon source changes (Dowzer *et al.*, 1989) or PacC, mediating pH (Tilburn *et al.*, 1995).

1.2.1.2 Epigenetic control

Chromatin is involved in all genetic processes in eukaryotic nuclei and changes in its structure go along with activated or silenced transcription of genes. Recent studies in fungi revealed, that this epigenetic control plays an important role in expression of biosynthetic gene clusters (Bok *et al.*, 2009, Reyes-Dominguez *et al.*, 2010, Shwab *et al.*, 2007).

Chromatin consists of nuclear DNA, wrapped around an octamer of histone proteins. By post-translational modifications of histones, gene transcription is activated or silenced. These modifications include acetylation and methylation of lysines and arginines, phosphorylation of serines and threonines, and ubiquitination of lysines. Depending on its conformation induced by these modifications, chromatin is divided into active euchromatin or silenced heterochromatin. Hyperacetylated histones H3 and H4 correlate with transcriptional activity, whereas decreased acetylation is associated with transcriptional repression. However, methylations show different impacts on chromatin conformation. Methylated H3K4 facilitates euchromatin formation, whereas methylated H3K9, H3K27 and H4K20 are typical for heterochromatic states (Strauss *et al.*, 2011), in which genes are silenced or repressed.

1.2.1.2.1 Methylation by S-adenosylmethionine (SAM)

Methylations of histones usually occur by transfer of a methyl group from S-adenosylmethionine (SAM, AdoMet). SAM was first discovered in 1953 by Catoni (Catoni, 1953) and since then extensively investigated, especially in mammals as it is proposed to have therapeutic benefits in human diseases (Chiang *et al.*, 1996). Besides ATP, the ubiquitous enzyme substrate SAM is one of the most frequently used substrates and the major methyl group donor in all living organisms. In addition to histone methylation, it is involved in many methylation processes as protein, DNA, RNA, and phospholipid methylations, in which the methyl group is transferred by a methyltransferase to the corresponding substrate (Mato *et al.*, 1997). About 15 methyltransferase superfamilies have been identified and their classifications are based on substrate specificity rather than sequence similarities (Loenen, 2006). Besides the function of SAM as methyl donor, it also acts as carboxy-aminopropyl donor in the synthesis of polyamines, like spermidine, the production of modified nucleotides in rRNA, or as transcriptional regulator by binding to riboswitches (Bjork *et al.*, 1987, Bowman *et al.*, 1973, Corbino *et al.*, 2005, McDaniel *et al.*, 2005, Winkler *et al.*, 2005).

S-Adenosylmethionine synthetase (EC 2.5.1.6) is the only known enzyme that catalyzes the synthesis of SAM (**18**, Fig. 6) from methionine (**17**, Fig. 6) with ATP (Tabor *et al.*, 1984). The catalytic reaction occurs in two steps, in which the triphosphate is cleaved from ATP and further hydrolyzed to PP_i and P_i before SAM is released (Mudd *et al.*, 1958). The first crystal structure of a SAM synthetase, namely MetK of *Escherichia coli*, was determined in 1996 (Takusagawa *et al.*, 1996a). MetK consists of four identical subunits forming two dimers among which the active sites lie. The triphosphate moiety interacts extensively with the amino acid residues in the active site of the enzyme in order to cleave it at both ends, while the adenine and ribose moiety shows weak interaction, what facilitates the release of the product (Takusagawa *et al.*, 1996b).

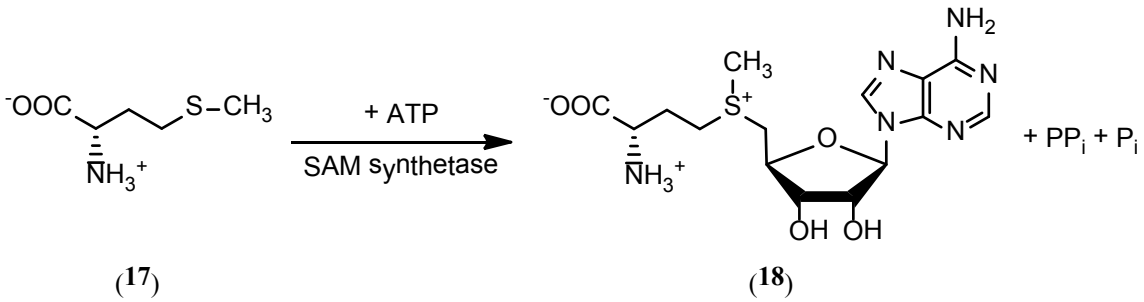

(**17**) (**18**)

Fig. 6: Biosynthesis of SAM. The SAM synthetase catalyzes the reaction from methionine (**17**) and ATP to the methyl group donor SAM (**18**).

1.2.1.2.2 The putative methyltransferase LaeA

LaeA (loss of *aflR* expression) was identified in 2004 as a regulator that complements an ST mutant strain, which was unable to express the pathway-specific regulator *aflR* (Bayram *et al.*, 2011, Bok *et al.*, 2004). Interestingly, it turned out that besides ST, LaeA was able to regulate the expression of many other secondary metabolites, like the antibiotic penicillin, the immunosuppressive gliotoxin, the cholesterol-lowering drug lovastatin, and several mycelial pigments. Due to its crucial function, LaeA has become famous as master regulator of secondary metabolism. LaeA is conserved in filamentous fungi, but not in *S. cerevisiae*, which possesses no secondary metabolism. LaeA is a nuclear protein with a classical nuclear localization signal (NLS) motif and a SAM-binding motif, showing sequence similarities to arginine and histone methyltransferases, indicating that LaeA acts by chromatin remodeling (Fig. 7). This hypothesis was corroborated by the finding that artificial introduction of additional genes into the ST gene cluster, which is under control of LaeA, resulted in LaeA dependent expression patterns (Bok *et al.*, 2006a).

In *A. nidulans* it had been shown, that the silent ST gene cluster is marked by H3K9 trimethylation with high amounts of the heterochromatin protein HepA (Reyes-Dominguez *et al.*, 2010). When the ST cluster is activated, trimethylated H3K9 and HepA levels decrease, whereas acetylated histone H3 levels increase. These chromatin modifications are restricted to genes located inside the cluster, while heterochromatic marks endure directly outside the cluster. It was suggested that LaeA counteracts H3K9 methylation inside the ST cluster, and by this, activates the specific TF AflR (Reyes-Dominguez *et al.*, 2010). This epigenetic control explains why biosynthetic genes are clustered in fungi.

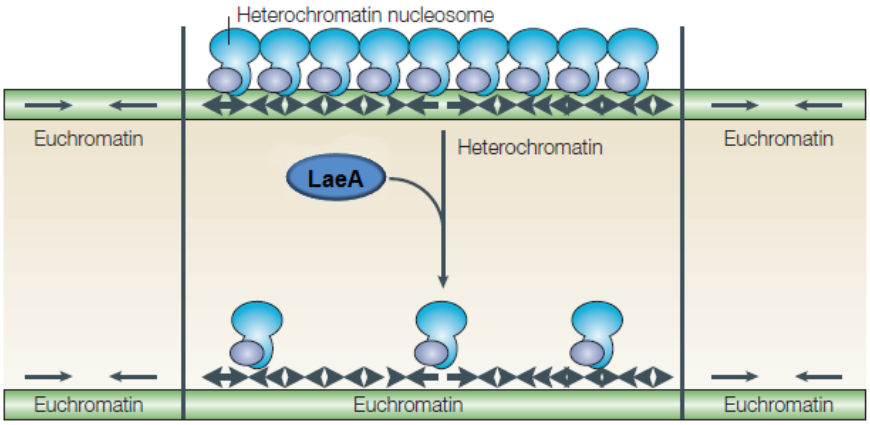

Fig. 7: Heterochromatic function of LaeA on the ST gene cluster. Modified from Keller *et al.*, 2005. LaeA probably converts heterochromatin to euchromatin by interfering with deacetylases or methylases, and subsequently activates transcription of the ST gene cluster.

1.3 Activation of silent biosynthetic gene clusters

Discovery of new bioactive natural products becomes more and more important as antibiotic resistances are spreading (see chapter 1.1.1). In 2002, infectious diseases were the third leading cause of death in the industrial nations and even the second-leading cause worldwide (Nathan, 2004). For this reason and to deal with the problem of cross-resistances, the discovery and development of new antibiotics, attacking new targets, is inevitable.

Different approaches were applied in recent years to find novel bioactive molecules either in new species or in already established model organisms. New geographical spots exhibiting extreme conditions, including hot springs or glacial ice, were explored in order to find new species producing yet unknown natural products (Sonjak *et al.*, 2005, Wilson *et al.*, 2009). An alternative approach is the exploration of the full genomic potential of already known species

by genomic mining (Bok *et al.*, 2006b). Genomic sequencing revealed, that there are many more genes for biosynthesis of secondary metabolites than metabolites already identified (Brakhage *et al.*, 2011). The *A. nidulans* genome carries genes for 31 PKSs, 27 NRPSs, one PKS/NRPS hybrid and 6 dimethylallyl tryptophan synthases (DMATSs), but only a quarter of them could be assigned to a produced metabolite yet (Tab. 1) (Bok *et al.*, 2006b).

Tab. 1: List of all genes encoding PKSs, NRPSs, and DMATSs, and their produced secondary metabolites in the genome of *A. nidulans*. Minus = not identified.

PKS	natural products	NRPS	natural products	DMATS	natural products
AN0150	monodictyphenone	AN0016	-	AN6784	prenylxanthones
AN0523	-	AN0607	-	AN8514	terrequinone A
AN1034	asperfuranone	AN1242	-	AN10289	-
AN1036	asperfuranone	AN1680	-	AN11080	-
AN1784	-	AN2064	-	AN11194	-
AN2032	-	AN2545	emericellamides	AN11202	-
AN2035	-	AN2621	penicillin		
AN2547	emericellamides	AN2924	-		
AN3230	-	AN3396	-		
AN3273	-	AN3495	-		
AN3386	-	AN3496	-		
AN3612	-	AN4827	-		
AN5475		AN5318	-		
AN6000	asperthecin	AN6236	-		
AN6431	-	AN6444	-		
AN6448	-	AN7884	-		
AN6791	-	AN8105	-		
AN7071	-	AN8504	-		
AN7084	-	AN8412[1]	terrequinone A		
AN7825	sterigmatocystin	AN8513	terrequinone A		
AN7903	DHMBA (this study)	AN9129	-		
AN7909	orsellinic acid	AN9226	-		
AN8209	YWA1, isocoumarins	AN9243	-		
AN8383	austinols	AN9244	-		
AN8412[1]	terrequinone A	AN10486	-		
AN8910	-	AN10576	-		
AN9005	-	AN11820	-		
AN10430	-	AN12117	-		
AN11191	-				
ANID_12066	-				
ANID_12168	-				
AN12331	-				

[1] PKS/NRPS hybrid

As described before, biosynthetic genes are often clustered (see chapter 1.2), but most of them are silenced or rarely expressed under laboratory conditions (Hertweck, 2009). Two major strategies were developed to activate hidden genes by (i) changing the environment or by (ii) genetic engineering (Sanchez *et al.*, 2011). These strategies are summarized in Fig. 8.

(i) The OSMAC approach (one strain many compounds) activates silent gene clusters by cultivating microorganisms under different media and growth conditions (Bode *et al.*, 2002,

Zähner *et al.*, 1982). Possible changing parameters include growth medium, growth period, temperature, type of culture vessel, aeration, and the addition of enzyme inhibitors or limited precursor molecules, like acetate for polyketide production. Alternatively, physical contact with an opponent results in uncovering hidden clusters by activating defense mechanisms. With this method the orsellinic acid gene cluster (see chapter 1.2) in *A. nidulans* was discovered. A direct bacterial-fungal interaction of the actinomycete *Streptomyces rapamycinicus* with *A. nidulans* led to the activation of this cluster, producing orsellinic acid, F-9775A and F-9775B.

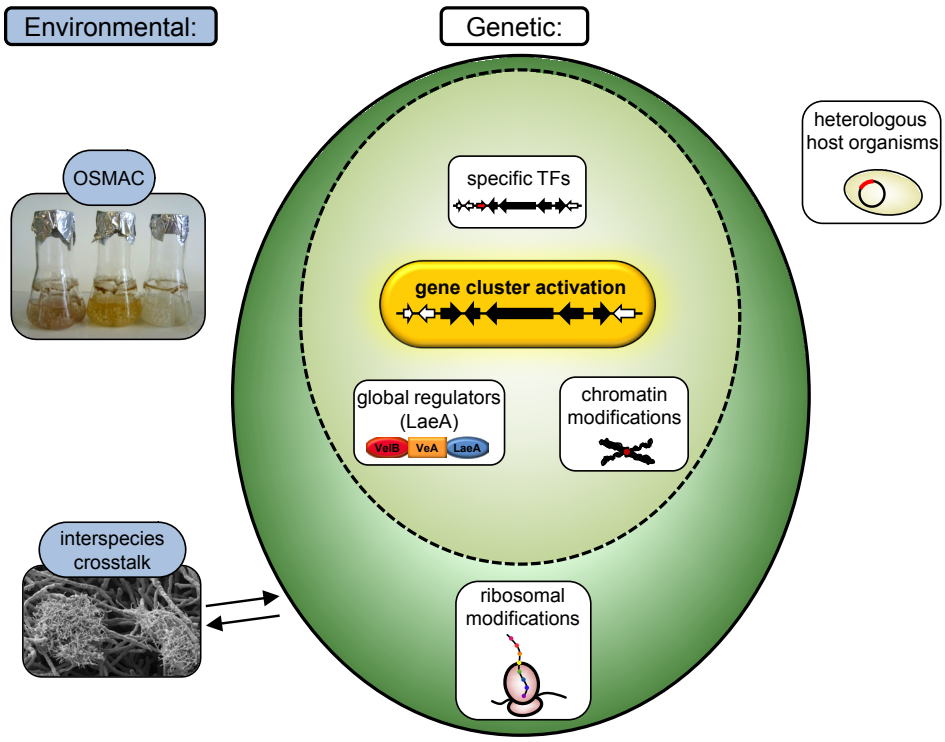

Fig. 8: Schematic presentation of environmental and genetic approaches to activate silenced biosynthetic gene clusters. Environmental approaches are the OSMAC (one strain many compounds) approach and the interspecies crosstalk approach, according to which microorganisms are cultivated under different media and growth conditions or are brought into contact with a competitor. Genetic approaches are the expression of complete gene clusters in heterologous host organisms, modifications of the ribosomal machinery or the chromatin structure, and activations of global or specific transcription factors.

(ii) Genetic engineering primarily focuses on expressing complete gene clusters in heterologous host organisms (Sakai *et al.*, 2008) or on altering the cellular protein synthesis machinery (Bok *et al.*, 2006b, Bok *et al.*, 2009, Ochi *et al.*, 2004, Shwab *et al.*, 2007). Secondary metabolite synthesis was enhanced by changing genes with general regulatory functions, like the putative methyltransferase gene *laeA* (see chapter 1.2.1.2.2). By microarray

analyses of strains overexpressing and deleted for *laeA*, the terrequinone A gene cluster in *A. nidulans* was identified (Bok *et al.*, 2006b). Chromatin is involved in activation or silencing of huge metabolic cluster regions (see chapter 1.2.1.2). By altering genes with chromatin modifying activities a general natural product synthesis enhancement is achieved. For example, the disruption of the histone deacetylase encoding gene *hdaA* in *A. nidulans* enhances production of ST and penicillin (Shwab *et al.*, 2007). By targeting genes involved in ribosomal functions, like ribosomal proteins or RNA polymerases, an increase in secondary metabolism by changing transcription and translation machineries occurs (Ochi *et al.*, 2004). A more selective approach is the artificial expression of a specific transcription factor (TF) gene (see chapter 1.2.1.1), which is embedded in a gene cluster (Hertweck, 2009). Replacement of the native TF promoter by an inducible promoter results in targeted expression and activation of the complete gene cluster.

This already established repertoire and prospectively developed approaches to activate silent biosynthetic gene clusters will help to make cryptic pathways a valuable resource for new therapeutics.

1.4 The model organism *Aspergillus nidulans*

Aspergillus nidulans (*Emericella nidulans*) is a fast-growing, ubiquitous saprophytic soil organism. It was introduced into science in 1953 by the Italian Guido Pontecorvo (Pontecorvo *et al.*, 1953) and due to its haploid, homothallic growth and the fact that it can undergo an asexual and a sexual reproduction cycle, *A. nidulans* established as a model organism. The filamentous fungus has been extensively studied in respect to genetic and metabolic regulation, development, cell cycle control, cell polarity, and chromatin structure. Its complete genome, consisting of 13.6 Mb distributed over eight chromosomes, containing an estimated 11,000 genes, has been sequenced (Galagan *et al.*, 2005), what facilitates genetic work. Molecular findings in this non-pathogenic organism can be transferred to its pathogenic (*A. fumigatus*, *A. flavus*, *A. terreus*) or its industrial used relatives (*A. niger*, *A. oryzae*) or even to higher eukaryotes.

After germination, *A. nidulans* grows as vegetative hyphae by apical extension of the Spitzenkörper. By repeated branching and nuclear mitosis, a multinucleate cellular network arises, which is called mycelium. After 16-20 hours of growth, the mycelium gains competence and, induced by environmental signals, can undergo the asexual or the sexual

reproduction cycle. In submerged cultures, only vegetative growth occurs, whereas for asexual and sexual development an air-medium interface is required.

1.4.1 Asexual development

During asexual development, *A. nidulans* forms mitotically derived green conidiospores about 48 hours after germination. The environmental signals for asexual reproduction include solid medium, light and a sufficient oxygen/carbon dioxide ratio. After achieving developmental competence, the mycelium differentiates a foot cell, which apically extends to a stalk (Fig. 9). The stalk tip swells and two rows of mononuclear sterigmata, the metulae and the phialides, originate by budding. From the phialides, long rows of isogenic, haploid conidiospores arise (Adams *et al.*, 1998). A complete asexual structure is called conidiophore. The green color of conidiospores originates from a polyketide-derived pigment derived from the yellow heptaketide naphthopyrone intermediate YWA1 (Tab. 1) (Watanabe *et al.*, 1999). In the biosynthesis cascade, the PKS gene *wA*, mediating formation of yellow condiospores, is followed by the laccase gene *yA*, involved in formation of green conidiospores (Aramayo *et al.*, 1990, Mayorga *et al.*, 1992).

1.4.2 Sexual development

The sexual reproduction cycle results in the formation of meiotically derived red ascospores (Braus *et al.*, 2002, Champe *et al.*, 1994, Poeggeler *et al.*, 2006, Timberlake, 1990). For induction, besides solid medium, darkness and a reduced oxygen/carbon dioxide ratio (compared to asexual development) is required. Sexual structure formation starts around 50 hours after germination with the fusion of ascogenous hyphae, which are surrounded by a specialized tissue called nest containing Hülle cells. These Hülle cells, surrounding the later fruiting body, are supposed to be nursing cells (Sarikaya Bayram *et al.*, 2010). Within the nest, a primordium arises which differentiates to a microcleistothecium (Fig. 9). A morphological bipartition into an outer sterile hyphal layer and an inner fertile cellular mass occurs. The outer hyphae differentiate to the later cleistothecial wall. In the inner, fusion of two haploid nuclei results in formation of asci. One meiotic and one mitotic cell division form eight haploid ascospores, which undergo mitosis without cell division, resulting in mature binucleate ascospores. The ascospore wall accumulates a red polyketide pigment called

asperthecin (see Tab. 1). A mature cleistothecium with a diameter of approximately 200 µm contains up to 80,000 robust ascospores that can endure a long period of time in the soil.

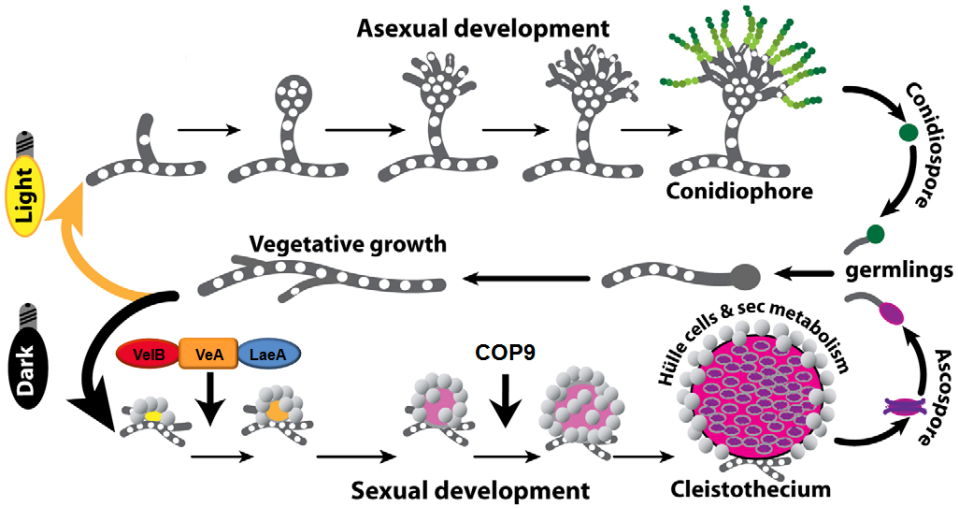

Fig. 9: Developmental programs in *A. nidulans*. Modified from Sarikaya Bayram *et al.*, 2010. In the light, vegetative hyphae develop asexual and form conidiophores with green conidiospores at their ends. In the dark, the sexual program is initiated, resulting in cleistothecia containing red ascospores. The velvet complex and the COP9 signalosome (CSN complex) are involved in regulation of development and secondary metabolism.

1.4.3 Correlation of development and secondary metabolism

A correlation between secondary metabolism and development of an organism has been recognized for a long time. Numerous examples of natural products influencing development in different organisms exist. These metabolites can be divided into three groups: (i) sporulation activating metabolites, (ii) pigments required for sporulation structures, and (iii) toxins secreted at the time of sporulation.

(i) Usually, synthesis of natural products commences at late stages, when primary metabolism is completed and the organism enters the stationary or resting phase. But some natural products, that are sporogenic factors, are produced at the approximate time of sporulation. In *A. nidulans*, the ratio of oleic acid- and linoleic acid-derived psi factors regulate asexual and sexual spore production (Brodhun *et al.*, 2009a, Brodhun *et al.*, 2009b, Tsitsigiannis *et al.*, 2004). In *Fusarium graminearum*, the estrogenic mycotoxin zearalenone enhances perithecial production, while inhibition of zearalenone synthesis blocks sexual development (Wolf *et al.*, 1973).

(ii) The most common pigments are melanins that are produced by oxidative polymerization of phenolic compounds. Besides their function as protector against damaging UV light, they also function as virulence factors. In *Colletotrichum lagenarium*, melanin biosynthesis is associated with the formation of the infection structure appressoria, required for host penetration (Takano *et al.*, 2000). In *A. fumigatus*, disruption of the spore pigment PKS gene *alb1* leads to diminished infection of a murine model (Tsai *et al.*, 1998).

(iii) Mycotoxins are the most harmful secondary metabolites of fungi. In *A. nidulans* and *A. parasiticus*, inhibited polyamine biosynthesis results in inhibition of sporulation and ST/AF production (Guzman-de-Pena *et al.*, 1997, Guzman-de-Pena *et al.*, 1998).

All these examples raised the suggestion that secondary metabolism and development are connected, but genetic evidence was missing. In recent years, factors connecting development and secondary metabolism have been identified by genetic and biochemical means.

1.4.3.1 Protein complexes at the interface of development and secondary metabolism

1.4.3.1.1 The G-protein signal transduction pathway

The G-protein signal transduction pathway in *Aspergillus nidulans* was first studied in 1997 (Hicks *et al.*, 1997) and it is known from different species that the pathway is essential for fungal growth (Lengeler *et al.*, 2000). In *A. nidulans*, characterization of fluffy mutants provided insight into this pathway. Fluffy mutants are deficient in conidiophore formation due to deficient expression of the specific transcription factor BrlA, resulting in a white, 'fluffy' phenotype. The fluffy gene *fluG* acts upstream of the signaling cascade (see Fig. 10A) and is involved in production of a factor activating a conidiation and ST production pathway (Lee *et al.*, 1994a). Deletion of *fluG* results in an aconidial and non-ST-producing phenotype (Hicks *et al.*, 1997). The fluffy gene *flbA* encodes a regulator of G-protein signaling and deletion shows the same phenotype as Δ*fluG* (Hicks *et al.*, 1997, Lee *et al.*, 1994b). FlbA negatively regulates the α-subunit of a heterotrimeric G-protein FadA (Hicks *et al.*, 1997, Yu *et al.*, 1996b), which itself has a negative effect on conidiation and ST production. The cAMP-dependent protein kinase catalytic subunit PkaA acts downstream of FadA (Shimizu *et al.*, 2001). It negatively regulates BrlA and also AflR, probably mediated by the secondary metabolism regulator LaeA (Shimizu *et al.*, 2003).

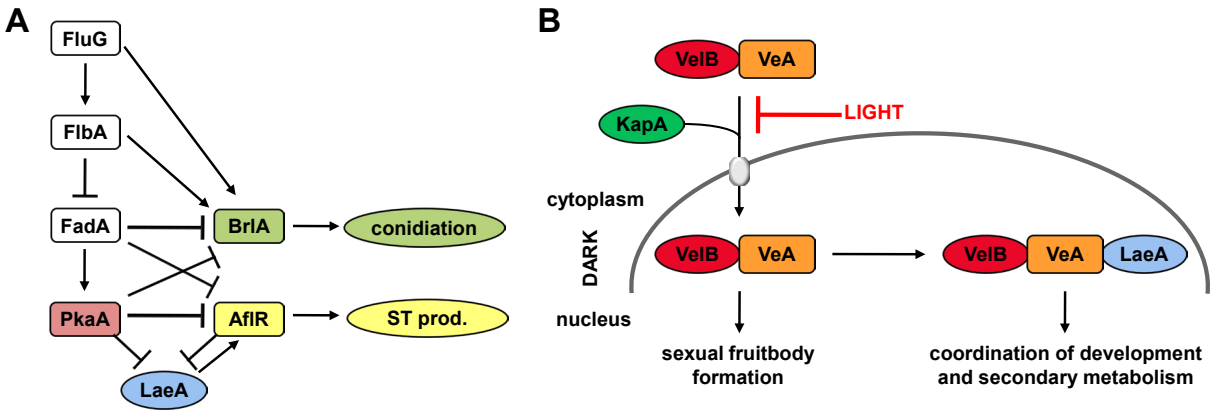

Fig. 10: Pathways connecting secondary metabolism and development in *A. nidulans*. **A:** The G-protein signal transduction pathway. FluG (fluffy protein, involved in synthesis of an extracellular conidiation factor), FlbA (fluffy protein, regulator of G-protein signaling), FadA (α-subunit of a heterotrimeric G-protein), PkaA (cAMP-dependent protein kinase catalytic subunit), LaeA (putative methyltransferase and master regulator of secondary metabolism), BrlA (transcription factor for conidiation), AflR (transcription factor for ST gene cluster). Modified from Calvo *et al.*, 2002. **B:** The velvet complex. VeA (velvet protein A), VelB (velvet-like protein B), KapA (importin α). Modified from Sarikaya Bayram *et al.*, 2010.

1.4.3.1.2 The velvet complex

The second important protein interplay, displaying the missing genetic link between secondary metabolism and development, is the trimeric velvet complex, discovered in 2008 in *Aspergillus nidulans* (Bayram *et al.*, 2008). The velvet superfamily harbors conserved fungal regulatory proteins. The most prominent among them is VeA (velvet A), first described in 1965 (Kaefer, 1965). VeA is involved in light response and connects development and secondary metabolism. Deletion of *veA* in *Aspergillus nidulans* results in a loss of sexual fruiting bodies and aberrant natural product synthesis. Loss of a second velvet-like protein VelB (*ve*lvet-like B) leads to the same phenotype. In the light, the predominantly cytoplasmic VeA interacts with VelB inducing asexual spore formation. In the dark, VeA and VelB are transported by the importin α KapA into the nucleus, where they form the heterotrimeric velvet complex together with the master regulator of secondary metabolism LaeA (see chapter 1.2.1.2.2) for coordination of sexual development and secondary metabolism (Fig. 10B). Recently, an additional role for LaeA in asexual development and formation of Hülle cells during sexual reproduction was discovered (Sarikaya Bayram *et al.*, 2010).

1.4.3.1.3 The COP9 signalosome

The multiprotein COP9 signalosome (constitutively photomorphogenic, also called CSN complex) is highly conserved in eukaryotes (Wei *et al.*, 1994) and plays a crucial role in

control of ubiquitin-mediated protein degradation in the cell by the proteasome pathway (Fig. 11) (Braus *et al.*, 2010). The CSN complex consists of eight subunits CSN1 to CSN8, with CSN5 being the only subunit conserved among all eukaryotes (Deng *et al.*, 2000, Maytal-Kivity *et al.*, 2003). In CSN5 resides a deneddylase catalytic activity, which detaches the ubiquitin-like protein Nedd8 from cullin-based ubiquitin E3 ligases. The covalent linkage of Nedd8 to a lysine residue of cullins activates E3 enzymes, which control ubiquitin-mediated protein degradation in the cell (Braus *et al.*, 2010).

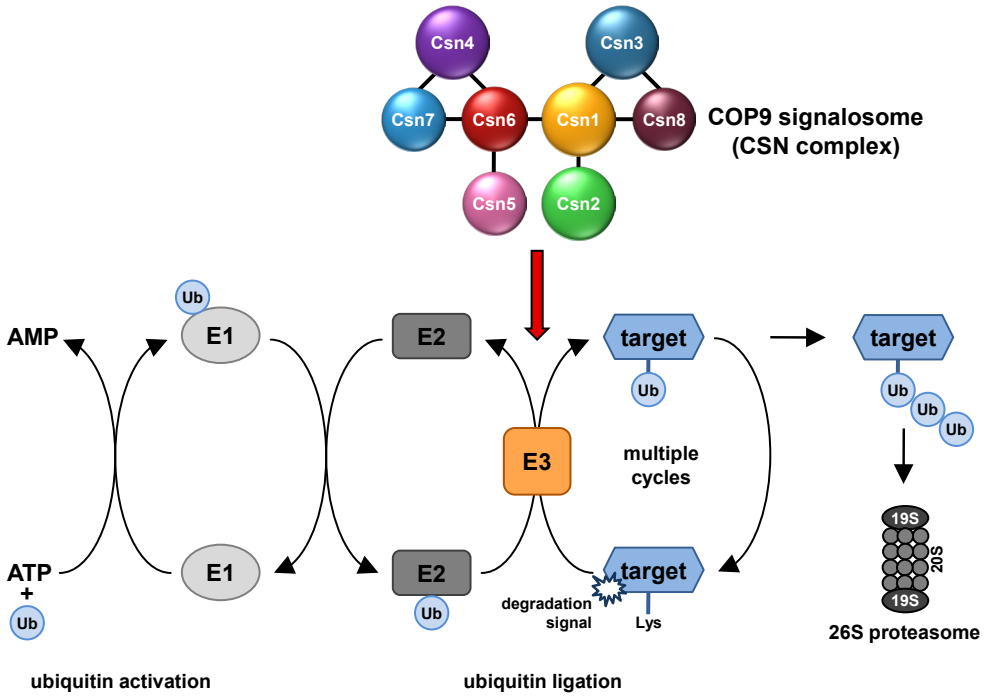

Fig. 11: Model for the protein degradation by ubiquitin labeling. Ubiquitin is activated by an E1 activating enzyme and transferred to an E2 ubiquitin conjugating enzyme. The E3 ubiquitin ligase mediates ubiquitination of a lysine residue of the target protein. By multiple repetitions, the target protein is labeled with a ubiquitin chain and degraded by the 26S proteasome. The COP9 signalosome (CSN complex) regulates the activity of the E3 ubiquitin ligase during protein degradation. Modified from Sharon *et al.*, 2009 and Watson *et al.*, 2006.

Since its discovery in *Arabidopsis thaliana* as a suppressor of light-dependent development (Wei *et al.*, 1994), CSN has been identified in mammalian cells, insects, yeasts, and fungi (Busch *et al.*, 2003, Freilich *et al.*, 1999, He *et al.*, 2005, Mundt *et al.*, 1999, Seeger *et al.*, 1998). It is involved in a variety of cellular processes, like cell cycle regulation, hormone signaling, DNA repair, and circadian clock regulation (Braus *et al.*, 2010, Wei *et al.*, 2003). CSN is an essential regulator of development and deletion of one of the subunits results in embryonic death in plants or animals (Wei *et al.*, 2008). In *A. nidulans*, all eight subunits of

CSN are conserved and deletion results in viable mutants, what makes it a suitable model organism for analysis of CSN (Busch *et al.*, 2003). The *A. nidulans* mutants are blocked in sexual fruiting body development at the level of primordia, but produce excessive amounts of nests and Hülle cells even in light (Busch *et al.*, 2007). Additionally, they are strongly impaired in secondary metabolite production and show an abnormal pigmentation.

1.5 Scope and aim of this work

Secondary metabolism is a fascinating process occurring in fungi, bacteria, plants and animals. Although not needed for survival of the organism, secondary metabolites confer advantages in response to the environment, including protection against UV-damages by pigments, and weaponry against competitors. With 1.5 million members, filamentous fungi are a promising fungal group for the discovery of new bioactive secondary metabolites that can be applied in human therapy.

The filamentous fungus *Aspergillus nidulans* is a suitable model organism for the study of secondary metabolism. It produces important metabolites, like the antibiotic penicillin, but also damaging compounds, like the aflatoxin precursor sterigmatocystin. The complete genome of *A. nidulans* was sequenced and therefore, clusters can be easily identified. The major problem is the silencing of many biosynthetic gene clusters under standard laboratory conditions, and consequently, the development of approaches to activate expression of those clusters is necessary.

In the first part of this work, the application of a novel approach based on protein degradation impairment is described. A previously silenced and orphaned biosynthetic PKS gene cluster, identified by transcriptional profiling of a *CSN5*/*csnE* deletion strain impaired in deneddylase activity of CSN, was characterized. This study aims on activation of the novel gene cluster, determination of its boundaries and the isolation and identification of the metabolites synthesized by its gene products.

Expression of biosynthetic gene clusters is partially controlled by heterochromatin formation, in which methylations play a crucial role. Methylations occur by methyl group transfer from the ubiquitous donor S-adenosylmethionine (SAM), which is synthesized by SAM synthetases. The second part of this work focuses on the characterization of the SAM synthetase SasA in *Aspergillus nidulans*. SAM synthetases are well-studied in other organisms like human, yeast, bacteria, and plants, but less is known about them in filamentous

fungi. We studied the role of SasA in growth, development and secondary metabolism of *A. nidulans* by analyzing protein localization and interactions, and by constructing *sasA* deletion and overexpression mutants.

2 Materials and Methods

2.1 Growth media and growth conditions

Aspergillus nidulans strains were grown on minimal medium (0.52 g/l KCl, 0.52 g/l $MgSO_4$, 1.52 g/l KH_2PO_4, 0.1% trace element solution, pH 6.5) (Barratt *et al.*, 1965) or on minimal medium with 0.1% casein hydrolysate at 30°C or 37°C and supplemented appropriately with 1 µg/ml pyridoxine-HCl, 1 µg/ml uracil, 0.25 µg/ml uridine, 1 µg/ml 4-aminobenzoic acid, 1 µg/ml pyrithiamine (Takara Bio Inc, Münsing, Germany), 120 µg/ml nourseothricin-dihydrogen sulfate (clonNAT, Werner BioAgents, Jena, Germany) and 80 µg/ml phleomycin (Cayla-InvivoGen, Toulouse, France). 10 mM nitrate, ammonium or proline served as nitrogen source and 1% D-glucose as carbon source. For solid medium, 2% agar was added. For induction of sexual development, cultures were grown in dark under oxygen limitation conditions and for induction of asexual development, cultures were grown in light (Clutterbuck, 1974). *Escherichia coli* strains were cultivated in LB medium (1% tryptone, 0.5% yeast extract, 1% NaCl) supplemented with 100 µg/ml ampicillin or 50 µg/ml kanamycin, respectively. Bacterial strains for bioactivity tests were propagated on LB medium. *Sordaria macrospora* was grown on biomalt maize medium (2.5% maize meal, 0.8% biomalt, pH 6.5) (Esser, 1982). *Verticillium longisporum* was propagated on simulated xylem medium (0.2% sodium pectin, 0.4% casein, 0.52 g/l KCl, 0.52 g/l $MgSO_4$, 1.52 g/l KH_2PO_4, 0.1% trace element solution, pH 6.5), *Neurospora crassa* on Vogel's minimal medium with 2% sucrose (Vogel, 1956), and *Aspergillus fumigatus* on minimal medium.

2.2 Strains

2.2.1 *Escherichia coli* strains

Escherichia coli strains MACH-1 (Invitrogen GmbH, Karlsruhe, Germany) and DH5α [F^-, Φ80Δ(*lacZ*)$M15^{-1}$, Δ(*lacZYA-argF*) U169, *recA1*, *endA1*, *hsdR17* (r_K^-, m_K^+), *supE44*, λ^-, *thi1*, *gyrA96*, *relA1*] (Woodcock *et al.*, 1989) were used.

2.2.2 *Aspergillus nidulans* strains

Strains generated and used in this study are listed in Tab. 2.

Tab. 2: Strains constructed and used in this study.

Strain name	Strain no.	Genotype	Reference
A4	A4	Glasgow wild type	FGSC[2]
TNO2A3	TNO2A3	*pyroA4; pyrG89; argB2; ΔnkuA::argB; veA1*	(Nayak *et al.*, 2006)
AGB154	AGB154	*pabaA1; yA2*	(Bayram *et al.*, 2009)
AGB160	AGB160	*pyroA4; pyrG89; pyr-4*$^{+}$	(Busch *et al.*, 2003)
AGB506	AGB506	^{p}*gpdA::mrfp::h2A/nat*^{R}*; pyroA4; pyrG89*	(Sarikaya Bayram *et al.*, 2010)
AGB552	AGB552	*pabaA1; yA; ΔnkuA::argB*	this study
Δ*csnE*	AGB209	*pyroA4; pyrG89; ΔcsnE::pyr-4*$^{+}$	(Busch *et al.*, 2003)
Δ*dbaI*	AGB523	*ΔdbaI::ptrA; pyroA4; pyrG89; pyr-4*$^{+}$	this study
Δ*dbaI*/ΔcsnE	AGB524	*ΔdbaI::ptrA; ΔcsnE::pyr-4*$^{+}$*; pyroA4; pyrG89*	this study
Δ*dbaI*/Δ*csnE* + *csnE*$^{ect.}$	AGB526	*ΔdbaI::ptrA; ΔcsnE::pyr-4*$^{+}$*; pyroA4; pyrG89, csnE*$^{ect.}$	this study
Δ*dbaI*/Δ*csnE* + *gpdA::dbaI*$^{ect.}$	AGB661	*ΔdbaI::ptrA; ΔcsnE::pyr-4*$^{+}$*; pyroA4; pyrG89, gpdA::dbaI*$^{ect.}$	this study
dbaA OE	AGB527	*ptrA::*^{p}*niiA::dbaA; pyroA4; pyrG89; argB2; ΔnkuA::argB; veA1*	this study
dbaG OE	AGB528	*ptrA::*^{p}*niiA::dbaG; pyroA4; pyrG89; argB2; ΔnkuA::argB; veA1*	this study
Δ*dbaA*	AGB529	*ΔdbaA::ptrA; pyroA4; pyrG89; argB2; ΔnkuA::argB; veA1*	this study
Δ*dbaA*/Δ*csnE*	AGB530	*ΔdbaA::ptrA; pyroA4; pyrG89; ΔcsnE::pyr-4*$^{+}$	this study
Δ*dbaB*	AGB531	*ΔdbaB::ptrA; pabaA1; yA; ΔnkuA::argB*	this study
Δ*dbaC*	AGB532	*ΔdbaC::ptrA; pabaA1; yA; ΔnkuA::argB*	this study
Δ*dbaD*	AGB533	*ΔdbaD::ptrA; pabaA1; yA; ΔnkuA::argB*	this study
Δ*dbaE*	AGB534	*ΔdbaE::ptrA; pabaA1; yA; ΔnkuA::argB*	this study
Δ*dbaF*	AGB535	*ΔdbaF::ptrA; pabaA1; yA; ΔnkuA::argB*	this study
Δ*dbaG*	AGB536	*ΔdbaG::ptrA; pabaA1; yA; ΔnkuA::argB*	this study
Δ*dbaH*	AGB537	*ΔdbaH::ptrA; pabaA1; yA; ΔnkuA::argB*	this study

[2] Fungal Genetics Stock Center (University of Kansas Medical Center, Kansas City, KS, USA); Dave Geiser (Penn State University, University Park, PA, USA); Gregory May (University of Texas, Houston, TX, USA).

Tab. 2 continued: Strains constructed and used in this study.

Strain name	Strain no.	Genotype	Reference
Δ*dbaB*/*dbaA* OE	AGB538	Δ*dbaB:: AfpyrG; ptrA::*^{p}*niiA::dbaA; pyroA4; pyrG89; argB2;* Δ*nkuA::argB; veA1*	this study
Δ*dbaC*/*dbaA* OE	AGB539	Δ*dbaC:: AfpyrG; ptrA::*^{p}*niiA::dbaA; pyroA4; pyrG89; argB2;* Δ*nkuA::argB; veA1*	this study
Δ*dbaD*/*dbaA* OE	AGB540	Δ*dbaD:: AfpyrG; ptrA::*^{p}*niiA::dbaA; pyroA4; pyrG89; argB2;* Δ*nkuA::argB; veA1*	this study
Δ*dbaE*/*dbaA* OE	AGB541	Δ*dbaE:: AfpyrG; ptrA::*^{p}*niiA::dbaA; pyroA4; pyrG89; argB2;* Δ*nkuA::argB; veA1*	this study
Δ*dbaF*/*dbaA* OE	AGB542	Δ*dbaF:: AfpyrG; ptrA::*^{p}*niiA::dbaA; pyroA4; pyrG89; argB2;* Δ*nkuA::argB; veA1*	this study
Δ*dbaG*/*dbaA* OE	AGB612	Δ*dbaG:: AfpyrG; ptrA::*^{p}*niiA::dbaA; pyroA4; pyrG89; argB2;* Δ*nkuA::argB; veA1*	this study
Δ*dbaH*/*dbaA* OE	AGB613	Δ*dbaH:: AfpyrG; ptrA::*^{p}*niiA::dbaA; pyroA4; pyrG89; argB2;* Δ*nkuA::argB; veA1*	this study
dbaA::*ctap*	AGB616	*dbaA::ctap::*^{p}*gpdA::nat*^{R}*; pabaA1; yA;* Δ*nkuA::argB*	this study
dbaA::*ctap*/Δ*csnE*	AGB617	*dbaA::ctap::*^{p}*gpdA::nat*^{R}*; pyroA4; pyrG89;* Δ*csnE::pyr-4*$^{+}$	this study
Δ*dbaA*/Δ*csnE* + *dbaA*$^{ect.}$	AGB618	Δ*dbaA::ptrA; pyroA4; pyrG89;* Δ*csnE::pyr-4*$^{+}$*, dbaA*$^{ect.}$	this study
Δ*dbaD*/*dbaA* OE + *dbaD*$^{ect.}$	AGB619	Δ*dbaD:: AfpyrG; ptrA::*^{p}*niiA::dbaA; pyroA4; pyrG89; argB2;* Δ*nkuA::argB; veA1, dbaD*$^{ect.}$	this study
Δ*dbaG*/*dbaA* OE + *dbaG*$^{ect.}$	AGB620	Δ*dbaG:: AfpyrG; ptrA::*^{p}*niiA::dbaA; pyroA4; pyrG89; argB2;* Δ*nkuA::argB; veA1, dbaG*$^{ect.}$	this study
Δ*dbaH*/*dbaA* OE + *dbaH*$^{ect.}$	AGB660	Δ*dbaH:: AfpyrG; ptrA::*^{p}*niiA::dbaA; pyroA4; pyrG89; argB2;* Δ*nkuA::argB; veA1, dbaH*$^{ect.}$	this study
sasA OE	AGB665	*ptrA::*^{p}*niiA::sasA; pyroA4; pyrG89; argB2;* Δ*nkuA::argB; veA1*	this study
sasA::*gfp*	AGB666	*sasA::sgfp::*^{p}*gpdA::nat*^{R}*; pyroA4; pyrG89; argB2;* Δ*nkuA::argB; veA1*	this study
sasA::*tap*	AGB667	*sasA::ctap::*^{p}*gpdA::nat*^{R}*; pyroA4; pyrG89; argB2;* Δ*nkuA::argB; veA1*	this study
sasA::*gfp*	AGB668	*sasA::sgfp::*^{p}*gpdA::nat*^{R}	this study
sasA::*tap*	AGB669	*sasA::ctap::*^{p}*gpdA::nat*^{R}	this study
veA::*ctap*	AGB273	^{p}*veA*::*veA*::*ctap, ptrA; pabaA1, yA2;* Δ*argB*::*trpC; trpC801,* Δ*veA*::*argB*	(Bayram *et al.*, 2008)
velB::*ctap*	AGB389	*velB*::*ctap*::^{p}*gpdA*::*nat*^{R}	(Bayram *et al.*, 2008)
veA::*ctap*/*velB*::*ctap*	AGB677	^{p}*veA*::*veA*::*ctap, ptrA; yA2*; Δ*argB*::*trpC*; *trpC801*, Δ*veA*::*argB*; *velB*::*ctap*::^{p}*gpdA*::*nat*^{R}	this study

2.2.2.1 Construction of strains for *dba* analysis

Primers and plasmids used for construction of strains are listed in Tab. 3, Tab. 4 and Tab. 5. For construction of overexpression strains *dbaA* OE (AGB527) and *dbaG* OE (AGB528), the nitrogen source driven 1.3 kb promoter ^{p}*niiA*, which can be induced by nitrate and repressed by ammonium containing medium, was amplified from pME3160 (Tab. 5) with primerpair JG92/93. The promoter was fused to the resistance marker gene *ptrA* (amplified from pPTRII with primer pair JG21/22) via fusion PCR using primers JG21 and JG93. For homologous integration of the overexpression cassette into the genome, 1 kb of 5'-UTR and 1 kb of target gene were amplified using oligos JG90/91 and JG94/95 for *dbaA* and JG98/99 and JG100/101 for *dbaG*, respectively. The flanking regions were fused to *ptrA*::^{p}*niiA* cassette with primers JG96/97 for *dbaA* and JG102/103 for *dbaG*. The overexpression constructs were transformed into strain TNO2A3.

For construction of deletion strains, TNO2A3, AGB160, AGB209, AGB552, and AGB527 served as wild type strains. The deletion cassettes containing *ptrA* or *pyrG* marker were integrated by using up to 2 kb flanking regions up- and downstream of the target genes. Primers used for amplification of deletion cassettes are listed in Tab. 3 and Tab. 4. Flanking regions were amplified from *Aspergillus nidulans* A4 genomic DNA. Marker gene *pyrG* was amplified from a deletion cassette with primer pair OZG483/484, and *ptrA* was amplified from plasmid pPTRII (Tab. 5) with primer pair JG21/22.

For construction of strains *dbaA*::*ctap* (AGB616) and *dbaA*::*ctap*/Δ*csnE* (AGB617), *ctap*-tag was cloned to ^{p}*gpdA*::*nat*^{R} (amplified from plasmid pNV1) with oligos OZG192/209 and subsequently fused to 5' and 3' flanking regions of target gene *dbaA* via PCR with primer pair JG160/OZG494. The cloning cassette was transformed into strains AGB552 and AGB209 homologously.

2.2.2.2 Construction of *dba* complementation strains

For complementation of *dbaA*, *dbaD*, *dbaG*, *dbaH*, and *dbaI* deletion strains (AGB530, AGB540, AGB612, AGB613, AGB524), plasmids pME3792, pME3793, pME3798, pME3837, and pME3800 were integrated into the fungal genome, resulting in strains AGB618, AGB619, AGB620, AGB660, and AGB661, respectively. For construction of plasmids see chapter 2.3.2.1.

For complementation of *csnE* in *ΔdbaI*/*ΔcsnE* strain (AGB524), plasmid pME2423 was integrated into the genome, resulting in strain AGB526.

Tab. 3: Primers used in this study.

Designation	Sequence	Basepairs
JG1	5'-ATGGATCCTCAGCAGCGTCATTTG-3'	24
JG2	5'-TTAATGGTAGTGAAGCTTGCCTGG-3'	24
JG3	5'-ATGTCAAAAGCCCAGAGCCCACC-3'	23
JG4	5'-CTAATGAACAGTTGAAGATTGAAAGGG-3'	27
JG5	5'-ATGGGCAGTGTCGAGACGATCC-3'	22
JG6	5'-TTATTTGAGCTTTTCACCAGTCTTCC-3'	26
JG19	5'-AAAGATATCCAAGGCTCGGAGTATCGTGTCG-3'	31
JG20	5'-CGTTACCAATGGGATCCCGTAATTGTAGCGCTCTCGCGGGGGC-3'	43
JG21	5'-ATTACGGGATCCCATTGGTAACG-3'	23
JG22	5'-GCATCTTTGTTTGTATTATACTGTC-3'	25
JG23	5'-GACAGTATAATACAAACAAAGATGCCCCGGCCATTAAGGCTACTCC-3'	46
JG24	5'-TTTGATATCCACTAATGGACCGGAAGATAACT-3'	32
JG25	5'-CAGCCAGGAGAGGCTGGGCAGG-3'	22
JG26	5'-GAGCGACGTCGTCGGCTGTGACC-3'	23
JG47	5'-AAAACTAGTAGCAGTACGGCCATACCCTTGAG-3'	32
JG48	5'-TACCAATGGGATCCCGTAATGGTGACGATGGTCTGAAAAAATGAG-3'	45
JG49	5'-TATAATACAAACAAAGATGCGCTCGTCGCTTAGGCTTGAATCC-3'	43
JG50	5'-TTTACTAGTCCTCTGGATAAAGACCATTTCTTCC-3'	34
JG51	5'-CCCTTCTTTCTTGCAGTTGGTTCG-3'	24
JG52	5'-GCCGGTAAGCTTTCGCGAAATTTC-3'	24
JG55	5'-AAAGAATTCATGGGCTCAGTCGCTACCCC-3'	29
JG56	5'-AAAGAATTCTTAGAACTTAAGGGCCTTGGGC-3'	31
JG83	5'-GTACTCTCAAGAAGATACGCAGCA-3'	24
JG84	5'-AGCGGTACGTGCGTGTAGAGCT-3'	22
JG85	5'-ACCATACCACCGCTACCACCGAACTTAAGGGCCTTGGCTGC-3'	42
JG86	5'-TGAGCATGCCCTGCCCCTGAGCTCGTCGCTTAGGCTTGAATCC-3'	43
JG87	5'-CTGGAACTGAGGAGGGTAGACAA-3'	23
JG88	5'-GTTCGAGGACATTGGAAGAATCACA-3'	25
JG89	5'-CTCTTACCACCGCTACCACCGAACTTAAGGGCCTTGGGCTGCT-3'	43
JG90	5'-CAGCCCGCCATGTACCGAATATC-3'	23
JG91	5'TACCAATGGGATCCCGTAATCGTCTAGCTGGGGTTCCTGAATC-3'	43
JG92	5'-TATAATACAAACAAAGATGCGATGGCGGGCGCGGTGATTGA-3'	41
JG93	5'-GTGAGAGTATGGGATAGGAAAATAAT-3'	26
JG94	5'-TTCCTATCCCATACTCTCACATGTCTCAACATGTCAAAAGCCCAG-3'	45
JG95	5'-ATGGCTAGCAGGAGCCATGCCT-3'	22
JG96	5'-CTGATATACCAATATACCCTTCTAG-3'	25
JG97	5'-TAGAACGAGTGTCCAATATTCTCAT-3'	25
JG98	5'-CGATAGCTAGGCTCTCTTTTCCTT-3'	24
JG99	5'-TACCAATGGGATCCCGTAATGGTGTCTGTGCCTGGCACCGG-3'	41
JG100	5'-TTCCTATCCCATACTCTCACATGCCTGAGGACGGACCCCCC-3'	41
JG101	5'-GGAAACACCGAGCAACACGGGA-3'	22
JG102	5'-TCGCTATCTCGCGTCAACTCATG-3'	23
JG103	5'-TGATACGGCGAGGGACTCAAGTA-3'	23
JG104	5'-TGGATGTCCTGTGGCTACACTGC-3'	23

Tab. 3 continued: Primers used in this study.

Designation	Sequence	Basepairs
JG105	5'-TGGGGCATGCTGGATGCAGGGT-3'	22
JG147	5'-TTAGAACTTAAGGGCCTTGGGCT-3'	23
JG149	5'-ATGGGCTCAGTCGCTACCCCC-3'	21
JG150	5'-TACCAATGGGATCCCGTAATGGTGACGATGGTCTGAAAAAATGA-3'	44
JG151	5'-TTCCTATCCCATACTCTCACATGGGCTCAGTCGCTACCCCC-3'	41
JG152	5'-GGAGGTCAAAGTTGTTGCGGATG-3'	23
JG158	5'-TCGGCGGCTATATTATCAGTCAAT-3'	24
JG159	5'-ATGGCGGATAGCCTGAGGAATC-3'	22
JG160	5'-CCCGAGAGCATTTTTGAAGGACT-3'	23
JG161	5'-TATAATACAAACAAAGATGCAAATTAAGACGGCCTTTTTCCTTT-3'	44
JG162	5'-GGATCATGGGATAAGCATCTGAC-3'	23
JG163	5'-AAAGCGGCCGCGGCGGCTCTGAGGTGCAGTGG-3'	32
JG164	5'-AAAGCGGCCGCTCAGGGGCAGGGCATGCTCATG-3'	33
JG165	5'-ATGACACGCACCTCACCCACTCT-3'	23
JG166	5'-CTAGACTGCAATCTCCGACAATTTT-3'	25
JG167	5'-ATGAAGTCTGTCTTGGCCAGCGG-3'	23
JG168	5'-TTAGTTATCGAGGTCATCCCGATC-3'	24
JG169	5'-ATGGCTCCAAATCACGTTCTTT-3'	22
JG170	5'-ATGGGTTGTAGTTGCCGTCTC-3'	21
JG173	5'-ATGTCTGAACAAAATGACTGGCTG-3'	24
JG174	5'-TTACTTCTGCTGGTTGGGAATTCT-3'	24
JG175	5'-ATGGCCGCCAACATCAACAACG-3'	22
JG176	5'-TCACAAAGAAACCACCACCTTCT-3'	23
JG177	5'-ATGACAGAACAACCTCCGCAGAA-3'	23
JG178	5'-TCACGCCTTCACTTTGAGCTTGA-3'	23
JG179	5'-ATGACCATCCGAATCCCCAGCG-3'	22
JG180	5'-TCAACACCAAGAATCCAAGACACC-3'	24
JG181	5'-ATGCCAGGTACCGTGCGCCCA-3'	21
JG182	5'-CTATTTTTCAACCGACCCCTCTG-3'	23
JG190	5'-ATGGCCCAACTCTACGACTGGC-3'	22
JG191	5'-CTACAAAGGCTTCCTAATCACGCA-3'	24
JG192	5'-ATGCCCCAAGAACCCACGCCT-3'	21
JG193	5'-CTATATCTTCTTCAAAATAACCATCC-3'	26
JG194	5'-ATGTCAAAAATCAGCCTCTTCGGA-3'	24
JG195	5'-CTACTCTCGCGTCCGCAAATAC-3'	22
JG196	5'-ATGGCAGCCCCTGGAGATATCA-3'	22
JG197	5'-TTAGAGCCCATTGAACTTATATACC-3'	25
JG198	5'-ATGGCCACTGAAAACAACCCACC-3'	23
JG199	5'-CTAATAATGCGGCCAGATCCCC-3'	22
JG200	5'-ATGAGAAACCTCAGTACCTGGCC-3'	23
JG201	5'-TCACTTCAGGGTGAGGAGCCCT-3'	22
JG204	5'-AAAATCGATAGCCCGCCATGTACCGAATATC-3'	31
JG205	5'-AAAATCGATCGGCACCACCATCACCATGAC-3'	30
JG208	5'-AAGATGCCATCAAAGCTCTCGGC-3'	23

Tab. 3 continued: Primers used in this study.

Designation	Sequence	Basepairs
JG209	5'-CCCGTGGCAAACAAGAAGATGATT-3'	24
JG210	5'-TATAATACAAACAAAGATGCTCCAGCTGAATTAGCACTAACTTAT-3'	45
JG215	5'-AGCTTCTAGCCTTCTTCTTTCCC-3'	23
JG216	5'-GTAGTGACTTCTCAAATACTTTTCA-3'	25
JG217	5'-TACCAATGGGATCCCGTAATGGTGATAGGCTATCTGGTTTAGC-3'	43
JG218	5'-TATAATACAAACAAAGATGCCTTACTTAGCGAGTATGCCTATG-3'	43
JG219	5'-CGTCTTGCTGATAGCTAGCCAC-3'	22
JG220	5'-TGGATGGCGTACTGCCTGGAT-3'	21
JG221	5'-TGTTGTCTTCATTCTGGTTGAGGT-3'	24
JG222	5'-GGAGGAGTACAATCTGGTGTTAG-3'	23
JG223	5'-TACCAATGGGATCCCGTAATTTCACTGGCGGAGCGGTTATG-3'	41
JG224	5'-TATAATACAAACAAAGATGCTCATTTGATCCATAGGACGTGGC-3'	43
JG225	5'-TCATCTAGCAGTCAGGAACTCCA-3'	23
JG226	5'-GGAATGGGCTAACACGAAGGGA-3'	22
JG227	5'-GCTGTCAGCAAACAGACGAGTTC-3'	23
JG228	5'-TCTACGAGTCCGAGATAGCTTGA-3'	23
JG229	5'-TACCAATGGGATCCCGTAATCGTAGGGATGATTTGGTAATTAATC-3'	45
JG230	5'-TATAATACAAACAAAGATGCTGTTTGGTGTTGAAATATTATCAGAG-3'	46
JG231	5'-CAGGGCAGATTCTAATGTCTAAGG-3'	24
JG232	5'-CTCCTGCAGGCTGCAAGAGCA-3'	21
JG233	5'-CCGAGCAATCTTCGCCCTCTTG-3'	22
JG234	5'-ATCTCTCGTTCTCTCCCTCATCT-3'	23
JG235	5'-TACCAATGGGATCCCGTAATTTTCTAATTGATTCTTAGTTAATTGAA-3'	47
JG236	5'-TATAATACAAACAAAGATGCCTATTTTTGATATCCCGGTTATAGC-3'	45
JG237	5'-CCCAACGGGCCTTACGACTTC-3'	21
JG238	5'-CGCTTTCTTACCTGACTCTTCAC-3'	23
JG253	5'-TACTAGTCTCATATCCAAGTCGGA-3'	24
JG254	5'-CTCCGATATCTTCTAAACATAACAC-3'	25
JG255	5'-TACCAATGGGATCCCGTAATGTTGACCGTGGTGTATTTTGAGAA-3'	44
JG256	5'-TATAATACAAACAAAGATGCTCGAGTGTTTAATGGAAAAAGTTCA-3'	45
JG257	5'-CATGACATTGCAGGCTCGGACT-3'	22
JG258	5'-ACGAAGTCCTATCCAACTTGCCA-3'	23
JG259	5'-CCCACCGATTCCGGAGAAGTG-3'	21
JG260	5'-CAGTATAGGCTCTCACAACGTGT-3'	23
JG261	5'-TACCAATGGGATCCCGTAATTGTACAAGATATAAAAGAGGTAGAAA-3'	46
JG262	5'-TATAATACAAACAAAGATGCCTAATTTCACCGTTGCTTCGCTC-3'	43
JG263	5'-ACCGCGTTCATAGAGTAGTTATAG-3'	24
JG264	5'-GGCCTAAAAGCACGTCCAAGATG-3'	23
JG290	5'-AATAGCATGCCATTAACCTAGGTA-3'	24
JG291	5'-AAGTCCCGATGACCAAGCATGGTGATGTCTGCTCAAGCGGG-3'	41
JG292	5'-ATGCTTGGTCATCGGGACTTCAC-3'	23
JG293	5'-ATTATTCTCATAGTCGCAGGCACA-3'	24
JG298	5'-CACTTAACGTTACTGAAATCGGTGATAGGCTATCTGGTTTAGC-3'	43
JG299	5'-CTTCAATATCATCTTCTGTCCTTACTTAGCGAGTATGCCTATG-3'	43

Tab. 3 continued: Primers used in this study.

Designation	Sequence	Basepairs
JG306	5'-CACTTAACGTTACTGAAATCGTTGACCGTGGTGTATTTTGAGAA-3'	44
JG307	5'-CTTCAATATCATCTTCTGTCTCGAGTGTTTAATGGAAAAAGTTCA-3'	45
JG308	5'-CACTTAACGTTACTGAAATCTTCACTGGCGGAGCGGTTATG-3'	41
JG309	5'-CTTCAATATCATCTTCTGTCTCATTTGATCCATAGGACGTGGC-3'	43
JG310	5'-CACTTAACGTTACTGAAATCTGTACAAGATATAAAAGAGGTAGAAA-3'	46
JG311	5'-CTTCAATATCATCTTCTGTCCTAATTTCACCGTTGCTTCGCTC-3'	43
JG312	5'-CACTTAACGTTACTGAAATCCGTAGGGATGATTTGGTAATTAATC-3'	45
JG313	5'-CTTCAATATCATCTTCTGTCTGTTTGGTGTTGAAATATTATCAGAG-3'	46
JG314	5'-CACTTAACGTTACTGAAATCTTTCTAATTGATTCTTAGTTAATTGAA-3'	47
JG315	5'-CTTCAATATCATCTTCTGTCCTATTTTTGATATCCCGGTTATAGC-3'	45
JG343	5'-CACTTAACGTTACTGAAATCGGTGTCTGTGCCTGGCACCGG-3'	41
JG344	5'-CTTCAATATCATCTTCTGTCTCCAGCTGAATTAGCACTAACTTAT-3'	45
OZG61	5‘-ATGTTTGAGATGGGCCCGGTGGG-3'	23
OZG62	5’-TTATCTTAATGGTTTCCTAGCCTGGT-3'	26
OZG192	5'-TCAGGGGCAGGGCATGCTCATGTAGAG-3'	27
OZG207	5'-GGTGGTAGCGGTGGTATGGTGAGC-3'	24
ÖZG209	5'-GGTGGTAGCGGTGGTAAGAGAAGATGGAAAAAGAATTTCATAG-3'	44
OZG337	5'-ATGGAGCCCCCAGCGATCAGCCAG-3'	24
OZG338	5'-TCAGGCGTGGCGGAGGATGCTGATC-3'	25
OZG339	5'-TCAGGCGTGGCGGAGGATGCTGAT-3'	24
OZG340	5'-TTATCTAAAGGCCCCCCCATCAACG-3'	25
OZG367	5'-ATGGGTTCAGTCAGCAAAGCCAATG-3'	25
OZG368	5'-CTAGGTCTGGCCGTTCTTGTTG-3'	22
OZG483	5'-GATTTCAGTAACGTTAAGTGGATC-3'	24
OZG484	5'-GACAGAAGATGATATTGAAGGAGCC-3'	28
OZG492	5'-CCATCTTCTCTTACCACCGCTACCACCATGAACAGTTGAAGATTGAAA GGGAC-3'	53
OZG493	5'-GCTCTACATGAGCATGCCCTGCCCCTGAAAATTAAGACGGCCTTTTTC CTTTCTTG-3'	56
OZG494	5'-GTTCTCCCTCGTCTCTAGCCCAC-3'	23
gpdA-5	5'-ATGGCTCCCAAGGTACGACATTTAG-3'	25
gpdA-3	5'-CTATTGGGCATCAACCTTGGAG-3'	22
tdiA-5	5'-ATGGCACCAAGCAAGACCGAG-3'	21
tdiA-3	5'-CTACAGGCCCCGCTCCCTCAG-3'	21

Tab. 4: Primers used for amplification and fusion of cloning cassettes.

Strain name	Strain no.	Primers for 5'-region	Primers for 3'-region	Primers for fusion	Strains used for
Δ*dbaA*	AGB529/530	JG91/159	JG158/161	JG160/162	TNO2A3/AGB209
Δ*dbaB*	AGB531	JG215/217	JG218/220	JG216/219	AGB552
Δ*dbaC*	AGB532	JG233/235	JG236/238	JG234/237	AGB552
Δ*dbaD*	AG533	JG253/255	JG256/258	JG254/257	AGB552
Δ*dbaE*	AGB534	JG221/223	JG224/226	JG222/225	AGB552
Δ*dbaF*	AGB535	JG259/261	JG262/264	JG260/263	AGB552
Δ*dbaG*	AGB536	JG98/99	JG208/210	JG102/209	AGB552
Δ*dbaH*	AGB537	JG227/229	JG230/232	JG228/231	AGB552
Δ*dbaI*	AGB523/524	JG19/20	JG23/24	JG25/26	AGB160/AGB209
dbaA OE	AGB527	JG90/91	JG94/95	JG96/97	TNO2A3
dbaG OE	AGB528	JG98/99	JG100/101	JG102/103	TNO2A3
Δ*dbaB*/*dbaA* OE	AGB538	JG215/298	JG220/299	JG216/219	AGB527
Δ*dbaC*/*dbaA* OE	AGB539	JG233/314	JG238/315	JG234/237	AGB527
Δ*dbaD*/*dbaA* OE	AGB540	JG253/306	JG258/307	JG254/257	AGB527
Δ*dbaE*/*dbaA* OE	AGB541	JG221/308	JG309/226	JG222/225	AGB527
Δ*dbaF*/*dbaA* OE	AGB542	JG259/310	JG264/311	JG260/263	AGB527
Δ*dbaG*/*dbaA* OE	AGB612	JG98/343	JG344/208	JG102/209	AGB527
Δ*dbaH*/*dbaA* OE	AGB613	JG227/312	JG313/232	JG228/231	AGB527
dbaA::*ctap*	AGB616/692	JG159/OZG492	OZG493/495	JG160/OZG494	AGB552/AGB209
sasA OE	AGB665	JG83/150	JG151/147	JG84/152	TNO2A3
sasA::*sgfp*	AGB666	JG83/85	JG86/88	JG84/87	TNO2A3
sasA::*ctap*	AGB667	JG83/89	JG86/88	JG84/87	TNO2A3
Δ*sasA*	lethal	JG47/48	JG49/50	JG51/52	TNO2A3

Tab. 5: Plasmids constructed and used in this study.

Plasmid	Description	Reference
pPTRII	autonomously replicating *A. nidulans* plasmid [*ptrA, AMA1, bla*]	Takara
pNV1	^{p}*gpdA::nat*^{R}	(Vogt *et al.*, 2008)
pME2423	^{p}*gpdA::ble::*^{t}*trpC; csnE*	(Busch *et al.*, 2003)
pME3160	^{p}*niiA*	(Bayram *et al.*, 2008)
pME3792	genomic *dbaA* with 1kb flanking regions in *Cla*I digested pNV1	this study
pME3793	genomic *dbaD* with 1.8 kb upstream and 1kb downstream flanking	this study
pME3798	genomic *dbaG* with 1 kb flanking regions in *Apa*I digested pNV1	this study
pME3799	^{p}*gpdA::nat*^{R} in *Not*I digested pME3835	this study
pME3800	^{p}*gpdA*::*dbaI*$^{1\text{-}1586bp}$ in *Ssp*I digested pME3799	this study
pME3835	*dbaI* in pCR-XL-TOPO	this study
pME3837	genomic *dbaH* with 1 kb flanking regions in *Xho*I digested pNV1	this study

2.2.2.3 Construction of strains for *sasA* analysis

For overexpression strain AGB665, the nitrogen source driven promoter ^{p}*niiA,* amplified from pME3160 with primers JG92/93, and *ptrA*, amplified from pPTRII with primers JG21/22, were fused via fusion PCR with primers JG21/93. The 1 kb upstream flanking region of *sasA* and 1.3 kb of *sasA* were amplified with primers JG83/150 and JG151/147 and fused to the *ptrA*::^{p}*niiA* cassette with primers JG84/152. The resulting cassette was subsequently cloned into strain TNO2A3 via homologous recombination.

For deletion of *sasA* the upstream and downstream flanking regions were amplified with primers JG47/48 and JG49/50 from genomic DNA and fused to *ptrA* with primers JG51/52. The deletion cassette was transformed into strain TNO2A3 via homologous recombination.

The C-terminally GFP- and TAP-tagged SasA strains AGB665 and AGB666 were generated by transformation via homologous recombination in strain TNO2A3. For both strains the 0.8 kb upstream flanking region and *sasA* were amplified with primers JG83/85 (GFP) or JG83/89 (TAP) and the 0.8 kb downstream flanking region was amplified with primers JG86/88 from genomic DNA. Subsequently, the amplicons were cloned to the *sgfp::gpdA::nat*^{R} or *ctap::gpdA::nat*^{R}cassette, respectively, with primers JG84/87. For generation of cassettes, *sgfp* tag was cloned to ^{p}*gpdA::nat*^{R} (amplified from plasmid pNV1) with oligos OZG192/207 and *ctap* with OZG192/209. For generation of AGB667 and AGB668, strains AGB665 and AGB666 were crossed with wild type strain AGB154.

For construction of double tap strain *veA*::*ctap*/*velB*::*ctap* (AGB677), the single tap strains *veA*::*ctap* (AGB273) and *velB*::*ctap* (AGB389) were crossed.

2.3 Genetic manipulations

2.3.1 Transformation

Transformation in *A. nidulans* was performed by polyethylene glycol mediated fusion of protoplasts as described previously (Eckert *et al.*, 2000, Punt *et al.*, 1992). Transformation in *Escherichia coli* was performed with calcium/manganese treated cells (Hanahan *et al.*, 1991) as described (Inoue *et al.*, 1990).

2.3.2 Plasmids

Plasmids used and constructed in this study are listed in Tab. 5.

2.3.2.1 Plasmid constructs for complementation studies

Plasmids pME3792, pME3793, pME3798, and pME3837, and pME3800 were constructed for complementation of *dbaA*, *dbaD*, *dbaG*, *dbaH*, and *dbaI* deletion strains, respectively.

For construction of pME3792, the open reading frame of *dbaA* with 1 kb of up- and downstream flanking regions was amplified from *A. nidulans* A4 genomic DNA with primers JG204/205 and cloned into plasmid pNV1 via *Cla*I restriction sites. Plasmid pME3793 was constructed by cloning genomic *dbaD* with 1.8 kb upstream and 1 kb downstream flanking regions amplified with JG254/257 in *Apa*I digested pNV1. For construction of pME3798, genomic *dbaG* with 1 kb flanking regions was amplified with primers pJG102/209 and cloned into pNV1 digested with *Apa*I resulting in pME3798. For pME3837, genomic *dbaH* with 1 kb flanking regions was amplified with primers JG228/231 and cloned into pNV1 cut with *Xho*I.

Plasmids pME3799, pME3800, and pME3835 were constructed for complementation of *dbaI* deletion strain.

For pME3800 construction, the ^{p}*gpdA* promoter was amplified with primers JG290/291 from plasmid pNV1 and fused to the beginning of *dbaI* (1-1586 bp), amplified with primers JG292/293. The construct was cloned blunt into plasmid pME3799 digested with *Ssp*I. For generation of pME3799, first genomic *dbaI*, amplified with primers JG104/105, was cloned into pCR-XL-TOPO (Invitrogen GmbH, Karlsruhe, Germany), resulting in pME3835 and subsequently, the ^{p}*gpdA*::*nat*^{R} resistance cassette amplified with JG163/164 from plasmid pNV1 was cloned into pME3835 digested with *Not*I, resulting in pME3799.

2.3.3 Sequence analysis

BLAST searches were performed at NCBI (http://www.ncbi.nlm.nih.gov/). For sequence alignment ClustalW2 (http://npsa-pbil.ibcp.fr/) was used. Phylogenetic analysis was conducted in MEGA5 (Tamura *et al.*, 2011). DNA was sequenced at the Labor für Genomanalyse in Göttingen (Germany). Sequences were analyzed with the software Lasergene (DNASTAR, Inc., Madison, WI, USA).

2.3.4 Recombinant DNA methods

Recombinant DNA technologies were performed according to the standard methods (Sambrook *et al.*, 1989). For PCR reactions *Taq* polymerase, Platinum® *Taq* Polymerase (Fermentas GmbH, St. Leon Rot, Germany), or Phusion® High Fidelity DNA Polymerase (Finnzymes, Vantaa, Finland) were used. Oligonucleotides were ordered from Eurofins MWG

GmbH (Ebersberg, Germany). Restriction enzymes and DNA modifying enzymes were obtained from Fermentas GmbH (St. Leon-Rot, Germany).

2.3.5 DNA isolation and hybridization

Genomic DNA was extracted from mycelia obtained from vegetative grown cultures. Mycelia were ground in liquid nitrogen and lysed in appropriate buffer (50 mM Tris (pH 7.2), 50 mM EDTA, 30 g/l SDS, 10 ml/l β-mercaptoethanol) at 65°C. Genomic DNA was extracted twice with phenol/chloroform (1:1 (v/v)) and subsequently precipitated with isopropanol and 50 mM sodium acetate (Kolar *et al.*, 1988). Genomic DNA was dissolved in RNAse A treated elution buffer (Qiagen, Hilden, Germany) and stored at 4°C.

Plasmid DNA from *E. coli* was purified using Qiagen Plasmid Midi or Mini Kit (Qiagen, Hilden, Germany) according to the manual. DNA gel extraction was performed using the QIAquick Gel Extraction Kit (Qiagen, Hilden, Germany).

Southern hybridization was performed according to standard protocols (Busch *et al.*, 2003) with nonradioactively labeled probes (Amersham Bioscience, Buckinghamshire, U.K.). For probe preparations, DNAs were amplified from genomic DNA by PCR using primers listed in Tab. 3 and Tab. 6.

Tab. 6: Primers used for amplification of Southern probes.

Probe	Primers
dbaA OE 5'-UTR	JG91/159
dbaG OE 5'-UTR	JG98/99
dbaA::*ctap* 3'-UTR	OZG493/495
Δ*dbaA* 3'-UTR	JG158/161
Δ*dbaA*/Δ*csnE* 5'-UTR	JG91/159
Δ*dbaI* 5'-UTR	JG19/20
Δ*dbaB* 5'-UTR	JG215/217
Δ*dbaC* 3'-UTR	JG236/238
Δ*dbaD* 3'-UTR	JG256/258
Δ*dbaE* 5'-UTR	JG221/223
Δ*dbaF* 5'-UTR	JG259/261
Δ*dbaG* 5'-UTR	JG98/99
Δ*dbaH* 5'-UTR	JG227/229
Δ*dbaB/dbaA* OE 3'-UTR	JG220/299
Δ*dbaC/dbaA* OE 5'-UTR	JG233/314
Δ*dbaD/dbaA* OE 3'-UTR	JG258/307
Δ*dbaE/dbaA* OE 5'UTR	JG221/308
Δ*dbaF/dbaA* OE 5'-UTR	JG259/310

Tab. 6 continued: Primers used for amplification of Southern probes.

Probe	Primers
Δ*dbaG/dbaA* OE 3'-UTR	JG208/344
Δ*dbaH/dbaA* OE 5'-UTR	JG227/312
sasA OE 5'-UTR	JG83/150
sasA::s*gfp* 3'-UTR	JG86/88
sasA::c*tap* 3'-UTR	JG86/88

2.3.6 Heterokaryon rescue

Heterokaryon rescue was performed according to the protocol by Osmani (Nayak *et al.*, 2006). First, conidiospores of primary transformants of a standard *Aspergillus nidulans* transformation were picked and plated on selective and non-selective medium. Second, primary transformants were excised together with agar, put on an agar plate with selective medium and grown 3 days at 30°C. A fresh agar piece was cut out, put in liquid selective medium and grown for 3 days at 30°C. Mycelia were harvested and genomic DNA extracted. Diagnostic PCR was performed.

2.4 RNA methods

2.4.1 RNA isolation and hybridization

Strains were cultivated vegetatively in liquid medium and after achieving developmental competence, on solid medium for different time periods under asexual and sexual inducing conditions. Mycelia were ground in liquid nitrogen and mixed with Trizol (Invitrogen GmbH, Karlsruhe, Germany) and chloroform. After centrifuging, the upper phase was extracted twice with phenol/chloroform (1:1 (v/v)). RNA was precipitated with isopropanol over night, dissolved in 0.1%-DEPC-treated water and stored at -20°C.

Northern hybridization was performed according to the protocol of Brown and Mackey (Brown *et al.*, 1997). The gel was loaded with 10-30 µg RNA. DNA for probes were amplified from genomic DNA with primers listed in Tab. 3 and Tab. 7. Probes were labeled with [α-^{32}P]-dATP using the Prime-It®-II kit (Stratagene Europe, Amsterdam, Netherlands) (Feinberg *et al.*, 1983). Autoradiographs were produced utilizing BioMaxMS films (Kodak Molecular Imaging, New Haven, CT, USA).

Tab. 7: Primers used for amplification of Northern probes.

Probe	Primers
AN7893	JG5/6
AN7894	JG173/174
AN7895	JG175/176
dbaA	JG3/4
dbaB	JG165/166
dbaC	JG190/191
dbaD	JG177/178
dbaE	JG179/180
dbaF	JG167/168
dbaG	JG100/101
dbaH	JG181/182
dbaI	JG1/2
AN7904	JG192/193
AN7905	JG194/195
AN7906	JG196/197
AN7907	JG198/199
AN7908	JG200/201
orsA	JG169/170
sasA	JG147/149
ipnA	OZG367/368
laeA	OZG61/62
aflR	OZG337/338
stcU	OZG339/340
gpdA	gpdA-5/gpdA-3
tdiA	tdiA-5/tdiA-3

2.4.2 Microarray data analysis

Microarray data were generated by Krystyna Nahlik (Nahlik *et al.*, 2010) and are deposited in NCBI's Gene Expression Omnibus (http://www.ncbi.nlm.nih.gov/geo/query/acc.cgi?token=pluhlwwaocgqmpa&acc=GSE22442). Briefly, purified RNA, extracted from 2 ml of ground fungal mycelium, was amplified using the Message Amp II kit (Ambion, Darmstadt, Germany) and 2 µg resulting aRNA was labelled with *N*-hydroxysuccinimide -activated Cy-3 or Cy-5 dyes (Amersham Bioscience). RNAs from two independent biological replicates were analyzed and four technical replicates were performed. The TIGR *A. nidulans* microarrays were provided by the National Institute of Allergy and Infectious Diseases (National Institutes of Health, USA). 'Contrasts' refer to $\log_2$ normalized intensity ratios between wild type and

Δ*csnE* samples. Genes with $\log_2$ ratios of ≥ 3.0 and adjusted p-values of ≤ 0.01 were regarded as significantly regulated and genes with $\log_2$ ratios of ≥ 2 and adjusted p-values of ≤ 0.01 were regarded as moderately regulated.

2.5 Protein methods

2.5.1 Protein isolation and Western blot

For isolation of proteins, crude extracts from vegetative grown cultures were prepared by grinding mycelia and extracting proteins with B300 buffer (100 mM Tris-HCl, pH 7.5, 300 mM NaCl, 10% glycerol, 2 mM EDTA, pH 8) at 4°C with addition of Complete Protease Inhibitor Cocktail (Roche, Mannheim, Germany). After centrifugation, the supernatant was directly used for further analyses.

For Western experiments, the protein extracts were separated by polyacrylamide gel electrophoresis and transferred onto a nitrocellulose membrane by electroblotting. As first antibody Anti-Calmodulin Binding Protein Epitope Tag (Biomol, Hamburg, Germany) and as second antibody goat-anti-rabbit IgG HRP (MoBiTec, Göttingen, Germany) was used. PrestainedPageRuler (Fermentas GmbH, St. Leon-Rot, Germany) was utilized as marker. As detection reagent, the ECL technology (GE Healthcare Life Sciences, Munich, Germany) products were used.

2.5.2 Tandem Affinity Purification

TAP experiments were performed as described previously (Bayram *et al.*, 2008). Vegetative cultures were grown over night at 30°C in liquid medium and the mycelia was shifted to solid minimal medium with 0.1% casein hydrolysate and grown under asexual or sexual inducing conditions. The cells were washed, ground in liquid nitrogen and added to appropriate buffer (100 mM Tris-HCl (pH 7.6), 250 mM NaCl, 10% glycerol, 0.05% NP-40, 1 mM EDTA, 2 mM DTT) supplemented with EDTA-free protease inhibitor mix (Roche GmbH, Mannheim, Germany), phosphatase inhibitors (Merck, Darmstadt, Germany) and specified protease inhibitors (http://depts.washington.edu/yeastrc/pages/ms_tap1.html). Crude extracts were centrifuged and the obtained protein extracts were incubated for 2 hours with 400 µl of IgG sepharose 6 Fast Flow (GE Healthcare Life Sciences, Munich, Germany) at 4°C. Hence, the NCCR standard protocol was followed (http://depts.washington.edu/yeastrc/pages/ms_tap1.html) beginning with step 14. For TEV cleavage, 350 U of AcTEV™

(InvitrogenGmbH, Karlsruhe, Germany) in the presence of 1 µM E-64 (Calbiochem Merck Biosciences Ltd., Nottingham, UK) was added and incubated over night at 4°C. The proteins were precipitated with trichloroacetic acid, separated on a 10% polyacrylamide gel and stained with Coomassie Brilliant Blue G (Sigma-Aldrich Chemie GmbH, Steinheim, Germany). Protein bands were cut out and submitted for mass spectrometry. In addition to this standard protocol, modified purifications were performed. For fixation of proteins, 28 ml/l formaldehyde was added after 20 hours of vegetative growth. After 20 min of incubation, 2.5 M glycine was added, and after 5 min cultures were harvested as described before. A second modification was to change buffer composition and concentration. Buffers were used without phosphatase inhibitors and instead of IPP300 the buffer IPP150 was used twice during washing steps. 4-8 µM S-adenosylmethionine was added to all buffers. In a shortened purification, directly after washing with IPP150, glycine buffer (0.1 M glycine, 150 mM NaCl, 0.1% Triton X-100, pH 2) was added. Proteins were eluted after 5 min of incubation and precipitated with trichloroacetic acid.

2.5.2.1 LC-MS/MS protein identification

Polyacrylamide gel pieces of stained protein bands were digested with trypsin according to Shevchenko *et al*. (Shevchenko *et al.*, 1996). Tryptic peptides were extracted and injected onto a reversed-phase liquid chromatographic column (Dionex-NAN75-15-03-C18 PM) by using the *ultimate* HPLC system (Dionex, Amsterdam, Netherlands) to further reduce sample complexity prior to mass analyses with an LCQ DecaXP mass spectrometer (Thermo Electron Corp, San Jose, CA) equipped with a nanoelectrospray ion source. Cycles of MS spectra with m/z ratios of peptides and four data-dependent MS2 spectra were recorded by mass spectrometry. The "peak list" was created with extracts provided by the Xcalibur software package (BioworksBrowser 3.1). The MS2 spectra with a total ion current higher than 10,000 were used to search for matches against a public *A. nidulans* genome-wide protein sequence database of the BROAD INSTITUTE (http://www.broad.mit.edu/annotation/genome/*Aspergillus*_nidulans/Home.html) (9542 sequences, December 2005, plus 180 sequences of the most commonly appearing contaminants, e.g. keratins and proteases, provided with the BioworksBrowser package) using the TurboSEQUEST algorithm (Eng *et al.*, 1994) of the Bioworks software (Version 3.1, Thermo Electron Corp.). The search parameters included based on the TurboSEQUEST algorithm were: (i) precursor ion mass tolerance less than 1.4 amu, (ii) fragment ion mass tolerance less than 1.0 amu, (iii) up to three missed tryptic cleavages allowed, and (iv) fixed cysteine modification by carboxyamidomethylation (plus

57.05 amu) and variable modification by methionine oxidation (plus 15.99 amu) and phosphorylation of serine, threonine, or thyrosine (plus 79.97 amu). In accordance with the criteria described by Link *et al.* (Link *et al.*, 1999) matched peptide sequences of identified proteins had to pass the following: (i) the cross-correlation scores (X_{corr}) of matches must be greater than 2.0, 2.5, and 3.0 for peptide ions of charge state 1, 2, and 3, respectively, (ii) ΔCn values of the best peptide matches must be at least 0.4, and (iii) the primary scores (Sp) must be at least 600. Protein identification required at least two different peptides matching these criteria. The degree of completeness of the b- and y-ion series for each SEQUEST result was manually checked for every protein identified. Peptides of identified proteins were individually blasted against the NCBI database (BLASTP at http://www.ncbi.nlm.nih.gov/BLAST/) to ensure their unambiguous assignment to the TurboSEQUEST-specified protein.

2.6 Microscopic analysis

Pictures of *A. nidulans* colonies and structures were taken with an Olympus SC30 digital camera (Olympus, Hamburg, Germany) used in combination with an Olympus SZX12 binocular. Olympus CellSens Dimension 1.4 software was used for editing pictures and the calibration of magnifications.

For fluorescence microscopy, *A. nidulans* strains (2000 spores) were inoculated in eight chambered borosilicate coverglass system (NUNC) supplemented with liquid medium or on glass slides covered with a thin layer of solid medium and incubated at 30°C. Fluorescence photographs were taken with an AXIOVERT OBSERVER. Z1 (ZEISS) microscope equipped with a QUANTEM: 512SC (PHOTOMETRICS) digital camera and the SLIDEBOOK 5.0 software package (INTELLIGENT IMAGING INNOVATIONS).

2.7 Chemical analysis

2.7.1 Sterigmatocystin analysis

For analysis of sterigmatocystin, plates were inoculated with 10^7 spores and grown 3 days at 37°C. An agarpiece (Ø = 1.5 cm) was homogenized in 3 ml water and subsequently extracted with an equivalent volume of chloroform. The organic phase was evaporated and the residual metabolites were dissolved in 50 µl methanol. 15 µl of the extract was separated on TLC in acetone/chloroform 4:1 (v/v) and derivatized with an alcoholic aluminum chloride solution (20% (w/v)). Metabolites were visualized under λ = 366 nm. As standard, sterigmatocystin

(Sigma-AldrichChemie GmbH, Steinheim, Germany) was used. The data were documented using CAMAG TLC Visualizer (CAMAG, Muttenz, Switzerland).

2.7.2 Analysis of DHMBA and DHPDI

2.7.2.1 General experimental procedures

^{1}H-NMR spectra were recorded on a *Varian* Mercury-Vx 300 (300 MHz) or a *Varian* VNMRS-300 (300 MHz) spectrometer, respectively. ^{13}C-NMR spectra were recorded on a *Varian* Inova-500 spectrometer (125.7 MHz). ESI-MS data were acquired using a *Finnigan* LC-Q mass spectrometer. HPLC was performed using a system by Instrumentelle Analytik Goebel GmbH (analytical HPLC: HPLC pump 420, autosampler SA 360, HPLC detector Celeno DAD UV, evaporative light scattering detector ELSD-Sedex 85, ERC, column Nucleodur 100-5 C18 ec, 250 mm x 3 mm, solvent system: A = H_2O + 0.1% TFA, B = acetonitrile + 0.1% TFA. Preparative HPLC: HPLC pump RAININ Dynamax SD-1, HPLC detector RAININ Dynamyx UV-1, column Nucleodur 100-5 C18 ec, 250 mm x 20 mm, solvent system: A = H_2O, B = acetonitrile).

2.7.2.2 Cultivation

For analysis of secondary metabolites, 1 l liquid minimal medium with nitrate or ammonium as nitrogen source was inoculated with 10^9 spores and grown at 37°C for 36 hours.

2.7.2.3 Extraction

Mycelia of cultures were removed by filtering with Miracloth and pH of the culture filtrate was adjusted to 5 by adding NaOH or HCl. The culture filtrate was extracted twice with an equivalent amount of ethyl acetate. The combined extracts were dried to yield the crude extract.

2.7.2.4 Analysis in HPLC/UV-DAD

The crude extracts were dissolved in 2 ml methanol and analyzed in HPLC using an analytical column (Nucleodur 100-5 C18 ec, 250 mm x 3 mm) under gradient conditions (20% B to 100% B in 20 minutes).

2.7.2.5 Isolation and chemical characterization of DHMBA

The crude extract of 2 l cultures of strain AGB527 (grown in inducing medium) was extracted with CH_2Cl_2. The resulting extract was concentrated and chromatographed by preparative HPLC under gradient conditions (20% B to 100% B in 20 minutes, flowrate: 14 ml/min). Detection was carried out at 230 nm. DHMBA (3.9 mg) was eluted at 14.4 min.
2,4-Dihydroxy-3-methyl-6-(2-oxopropyl)benzaldehyde (DHMBA): light yellow solid, ESI-MS: m/z (%) 231 $[M + Na]^+$, 207 $[M - H]^-$. ^{1}H-NMR (300 MHz, CD_2Cl_2): δ = 2.06 (s, 3H, 2'-H), 2.22 (s, 3H, 5'-H), 3.89 (s, 2H, 3'-H), 6.21 (s, 1H, 5-H), 9.85 (s, 1H, 1'-H), 12.64 (s, 1H, 2-OH). ^{13}C-NMR (125.7 MHz, CD_2Cl_2): δ = 6.98 (C-2'), 29.53 (C-5'), 46,78 (C-3'), 110.71 (C-3), 110.76 (C-5), 112.82 (C-1), 136.88 (C-6), 161.36 (C-4), 164.35 (C-2), 192.53 (C-1'), 205.15 (C-4'). UV λ_{max} (acetonitrile/H_2O/formic acid)/nm: 221, 296. NMR data are in good agreement with reported data (Suzuki *et al.*, 2001).

2.7.2.6 Isolation and chemical characterization of DHPDI

The crude extract of 7 l cultures of strain TNO (grown in inducing medium) was extracted with CH_2Cl_2. The resulting extract was concentrated and fractionated by preparative HPLC under gradient conditions (20% B to 100% B in 20 minutes, flowrate: 14 ml/min). Detection was carried out at 230 nm. The fraction eluted at 12.0 min was further chromatographed on a Sephadex column using methanol as solvent and yielded in 1.4 mg of compound DHPDI.
3,3-(2,3-Dihydroxypropyl)diindole (DHPDI): white solid, ESI-MS: m/z (%) 329 $[M + Na]^+$, 305 $[M - H]^-$. ^{1}H-NMR (300 MHz, CD_2Cl_2): δ = 3.55 (m, 2H, 2'-H), 4.47 (m, 1H, 5'-H), 4.70 (d, 1H, 3'-H), 6.90 (m, 2H, 5-H), 7.0 (m, 2H, 5-H), 7.15 (s, 1H, 1'-H), 7.30 (dd, 2H, 2-OH), 7.32 (s, 1H, 1'-H), 7.55 (dd, 2H, 2-OH). UV λ_{max} (acetonitrile/H_2O/formic acid)/nm: 229, 279. MS, NMR and UV data were consistent with the reported data (Porter *et al.*, 1977, Schröder, 2001).

2.7.3 Bioactivity tests

A potential antibiotic or antifungal activity of the isolated metabolites DHMBA and DHPDI was tested by agardiffusion tests. 25 µl of a methanolic solution of the substances (c = 1 mg/ml) was added on sterile filter discs (Ø = 9 mm) and put on agar plates inoculated with *Escherichia coli*, *Bacillus subtilis*, *Micrococcus luteus*, *Staphylococcus aureus*, *Salmonella enterica serovar typhimurium*, *Aspergillus fumigatus*, *Aspergillus nidulans*,

Verticillium longisporum, *Neurospora crassa* and *Sordaria macrospora*. Inhibition zones were measured after 1 to 5 days at 37°C or 25°C, respectively.

2.7.4 Metabolic fingerprinting by UPLC TOF-MS

For metabolic fingerprinting 10^9 spores of the wild type and the mutant strains (Δ*dbaI*, Δ*csnE*, Δ*csnE*/Δ*dbaI*) were inoculated in 1 l liquid minimal medium (with ammonium as N-source) in P-flasks and grown 10 days in dark. The culture filtrates (pH 5) were extracted twice with ethyl acetate. Two biological replicates of each sample were analyzed three times by Ultra Performance Liquid Chromatography (UPLC, ACQUITY UPLCTM System, Waters Corporation, Milford, USA) coupled with an photo diode array detector (UPLC eLambda 800 nm, Waters Corporation, Milford, USA) and with an orthogonal time-of-flight mass spectrometer (TOF-MS, LCT Premier™, Waters Corporation, Milford). For LC an ACQUITY UPLC™ BEH SHIELD RP18 column (1 x 100 mm, 1.7 µm particle size, Waters Corporation, Milford, USA) was used at a temperature of 40°C, a flow rate of 0.2 ml/min and with the following gradient for the analysis of the polar phase: 0-0.5 min 0% B, 0.5-3 min from 0% B to 20% B, 3-6 min from 20% B to 99% B, 6-9.5 min 99% B and 9.5-13 min 40% B (solvent system A: water/methanol/acetonitrile/formic acid (90:5:5:0.1 (v/v/v/v)); B: acetonitrile/formic acid (100:0.1 (v/v)). The TOF-MS was operated in negative as well as positive electrospray ionization (ESI) mode in W optics and with a mass resolution larger than 10,000. Data were acquired by MassLynx™ software (Waters Corporation, Milford, USA) in centroided format over a mass range of m/z 50-1200 with scan duration of 0.5 sec. and an interscan delay of 0.1 sec. The capillary and the cone voltage were maintained at 2,700 V and 30 V and the desolvation and source temperature at 250°C and 80°C, respectively. Nitrogen was used as cone (30 l/h) and desolvation gas (600 l/h). The Dynamic Range Enhancement (DRE) mode was used for data recording. All analyses were monitored by using Leucine-enkephaline ($[M+H]^+$ 556.2771 or $[M+H]^-$ 554.2615 as well as its ^{13}C-isotopomer $[M+H]^+$ 557.2803 or $[M+H]^-$ 555.2615, Sigma-Aldrich, Deisenheim, Germany) as lock spray reference compound at a concentration of 0.5 µg/ml in acetonitrile/water (50:50 (v/v)) and a flow rate of 30 µl/min. The raw mass spectrometry data of all samples were processed by the MarkerLynx™ Application Manager for MassLynx™ software (Waters Corporation, Milford, USA). The toolbox MarVis (http://marvis.gobics.de) was used for ranking, filtering, adduct correcting and combining the data as well as for clustering and visualization, respectively (Kaever *et al.*, 2009, Meinicke *et al.*, 2008). An ANOVA test was applied to extract a subset of high-quality marker candidates with a p-value < $1x10^{-6}$. The filtered data sets were adduct

corrected according to the following rules ($[M+H]^+$, $[M+Na]^+$, $[M+NH_4]^+$ for the positive and $[M-H]^-$, $[M+CH_2O_2-H]^-$, $[M+CH_2O_2+Na-2H]^-$ for the negative ionization mode). The combined data led to an overall data set with 895 marker candidates, which were used for clustering and visualization by means of a one-dimensional self-organizing-map (1D-SOM) model and for data base search within a mass window of 5 mDa (In-house-data base; KNApSAcK, http://kanaya.naist.jp/KNApSAcK/; Metacyc, http://metacyc.org; LIPID MAPS, http://www.lipidmaps.org; KEGG http://www.genome.jp/kegg/ligand.html). The identity of DHMBA, and orsellinic acid were confirmed by comparison of exact mass, retention time and UV/VIS spectra with authentic standards.

To identify metabolites specifically secreted by *dbaA* OE strain, the medium polar fractions (pre-separated by preparative HPLC) of ethyl acetate extracts of wild type and *dbaA* OE culture filtrates were also analyzed and compared by the metabolite fingerprinting approach. The UPLC ESI TOF-MS analysis was done as described above with the exception of the use of ACQUITY UPLC™ HSS T3 column (1 x 100 mm, 1.7 µm particle size, Waters Corporation, Milford, USA) for LC separation of more polar compounds with the following solvent gradient: 0-0.5 min 1% B, 0.5-3 min from 1% B to 20% B, 3-8 min from 20% B to 95% B, 8-10 min 95% B and 10-14 min 1% B (solvent system A: water/formic acid (100:0.1 (v/v)); B: acetonitrile/formic acid (100:0.1 (v/v)).

The raw mass spectrometry data of all samples were processed within a retention time range from 2.5 to 6 min using the MarkerLynx™ Application Manager. After filtering by Kruskal-Wallis test and adduct correction the data sets from the positive and the negative ionization mode were combined. Clustering and visualization of the resulting data set by the MarVis tool enabled us to detect 21 metabolite marker specifically secreted by Δ*dbaA* OE strain. Exact mass, retention time and UV/VIS maxima of these compounds are shown in Tab. 10.

3 Results

3.1 Activation of a silent PKS gene cluster in *A. nidulans*

3.1.1 The *A. nidulans* Δ*csnE* is impaired in secondary metabolism

Deletion of the fifth subunit *csnE* of the CSN complex in *A. nidulans* results in a viable mutant, which is blocked in sexual reproduction cycle at the early stage of primordia formation, but produces excessive amounts of nests and Hülle cells in the light (Busch *et al.*, 2003). The mutant is temperature- and oxidative stress-sensitive and secondary metabolism is impaired, visible by the accumulation of colored pigments in the growth medium (Fig. 12). Several of these pigments could be identified as orcinol (**12**, Fig. 5) and related phenylethers diorcionol (**13**, Fig. 5), cordyol C (**14**, Fig. 5), and violaceol I and II (**15**, **16**, Fig. 5) (Nahlik *et al.*, 2010).

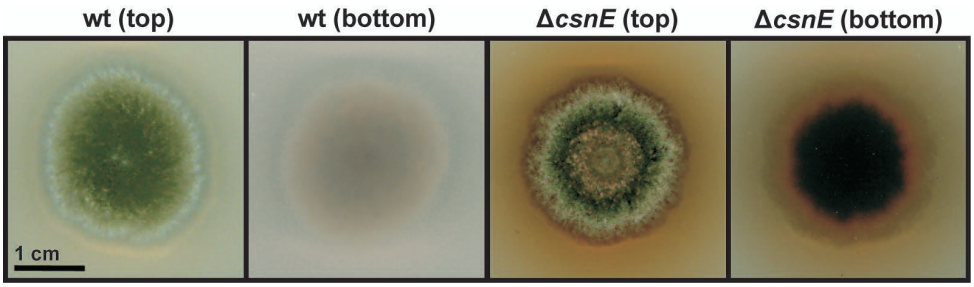

Fig. 12: Phenotype of Δ*csnE* and wild type after 3 days of asexual growth at 37°C. Pictures were taken from the top and the bottom of agar plates. Δ*csnE* accumulates pigments around colony margins.

We analyzed the influence of the *csnE* deletion on the well-studied sterigmatocystin (ST) gene cluster, which is under control of the specific transcription factor AflR and the general regulator of secondary metabolism LaeA. By Northern experiments, we determined the expression of *laeA*, *aflR*, and the oxidoreductase *stcU* (involved in oxidation of versicolorin A to demethylsterigmatocystin) in Δ*csnE* compared to wild type levels. Our results showed that expressions of *aflR* and *stcU* in Δ*csnE* are upregulated during early asexual stages in comparison to wild type, whereas *laeA* levels were unaffected (Fig. 13A).

In addition to Northern analysis, we performed TLC analysis for ST to check if also the production of the end product of the gene cluster has changed. ST production was determined after 2, 3, 4, and 5 days of asexual and sexual growth. Our results showed, that for all stages

of development the ST production was diminished in Δ*csnE* compared to wild type (Fig. 13B and C). This effect was most significant after 4 and 5 days of growth.

Additional microarray experiments and untargeted metabolite fingerprinting analysis verified these results and led to the hypothesis that intermediates of the ST pathway accumulate in Δ*csnE*, but production and secretion of ST was defective (Nahlik *et al.*, 2010).

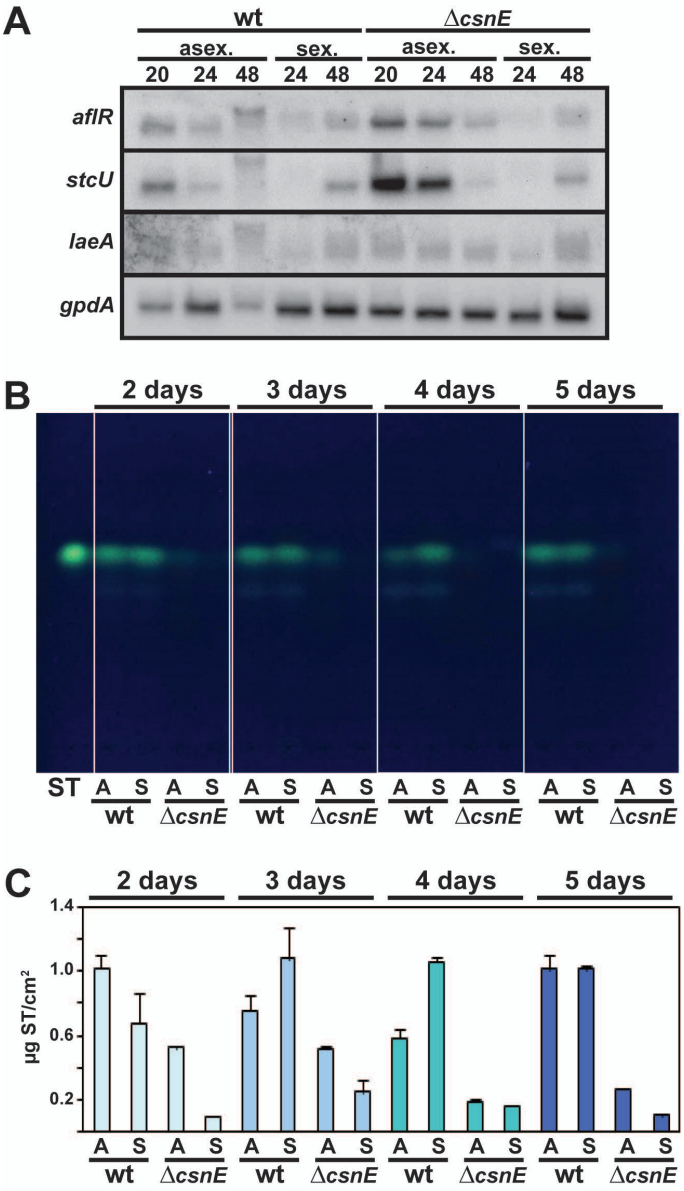

Fig. 13: The Δ*csnE* strain is impaired in ST biosynthesis. **A:** Northern hybridization of *aflR*, *stcU*, and *laeA* in Δ*csnE* and wild type. RNA was extracted after 20, 24, 48 hours of asexual and sexual development. Expression of *gpdA* is shown as equal loading control. **B:** ST analysis of wild type and Δ*csnE* after 2, 3, 4, and 5 days of asexual (A) and sexual (S) growth. Metabolite extracts were separated by thin layer chromatography (TLC) in acetone/chloroform 4:1 (v/v). ST was used as standard. **C:** Quantification of TLC results. The amount of secreted ST was determined per cm^2.

3.1.2 The *A. nidulans* Δ*csnE* activates a silent biosynthetic gene cluster comprising a polyketide synthase (PKS) gene

The fact that Δ*csnE* is impaired in secondary metabolism led to the assumption that interruption of the protein degradation machinery can lead to increased stabilization of regulators, including transcriptional activators for biosynthetic gene clusters.

For ascertainment, if the protein degradation impaired *A. nidulans* mutant Δ*csnE* bares new, unidentified secondary metabolites, we performed a genome-wide transcriptional profiling of Δ*csnE* during development (Nahlik *et al.*, 2010). The analysis revealed a putative gene cluster, comprising a yet unidentified PKS gene that was upregulated in the Δ*csnE* strain, but silenced in wild type (Tab. 8). The genes are upregulated in comparison to wild type at least at one developmental stage. The putative cluster was designated *dba* (derivative of benzaldehyde), referring to the identified PKS gene product described below (chapter 3.1.4). The putative gene cluster spans in total twelve genes, four of which encode putative oxygenases AN7893, *dbaB* (AN7897), *dbaF* (AN7900), and *dbaH* (AN7902). AN7895 encodes a putative alcohol dehydrogenase, *dbaE* (AN7899) encodes an esterase, *dbaD* (AN7898) encodes a putative MFS transporter and AN7894 and *dbaC* (AN11584) encode proteins with YCII domains of which the function is still unknown, but which are suggested to play a role in transcription initiation. Additionally, two putative transcription factor (TF) encoding genes are present, *dbaA* with a $Zn(II)_2Cys_6$-domain typical for fungal TFs, and *dbaG*, which encodes a protein showing significant similarities to other putative fungal TFs (*Nectria haematococca* (Gene ID: 9674136, 60% positives), *Neosartorya fischeri* (Gene ID: 4594276, 53% positives), *Aspergillus fumigatus* (Gene ID: 3503817, 61% positives)). Finally, the cluster encodes the PKS DbaI (AN7903). Besides this new PKS gene cluster, also the orsellinic acid gene cluster (*orsA*-*orsE*, AN7909-7914), which is located adjacent to our cluster, was partially upregulated in Δ*csnE* (Tab. 8).

For verification of the microarray results, the expression of three randomly selected genes of the new putative PKS gene cluster was analyzed by Northern hybridization (Fig. 14). The expression of the putative oxygenase gene AN7893, the putative TF gene *dbaA*, and the putative PKS gene *dbaI* were compared to wild type levels during vegetative growth or under conditions favoring in wild type asexual or sexual development. mRNA levels of all three genes of the putative gene cluster were substantially increased in the Δ*csnE* mutant during development which confirmed the initial microarray data (Tab. 8). This suggests that CSN is required for repression of this gene cluster in wild type *A. nidulans* cells.

Tab. 8: Transcriptional expression of genes in Δ*csnE* compared to wild type at different developmental stages (V = vegetative, A = asexual, S = sexual, 14 = 14 hours, 20 = 20 hours, 48 = 48 hours). Genes with $\log_2$ ratios ≥ 3.2 and adjusted p-values ≤ 0.01 were regarded as significantly regulated and genes with $\log_2$ ratios ≥ 2 and adjusted p-values ≤ 0.01 were regarded as moderately regulated. ↑ Significantly upregulated, ↗ moderately upregulated, ↘ moderately downregulated, 0 not regulated. Red frame: Putative new biosynthetic gene cluster.

Gene	$\log_2$ contrast wt - Δ*csnE*				Regulation			
	V14	V20	A48	S48	V14	V20	A48	S48
AN7892	0.58	2.37	-1.05	0.98	0	↘	0	0
AN7893	-3.85	-6.70	-4.50	-4.25	↑	↑	↑	↑
AN7894	-3.10	-6.45	-4.10	-4.30	↗	↑	↑	↑
AN7895	-2.90	-4.95	-4.00	-4.40	↗	↑	↑	↑
dbaA	-3.35	-3.50	-3.05	-3.35	↑	↑	↗	↑
dbaB	-2.80	-5.90	-3.20	-3.40	↗	↑	↑	↑
dbaC	-3.25	-6.00	-3.50	-4.10	↑	↑	↑	↑
dbaD	-3.15	-4.05	-2.05	-1.25	↗	↑	↗	0
dbaE	-3.45	-6.00	-1.65	-2.10	↑	↑	0	↗
dbaF	-5.35	-3.85	-1.65	-2.95	↑	↑	0	↗
dbaG	-3.00	-2.40	-1.30	-1.15	↗	↗	0	0
dbaH	-3.50	-7.00	-4.10	-4.50	↑	↑	↑	↑
dbaI	-2.84	-1.64	-0.07	-0.76	↗	0	0	0
AN7904	-0.26	0.48	0.40	0.77	0	0	0	0
AN7905	0.10	0.44	-0.72	-0.83	0	0	0	0
AN7906	-0.18	-0.09	0.25	-0.31	0	0	0	0
AN7907	0.54	0.80	1.97	1.27	0	0	0	0
AN7908	-0.12	-0.11	-1.52	-2.06	0	0	0	↗
orsA	0.00	-0.09	-0.36	-0.45	0	0	0	0
orsB	-0.71	0.45	-2.77	-2.65	0	0	↗	↗
orsC	-0.58	1.40	-2.34	-2.59	0	0	↗	↗
orsD	-0.74	1.22	-1.78	-1.79	0	0	0	0
orsE	-0.66	3.89	-2.21	-2.61	0	↑	↗	↗
AN7915	-0.07	1.27	0.34	0.61	0	0	0	0

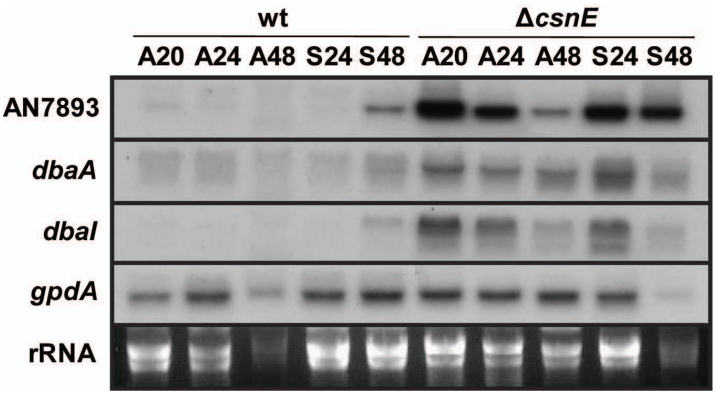

Fig. 14: Northern hybridization of three genes of the putative gene cluster. Samples were taken after 20, 24, and 48 hours of asexual growth (A20, A24, A48) and after 24 and 48 hours of sexual growth (S24, S48). Expression of *gpdA* was used as internal control. Expression of AN7893, *dbaA*, and *dbaI* are upregulated in Δ*csnE* compared to wild type.

3.1.3 Northern hybridization determines the borders of the *dba* gene cluster

Numerous gene clusters carry a specific transcriptional activator gene which is embedded within the cluster and regulates expression of the whole gene cluster (see chapter 1.2.1.1) (Bok *et al.*, 2006b). To determine the boundaries of the novel gene cluster and to discriminate the effect on secondary metabolism, we designed strains overexpressing the putative TF encoding genes *dbaA* (*dbaA* OE) or *dbaG* (*dbaG* OE), respectively, under the control of the inducible nitrate promoter, which can be activated by nitrate and repressed by ammonium containing medium (Fig. 15).

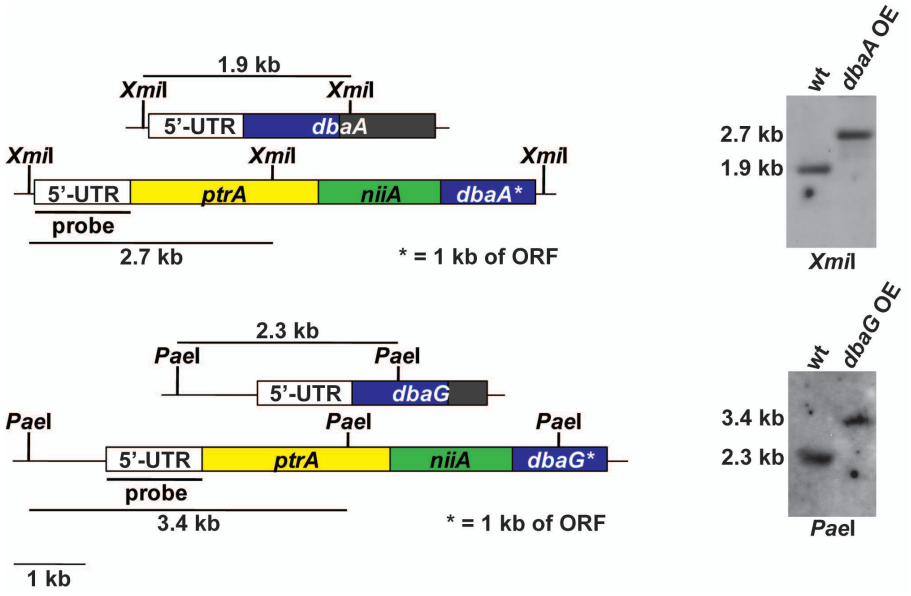

Fig. 15: Restriction maps and Southern hybridization of *dbaA* and *dbaG* overexpressing strains under the inducible nitrate promoter *niiA*.

Overexpression of *dbaG* led to no significant changes in phenotype, whereas overexpression of *dbaA* caused a strong production of pigments released to the growth medium (Fig. 16A). Additionally, the strain was reduced in colony diameter and conidiation. Interestingly, the pigmentation depends on pH and is reversible: in neutral and basic milieu the medium was yellow, while at pH < 3 the medium turned colorless (Fig. 16B).

We performed Northern hybridization experiments with the wild type and *dbaA* OE and *dbaG* OE strains (Fig. 16C). All genes starting from AN7893 to AN7909 (*orsA*) were used as probes, where we compared the promoter repressing and inducing conditions for the corresponding transcription factor. The *dbaG* overexpressing strain exhibited only increased expression of the putative oxidoreductase *dbaF*, whereas the expression of genes AN7893, *dbaC*, and *dbaD* were even decreased.

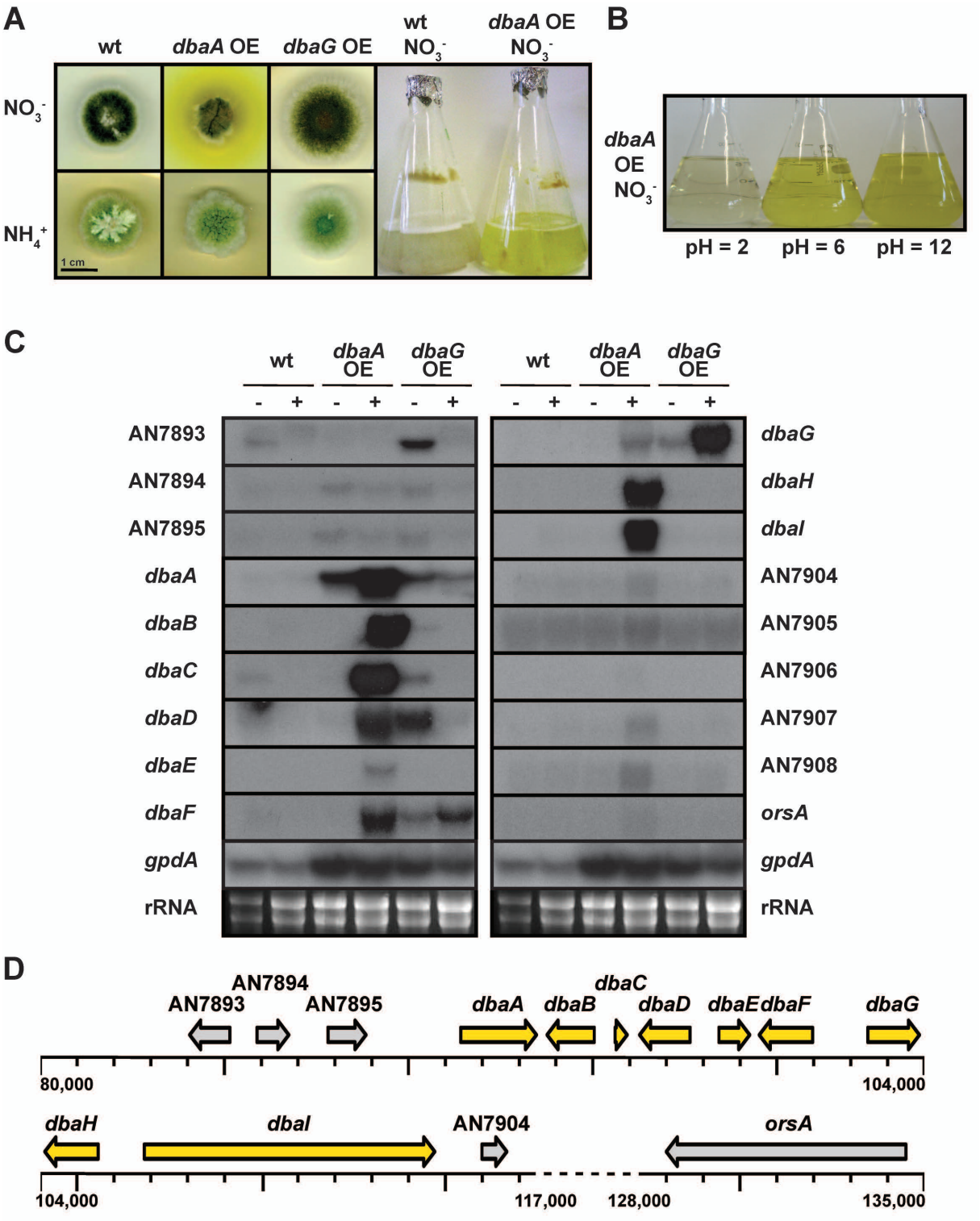

Fig. 16: Boundaries of *dba* gene cluster. **A:** Phenotypes of transcription factor *dbaA* and *dbaG* overexpressing strains. All strains were grown in inducing nitrate (NO_3^-) and repressing ammonium medium (NH_4^+). **B:** Reversible pH dependency of yellow metabolites produced in *dbaA* OE strain grown in inducing nitrate medium. **C:** Northern hybridization of genes AN7893 to *orsA* (AN7909) defines boundaries of *dba* gene cluster. Strains were grown in inducing nitrate (+) and repressing ammonium medium (-). Expression of *gpdA* was used as internal control. **D:** Scheme of *dba* gene cluster. Gene cluster starts with transcription factor *dbaA* (AN7896) and ends with PKS *dbaI* (AN7903). It is located on chromosome II neighbored to the orsellinic acid gene cluster.

In contrast, overexpression of *dbaA* coordinately upregulated all consecutive genes from AN7897 (*dbaB*) to the PKS encoding AN7903 (*dbaI*, Fig. 16C). Northern results indicate that these genes form a cluster which is controlled by the fungal $Zn(II)_2Cys_6$ transcription factor DbaA, encoded by the most 5'-upstream located gene (AN7896), and ends with the PKS encoding *dbaI* (An7903, Fig. 16D). The TF DbaA also controls expression of the second putative transcription factor gene *dbaG* (AN7901), suggesting a complex transcriptional control of the entire *dba* gene cluster. All encoded proteins of the cluster are summarized in Tab. 9.

Tab. 9: Encoded proteins of the *dba* gene cluster and their proposed functions.

Protein name	Accession no.	Proposed function	Predicted length
DbaA	AN7896	$Zn(II)_2Cys_6$ transcription factor	595 aa
DbaB	AN7897	FAD-binding monooxygenase	393 aa
DbaC	AN11584	protein with YCII domain	109 aa
DbaD	AN7898	general substrate transporter (major facilitator superfamily, MFS)	456 aa
DbaE	AN7899	esterase/lipase	278 aa
DbaF	AN7900	FAD-dependent oxidoreductase	476 aa
DbaG	AN7901	fungal transcription factor (no conserved domain)	421 aa
DbaH	AN7902	FAD-binding monooxygenase	462 aa
DbaI	AN7903	polyketide synthase	2605 aa

3.1.4 The *dba* gene cluster of *A. nidulans* synthesizes DHMBA (2,4-dihydroxy-3-methyl-6-(2-oxopropyl)benzaldehyde) as PKS product

In order to identify the secondary metabolites produced by the *dba* gene cluster, wild type and *dbaA* overexpressing (*dbaA* OE) strain were compared after cultivation in promoter inducing medium. Culture filtrates were extracted with ethyl acetate and subsequently analyzed by High Performance Liquid Chromatography coupled with an UV diode-array detector (HPLC-UV-DAD). The analysis revealed a major peak at 10.3 min retention time for *dbaA* OE and a peak at 10.6 min retention time in wild type strain (Fig. 17A). Although retention times of the two metabolites were rather similar, they showed differences in UV spectra. The wild type substance revealed absorption maxima at 231 and 276 nm, whereas the substance specific for *dbaA* OE showed absorption maxima at 221 and 296 nm. The structures of the two compounds were determined by nuclear magnetic resonance (NMR) spectroscopy and MS analysis after cultivating both strains in larger amounts and applying different chromatographic methods.

The first compound, isolated from the *dbaA* overexpressing strain, was identified as 2,4-dihydroxy-3-methyl-6-(2-oxopropyl)benzaldehyde (DHMBA, **19**, Fig. 17B). This substance was first isolated as side product from the New Zealand fungus *Sepedonium chrysospermum* in 2006 (Mitova *et al.*, 2006), but to our knowledge has not been discovered in an *Aspergillus* species so far. Until 2006, it had been only known as intermediate in the synthesis of azaphilones (Suzuki *et al.*, 2001).

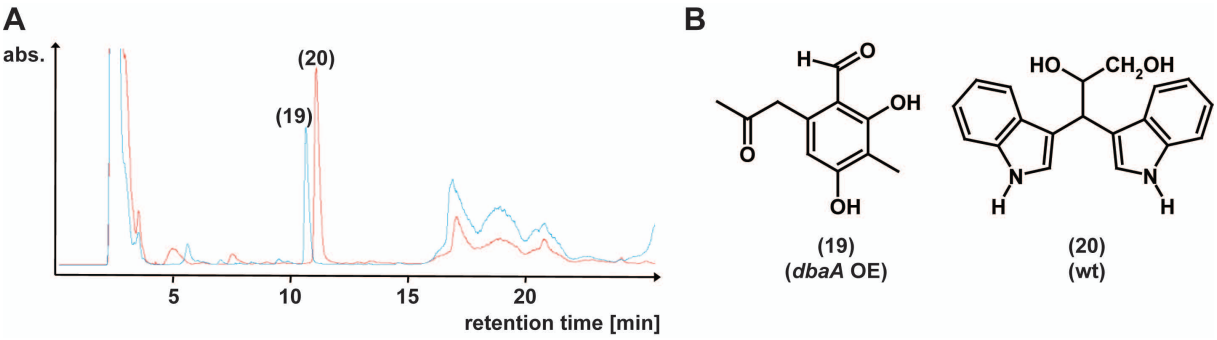

Fig. 17: Identification of *dba* gene cluster product. **A:** HPLC-UV-DAD chromatogram of wild type (red) and *dbaA* OE strain (cyan). **B:** Chemical structures of 2,4-dihydroxy-3-methyl-6-(2-oxopropyl)benzaldehyde (DHMBA, **19**) and 3,3-(2,3-dihydroxypropyl)diindole (DHPDI, **20**).

The second compound, isolated from the wild type, was identified as 3,3-(2,3-dihydroxypropyl)diindole (DHPDI, **20**, Fig. 17B). First, this indole alkaloid had been detected in mutants of *Saccharomyces cerevisiae*, which were blocked in tryptophan biosynthesis and accumulated different indole derivatives (Lingens *et al.*, 1967). In 1977, DHPDI had been isolated from *Balansia epichloë*, a fungus that parasitizes pasture grasses and causes ergot-type syndromes in grazing cattle. Toxicity studies on chicken embryos resulted in high mortality rates and indicated a possible involvement in disease symptoms (Porter *et al.*, 1977). Later, DHPDI was isolated from *Oceanibulbus indolifex*, a North Sea alphaproteobacterium (Schröder, 2001, Wagner-Dobler *et al.*, 2004). Interestingly, stability of DHPDI was pH dependent. While in basic milieu the diindole was stable, at pH < 3 it converted to 2-oxo-3-indolyl-(3)-propan-1-ol, indole and unknown indole polymers (Lingens *et al.*, 1967), which presumably explains the lack of DHPDI in ammonium-containing medium (Fig. 18). After cultivation in ammonium medium, pH of cultures was around 2.4, while cultivation in nitrate medium resulted in a pH of 6.3.

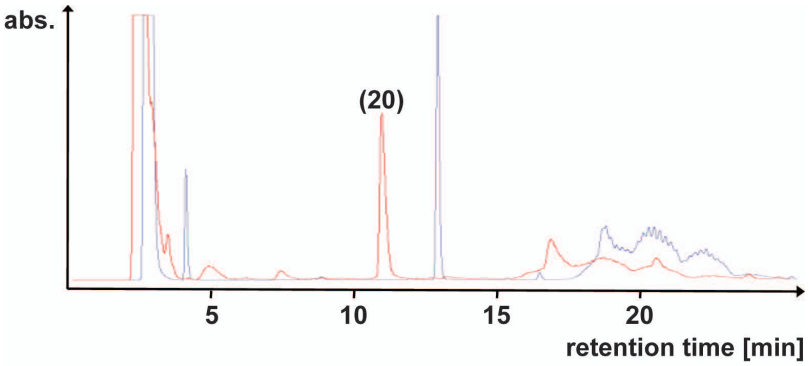

Fig. 18: HPLC-UV-DAD chromatogram overlay of ethyl acetate extracts of wild type grown in nitrate (red) and ammonium (blue) medium. DHPDI (**20**) is not produced by wild type cultivated in ammonium medium.

Besides the two major peaks, several minor peaks were present in the *dbaA* overexpressing strain in the HPLC-UV-DAD chromatogram (between 5 and 9 min retention time, Fig. 17). Some of these peaks showed UV/VIS maxima above 350 nm indicating that these compounds might contribute to the yellow color visible in the growth medium. Analysis by UPLC-TOF-MS revealed the exact masses of 21 compounds, which were produced in higher amounts in the *dbaA* OE strain than in wild type, 7 of them with UV maxima above 350 nm (Tab. 10). Due to minimal amounts of these metabolites, they could not be purified.

Tab. 10: UPLC-TOF-MS data for the 21 minor compounds of *dbaA* OE extracts.

Retention time [min]	Mass [Da]	UV maxima [nm]	Putative sum formula[3]
2.66	195.0545	197, 255	$C_9H_9NO_4$
2.72	182.0578	202, 289	$C_9H_{10}O_4$[4]
2.72	364.1173	202, 289	$C_{18}H_{20}O_8$
3.00	179.0585	-	$C_9H_9NO_3$[4]
3.03	205.0749	207, 265, 335	$C_{11}H_{11}NO_3$[4]
3.33	196.0730	-	$C_{10}H_{12}O_4$
3.41	224.0714	-	$C_{11}H_{12}O_5$
3.41	210.0898	194, 217, 358	$C_{11}H_{14}O_4$
3.66	194.0583	-	$C_{10}H_{10}O_4$
3.85	332.0900	197, 217, 290, 388	$C_{17}H_{16}O_7$[4]
4.10	540.1628	197, 229, 273	$C_{28}H_{28}O_{11}$
4.13	388.1163	218,275, 372	$C_{20}H_{20}O_8$[4]
4.16	346.1047	-	$C_{18}H_{18}O_7$
4.31	412.1159	-	$C_{22}H_{20}O_8$

[3] Sum formulas were derived from exact mass data (Elemental Composition tool for MassLynx™ software (Waters Corporation, Milford, USA)).

[4] Sum formulas could be confirmed by best fit to the isotopic pattern (Elemental Composition tool for MassLynx™ software (Waters Corporation, Milford, USA)).

Tab. 10 continued: UPLC-TOF-MS data for the 21 minor compounds of *dbaA* OE extracts.

Retention time [min]	Mass [Da]	UV maxima [nm]	Putative sum formula[3]
4.31	224.0688	217, 271, 304	$C_{11}H_{12}O_5$[4]
4.42	248.0681	202, 268, 302, 348	$C_{13}H_{12}O_5$[4]
4.43	344.0903	-	$C_{18}H_{16}O_7$
4.44	318.1112	-	$C_{17}H_{18}O_6$
4.60	208.0748	217, 387	$C_{11}H_{12}O_4$
4.70	224.0681	215, 250, 307, 378	$C_{11}H_{12}O_5$[4]
5.51	494.1519	221, 289, 362	$C_{27}H_{26}O_9$[4]

[3] Sum formulas were derived from exact mass data (Elemental Composition tool for MassLynx™ software (Waters Corporation, Milford, USA)).

[4] Sum formulas could be confirmed by best fit to the isotopic pattern (Elemental Composition tool for MassLynx™ software (Waters Corporation, Milford, USA)).

The *csnE* deletion strain showed reduced production of the well-studied metabolite sterigmatocystin (ST, Fig. 13A and B). Therefore, the influence of the *dbaA* and *dbaG* overexpressions on ST production was tested as well. Chloroform extracts of the two overexpression strains and the wild type strain grown on inducing nitrate medium were compared with thin layer chromatography (TLC, Fig. 19). All strains showed the same amount of ST and an interaction between the *dba* gene cluster and the ST gene cluster could be excluded.

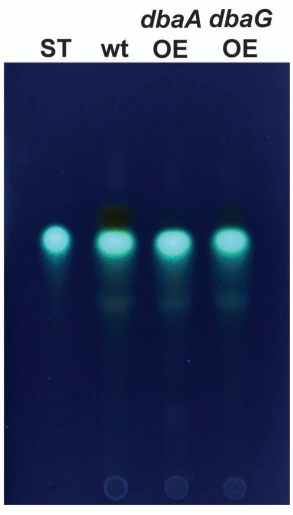

Fig. 19: Sterigmatocystin (ST) analysis of wild type, *dbaA* OE and *dbaG* OE strains. Metabolite extracts were separated by thin layer chromatography (TLC) in acetone/chloroform 4:1 (v/v). ST was used as standard.

3.1.5 DHMBA exhibits antibiotic activity in agar diffusion tests

DHMBA was only known as an intermediate in azaphilone synthesis (Suzuki *et al.*, 2001) and merely described as a side product in *S. chrysospermum* (Mitova *et al.*, 2006), while DHPDI was found to have toxic properties (Porter *et al.*, 1977). We analyzed the antibiotic activity of DHMBA and DHPDI. Agar diffusion tests with different Gram-positive and Gram-negative bacteria (*Escherichia coli*, *Bacillus subtilis*, *Micrococcus luteus*, *Staphylococcus aureus*, *Salmonella enterica serovar typhimurium*) as well as filamentous fungi (*Aspergillus fumigatus*, *Aspergillus nidulans*, *Verticillium longisporum*, *Neurospora crassa*, *Sordaria macrospora*) revealed no antibiotic activity for DHPDI. In contrast, DHMBA showed specifically antibacterial activity against the Gram-positive bacterium *Micrococcus luteus* with an inhibition zone of 2.5 cm diameter after 24 hours of growth (Fig. 20). This DHMBA mediated antibacterial activity, which might contribute to the survival of the fungus in the soil, supports our approach to use *csnE* mutant strains for exploring the secondary metabolism potential of filamentous fungi for bioactive compounds.

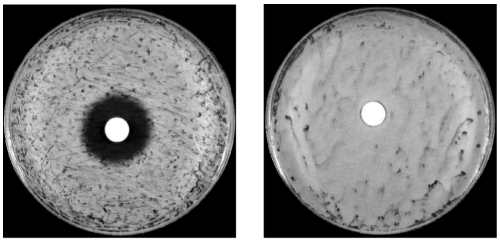

Fig. 20: Agar diffusion tests of DHMBA and DHPDI. 25 µl of DHMBA and DHPDI with a concentration of 1 mg/µl were spotted on filter discs. Agar plates were inoculated with *Micrococcus luteus* and grown for 24 hours at 37°C. The inhibition zone of DHMBA was 2.5 cm.

3.1.6 The *dba* gene cluster might be repressed by heterochromatin

Interestingly, the *dbaA* OE strain loses its ability for yellow pigment production after several generations, when the strain is grown on non-selecting medium. Also, the expression of *dbaA*, even under the inducible promoter, is gradually downregulated (Fig. 21A), indicating a heterochromatic effect on gene expression.

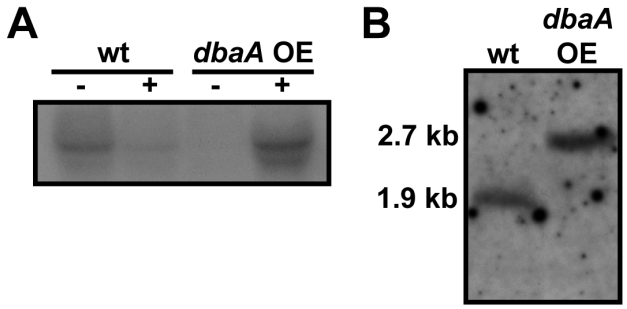

Fig. 21: Overexpression strain *dbaA* OE after several generations. **A:** Northern hybridization of wild type (wt) and *dbaA* OE strains. RNA was extracted from strains grown in inducing nitrate (+) and noninducing ammonium (-) medium for 24 hours. *dbaA* was used as probe. **B:** Southern hybridization of wt and *dbaA* OE strains.

We extracted genomic DNA from the colorless *dbaA* OE strain and performed Southern hybridization to verify correct integration of the overexpression cassette and to exclude contaminations. Southern hybridization showed the same bands as for the yellow *dbaA* OE strain (compare Fig. 15 and Fig. 21B), proving correct homologous integration and excluding contaminations with wild type. Taken together, these data suggest that a gradual heterochromatin spreading occurs in this part of the genome.

3.1.7 Deletion of the PKS gene *dbaI* in Δ*csnE* results in the loss of 184 metabolite marker candidates including DHMBA

For a comprehensive metabolite analysis of the *dba* gene cluster, we deleted the PKS encoding gene *dbaI* by replacement with a pyrithiamine marker containing deletion cassette via homologous recombination in wild type and Δ*csnE* background (Fig. 22). The lack of *pks* transcript was verified by Northern hybridization (Fig. 23A). As expected due to the silencing of the cluster, deletion of *dbaA* in wild type caused no phenotypical changes, but deletion in Δ*csnE* resulted in an alteration of Δ*csnE* specific pigments surrounding the colony margin (Fig. 23B). Introduction of the *csnE* genomic fragment restored the wild type and *dbaI* deletion phenotype, and ectopic introduction of a ^{p}*gpdA*::*dbaI* construct restored the *csnE* deletion phenotype.

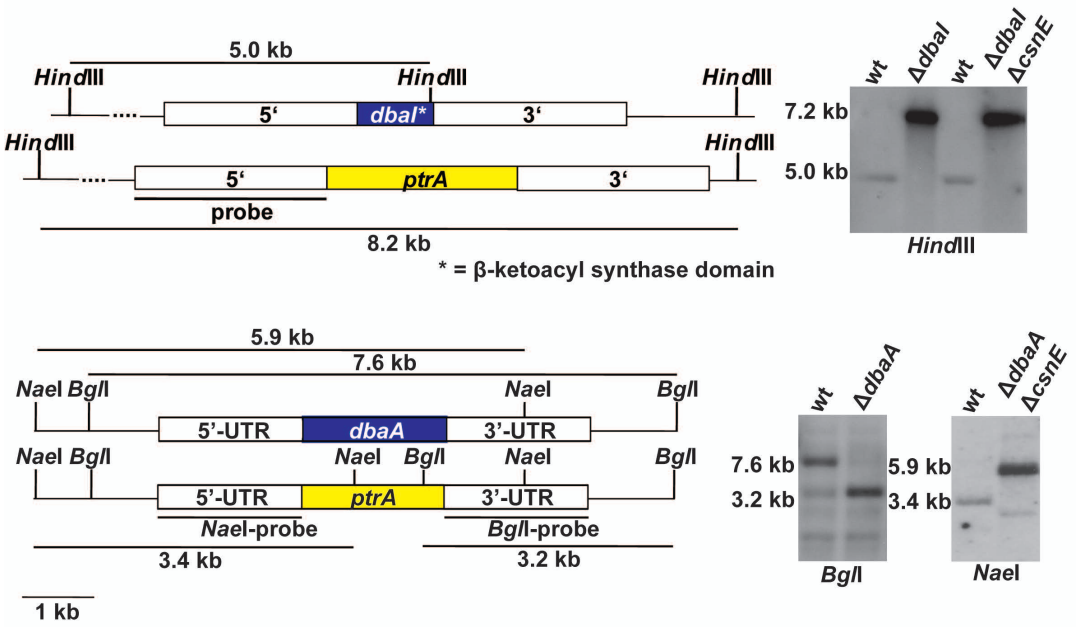

Fig. 22: Restriction maps and Southern hybridizations of *dbaI* and *dbaA* deletion strains.

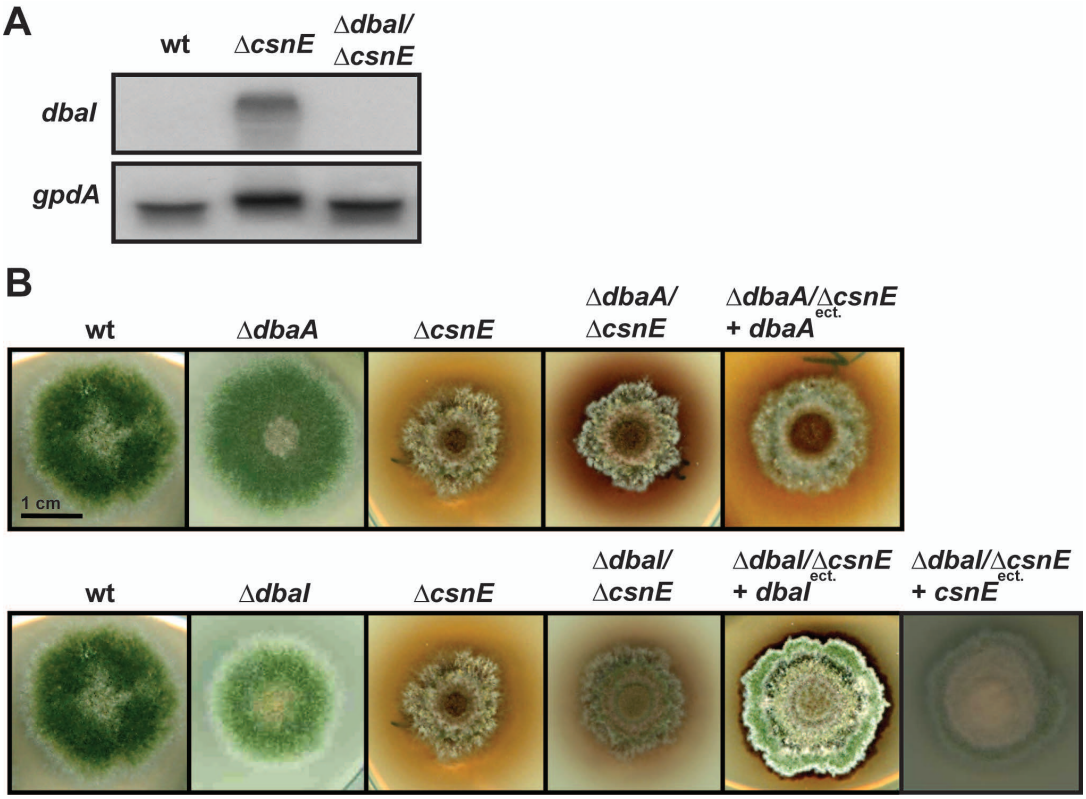

Fig. 23: Analysis of *dbaA* and *dbaI* deletion mutants. **A:** Northern hybridization of PKS deletion strain Δ*dbaI*/Δ*csnE*. Expression of *gpdA* was used as internal control. **B:** Phenotypes of TF *dbaA* and PKS *dbaI* gene deletions in wild type and Δ*csnE* background.

Metabolite production of the *A. nidulans* strain deficient in the COP9 signalosome was analyzed by a metabolite fingerprinting analysis. For that polar extracellular extracts of wild type, Δ*csnE*, Δ*dbaI*, and Δ*dbaI*/Δ*csnE* were analyzed by Ultra Performance Liquid Chromatography (UPLC) coupled with a time-of-flight mass spectrometer (TOF-MS). The intensity profiles of 895 marker candidates (p-value < $1x10^{-6}$) of the positive and negative ionization mode were clustered by training a one-dimensional self-organizing map model (Fig. 24A, 1D-SOMs) (Meinicke *et al.*, 2008) and grouped into 10 prototypes. Prototype 6 and 7 represent 184 marker candidates that are upregulated in Δ*csnE* but only when the PKS DbaI is present. Among them, DHMBA was detected in prototype 6 (Fig. 24B). Its production was enhanced in Δ*csnE* compared to wild type levels, but ceased when *dbaI* was deleted. Furthermore, the recently identified orsellinic acid (Schroeckh *et al.*, 2009) was detected in prototype 8 (Fig. 24B). As our microarray results suggested, its production was augmented in Δ*csnE* compared to wild type. In Δ*dbaI*/Δ*csnE* orsellinic acid production was diminished but not ceased, suggesting a crosstalk between the two PKSs DbaI and OrsA.

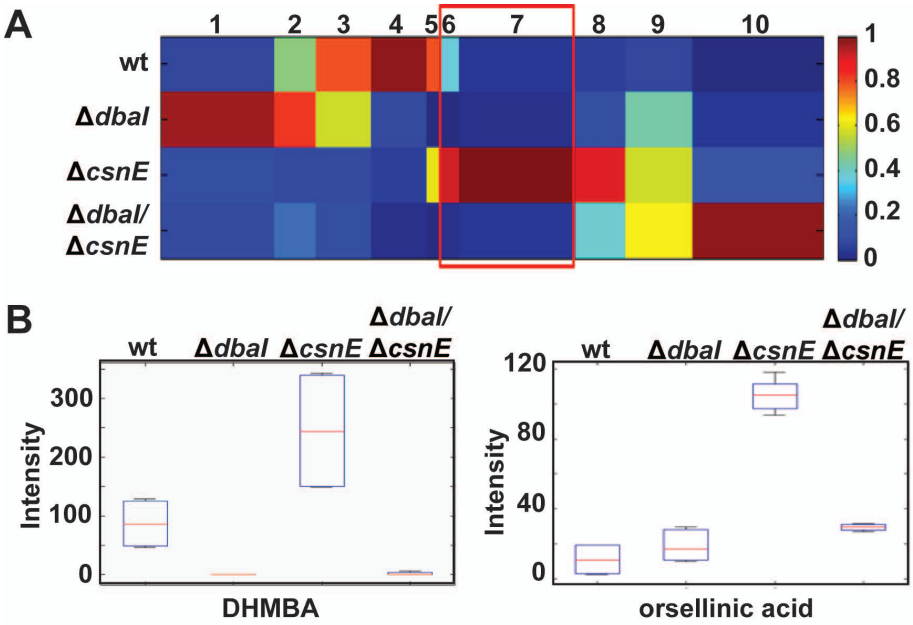

Fig. 24: Metabolic fingerprinting of *csnE* and *dbaI* deletion mutants. **A:** Clustering of the intensity profiles of 895 metabolite marker candidates of the ethyl acetate extraction phases of wild type, Δ*csnE*, Δ*dbaI*, and Δ*csnE*/Δ*dbaI* by 1D-SOM. The horizontal and vertical dimensions correspond to prototypes 1-10 and the analyzed fungal strains, respectively. Prototype 6 and 7 (red frame) represent metabolite markers, accumulating specifically in Δ*csnE*. Colors of matrix elements represent average intensity values. **B:** Box-Whisker plots show the relative abundance of 2,4-dihydroxy-3-methyl-6-(2-oxopropyl)benzaldehyde (DHMBA), which is detected in prototype 6, and of orsellinic acid, which is detected in prototype 8.

Furthermore, the influence of the TF DbaA on the *dba* gene cluster expression in Δ*csnE was* analyzed. Therefore, *dbaA* deletion strains were constructed in wild type and Δ*csnE* background similar to *dbaI* deletion strains (Fig. 22). Like the *dbaI* deletion, in wild type background no phenotypical changes were observed, while in Δ*csnE* background again a change of pigments was observed (Fig. 25A). For Δ*dbaA*/Δ*csnE*, the deletion phenotype was restored by ectopic integration of a *dbaA* genomic fragment.

We tested whether the deletion of *csnE* increases the amount of the TF DbaA. Therefore, a *tap*-(Tandem Affinity-Purification) tagged *dbaA* construct was designed and expressed in wild type and Δ*csnE* strains (Fig. 22). A Western blot experiment with an anti-calmodulin antibody, recognizing the calmodulin peptide of the TAP, showed the production of the tagged protein (Fig. 25B). A strong production was detectable in Δ*csnE* background but not in wild type background. Our results suggest that mRNA (Tab. 8) as well as protein levels (Fig. **25**) of the TF DbaA accumulate in the absence of CsnE.

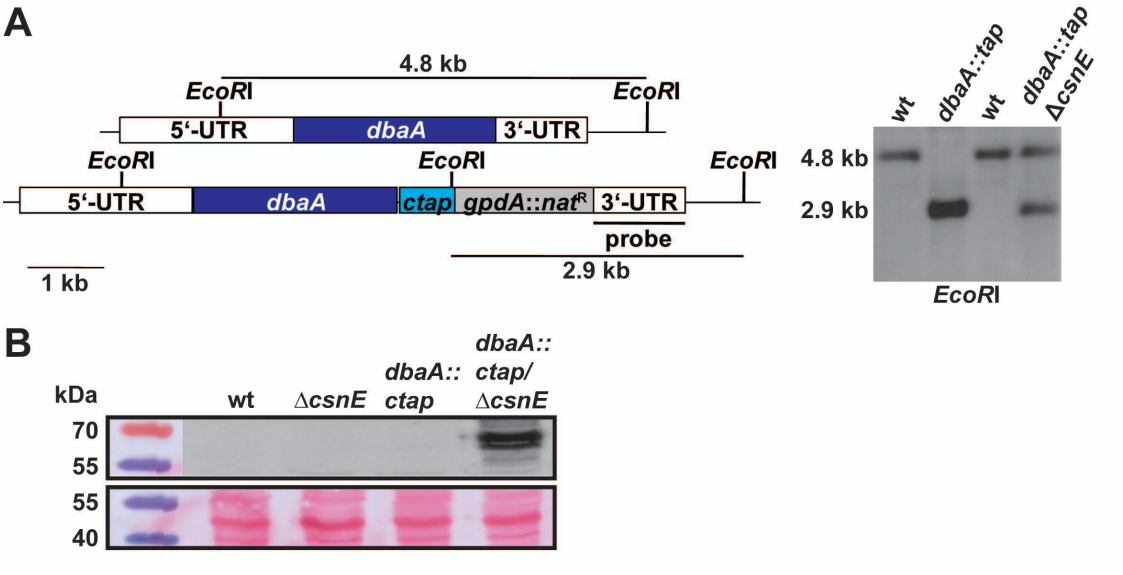

Fig. 25: C-terminally TAP tagged DbaA. **A:** Restriction maps and Southern hybridization of *dbaA::ctap* strains. **B:** Western blot of C-terminally TAP-tagged transcription factor DbaA. Ponceau staining is shown as equal loading control.

3.1.8 The oxygenase DbaH is required for yellow pigment production and involved in sexual development

Deletion mutants of all genes of the cluster (*dbaB-dbaH*) in *dbaA* OE and wild type background were designed in order to deepen our understanding of the new gene cluster and its possible function. The deletions were performed by homologous integration of *ptrA*

resistance marker and *A. fumigatus pyrG* marker containing cassettes (Fig. 26). Phenotypes of all deletions are summarized in Fig. 27. In wild type background, all deletions exhibited no obvious phenotype presumably due to the silencing of the gene cluster. During *dbaA* overexpression, strains Δ*dbaB,* Δ*dbaC*, Δ*dbaE*, Δ*dbaF*, Δ*dbaG*, and Δ*dbaH* were reduced in colony diameter and spore production. Interestingly, three of them (Δ*dbaD*, Δ*dbaG*, Δ*dbaH*) showed diminished or ceased yellow pigment production. These mutants are analyzed in detail below. A HPLC analysis of all deletion strains revealed that all of them still produced the polyketide DHMBA (Fig. 28). For strains Δ*dbaD*, Δ*dbaE* and Δ*dbaF* DHMBA production was reduced but still existent.

Overexpression of *dbaA* in the deletion strain of *dbaD*, containing the MFS transporter domain, resulted in a general diminished production of metabolites (Fig. 28). Synthesis of DHMBA was severely reduced and pigment production was only observed weakly in liquid but not on solid medium (Fig. 27). Conclusively, *dbaD* might be involved in transport of the metabolites to the environment. Interestingly, this strain showed no growth defects. In comparison to wild type, colony diameter and spore production remained unchanged, suggesting a toxic effect of secreted metabolites.

Deletion of the putative TF encoding gene *dbaG* in the *dbaA* OE strain showed metabolic changes. DHMBA was still synthesized but the pigment production was significantly diminished and only visible in submerged cultures.

Overexpression of *dbaA* in the deletion strain of *dbaH*, encoding a putative oxygenase, led to a visible pigment alteration as observable for Δ*dbaA*/Δ*csnE* and Δ*dbaI*/Δ*csnE*. However, HPLC analysis revealed for this strain a strong production of DHMBA and in addition several new components (Fig. 28). This leads to the conclusion that the putative oxygenase DbaH might be responsible for the synthesis of yellow pigments derived from oxidation of DHMBA. The block of this reaction by deleting *dbaH* led to the accumulation of the putative precursor of the yellow components, DHMBA. In addition to this metabolic phenotype, the developmental phenotype was also altered. The strain was impaired in sexual development and produced in comparison to the wild type very few colorless but fertile sexual fruiting bodies (cleistothecia) after 7 days of sexual growth (Fig. 27). At this stage, cleistothecia formation in wild type strain was completed. The production of Hülle cells, which are nursing cells to support fruiting body development (Sarikaya Bayram *et al.*, 2010), was not affected. The few cleistothecia gained color after 10 days of growth.

The results show that the *dba* gene cluster not only has impact on secondary metabolism but also on developmental processes of the fungus.

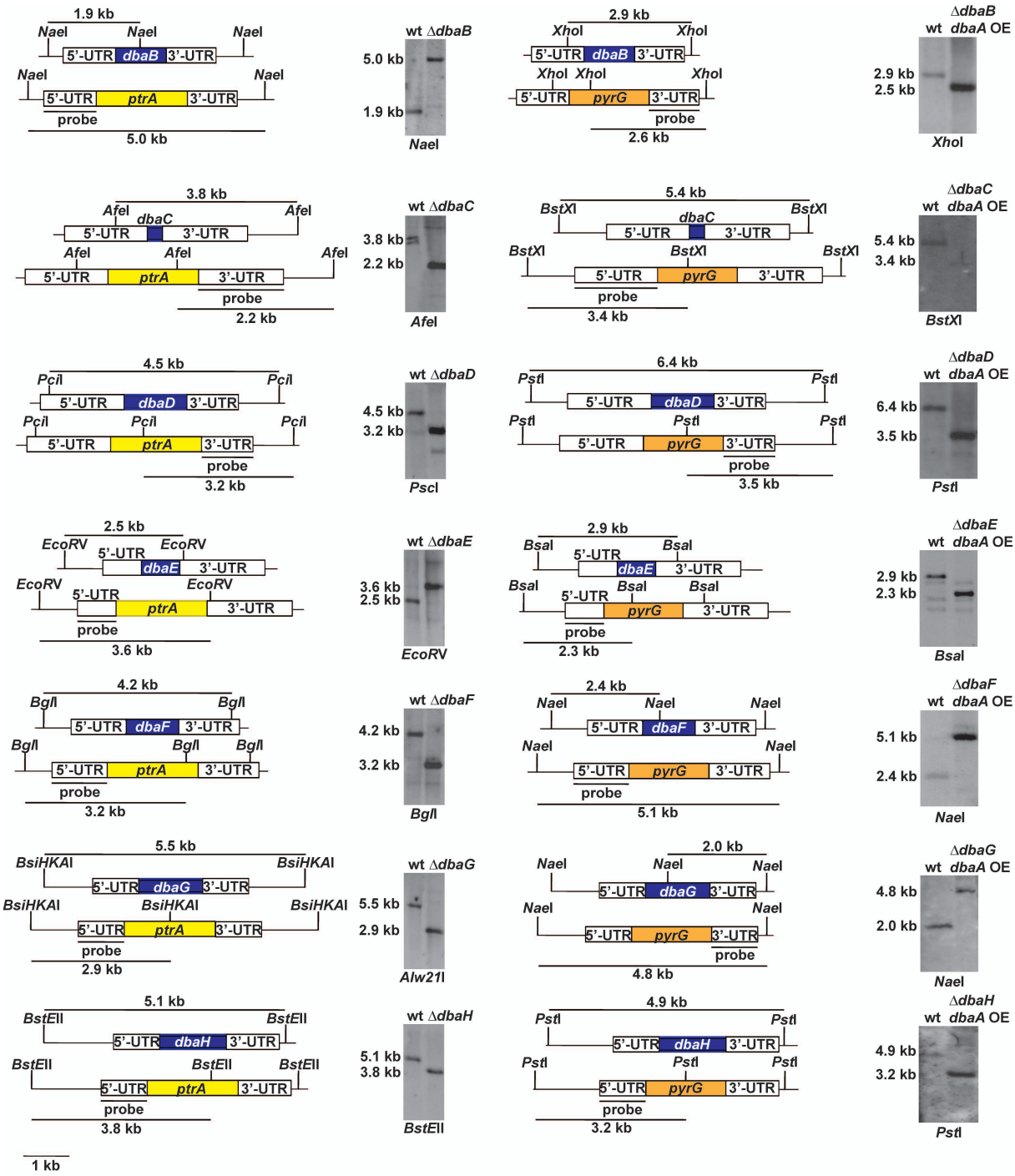

Fig. 26: Restriction maps and Southern hybridizations of *dba* deletions (*dbaB-dbaH*) in wild type background (left side) and in *dbaA* OE background (right side). For deletion in wild type background, *ptrA* was used as resistance marker gene. For deletion in *dbaA* OE background, *A. fumigatus pyrG* was used as marker gene.

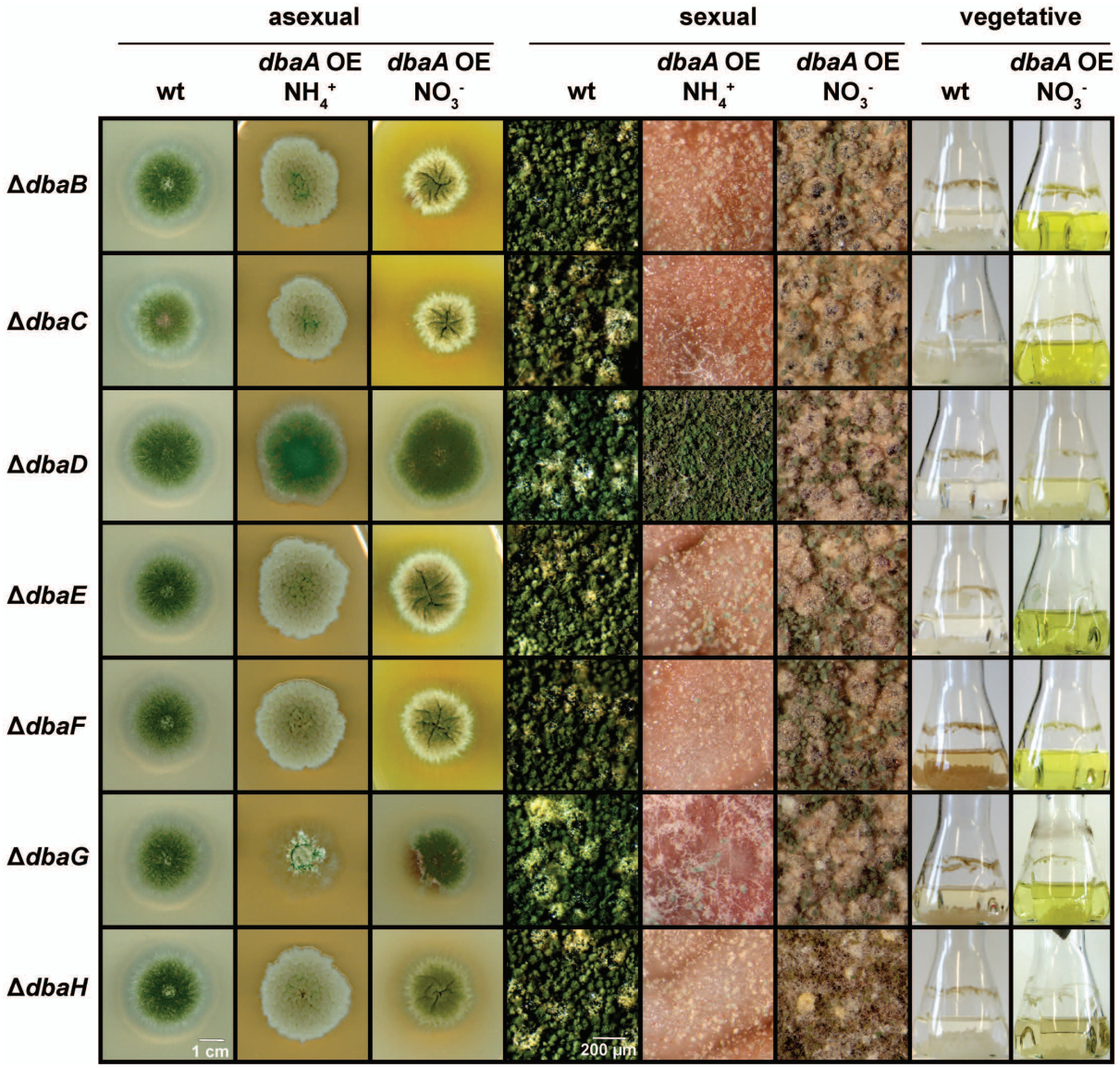

Fig. 27: Phenotypes of *dba* cluster deletions in wild type and *dbaA* OE background. Strains were grown in inducing nitrate (NO_3^-) and repressing ammonium (NH_4^+) medium. For asexual development, strains were grown 3 days at 37°C in light and for sexual development 7 days at 37°C in dark under limited oxygen level. For vegetative stage, strains were grown 24 hours in liquid medium.

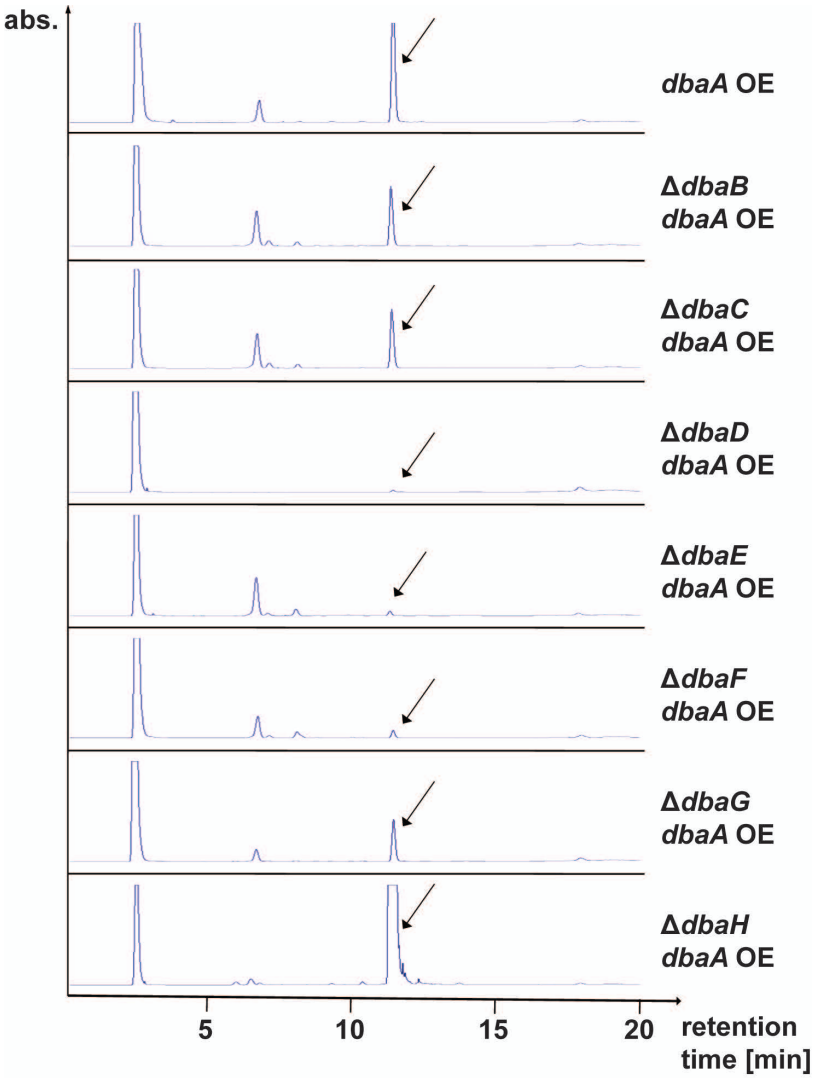

Fig. 28: HPLC-UV-DAD chromatograms of cluster deletion strains in *dbaA* OE background. DHMBA is produced by all strains. In Δ*dbaD,* Δ*dbaE,* and Δ*dbaF,* DHMBA production is reduced, while in Δ*dbaH* the production is enriched.

3.2 Characterization of the SAM synthetase in *A. nidulans*

Methylation plays a crucial role in regulation of biosynthetic gene clusters in filamentous fungi (see chapter 1.2.1.2). The most frequently used methyl group donor is the ubiquitous S-adenosylmethionine (SAM, chapter 1.2.1.2.1). Besides methylation of histones, SAM also methylates proteins, DNA, RNA, phospholipids and metabolites. The only protein known to catalyze the biosynthesis of SAM is the SAM synthetase (EC 2.5.1.6). In this study, the SAM synthetase of the filamentous fungus *A. nidulans* was characterized by genetic, cell biological and biochemical analysis.

3.2.1 *A. nidulans* genome contains one SAM synthetase gene with conserved motifs

In *A. nidulans*, the SAM synthetase encoding gene AN1222 consists of 1278 nucleotides (with two introns in the N-terminal region) encoding a putative protein with 388 amino acids and a predicted molecular mass of 42.2 kDa. According to the *Aspergillus nidulans* nomenclature, we named the gene as *sasA* (S-adenosylmethionine synthetase A). The deduced amino acid sequence of SasA exhibits two conserved motifs typical for all SAM synthetases (Fig. 30A). At the beginning of the central domain the hexapeptide GAGDQG is present, which binds the adenine moiety of ATP (Pajares *et al.*, 1991). In the C-terminal domain the glycine-rich nonapeptide GGGAFSGKD is present. This motif forms a P-loop-like structure and is proposed to be involved in binding the triphosphate of ATP (Takusagawa *et al.*, 1996b).

```
A.nidulans            114 LHYEEALEKLGAGDQGIMFGY...GWGAHGGGAFSGKDYSKVD 284
A.clavatus            113 LHYDEALEKLGAGDQGIMFGY...GWGAHGGGAFSGKDYSKVD 284
A.flavus 1            116 LHYDEALEKLGAGDQGIMFGY...GWGAHGGGAFSGKDYSKVD 286
A.flavus 2            110 SSGLEAPDDEPAGDQGMAFGY...GWGAHGGGAFSGKDFRQVD 280
A.fumigatus           113 LHYDEALEKLGAGDQGIMFGY...GWGAHGGGAFSGKDYSKVD 283
A.niger               113 LHYEEALEKLGAGDQGIMFGY...GWGAHGGGAFSGKDYSKVD 283
A.oryzae 1            116 LHYDEALEKLGAGDQGIMFGY...GWGAHGGGAFSGKDYSKVD 286
A.oryzae 2            110 SSGLEAPDDEPAGDQGMAFGY...GWGAHGGGAFSGKDFRQVD 280
E.coli                106 GVDRADPLEQGAGDQGLMFGY...GMARHGGGAFSGKDPSKVD 272
S.cerevisiae Sam1     108 VHEEKDLEDIGAGDQGIMFGY...GASSVGGGAFSGKDYSKVD 278
S.cerevisiae Sam2     110 LHYEKSLEDLGAGDQGIMFGY...GASSVGGGAFSGKDYSKVD 280
N.crassa              120 LHLDDRLENLGAGDQGIMFGY...GWGAHGGGAFSGKDFSKVD 290
H.sapiens MAT1A       121 VHLDRNEEDVGAGDQGLMFGY...GWGAHGGGAFSGKDYTKVD 291
H.sapiens MAT2A       121 VHLDRNEEDIGAGDQGLMFGY...GWGAHGGGAFSGKDYTKVD 291
D.melanogaster 1      132 VHINREEEDVGAGDQVSISKR...------------------
D.melanogaster 2      132 VHVNRAEEEIGAGDQGIMFGY...GWGAHGGGAFSGKDFTKVD 302
D.melanogaster 3      132 VHINREEEDVGAGDQGIMFGY...GWGAHGGGAFSGKDFTKVD 302
D.melanogaster 4      105 VHINREEEDVGAGDQGIMFGY...GWGAHGGGAFSGKDFTKVD 275
A. thaliana 1         109 GHFTKCPEEIGAGDQGHMFGY...GWGAHGGGAFSGKDPTKVD 279
A. thaliana 2         109 GHFFKRPEDIGAGDQGHMFGY...GWGAHGGGAFSGKDPTKVD 279
A. thaliana 3         109 GHLTKKPEDIGAGDQGHMFGY...GWGAHGGGAFSGKDPTKVD 279
A. thaliana 4         109 GHLTKKPEEVGAGDQGHMFGY...GWGAHGGGAFSGKDPTKVD 279
                                  ****         * .  *********  :**
```

Fig. 29: Amino acid sequence comparison of SAM synthetases from different organisms. The conserved motifs are shown in red. GenBank accession numbers for sequences are: *Aspergillus nidulans* (CBF87906), *Aspergillus clavatus* (EAW07774), *Aspergillus flavus* isoforms 1 and 2 (EED50079, EED51490), *Aspergillus fumigatus* (EDP56296), *Aspergillus niger* (CAK45307), *Aspergillus oryzae* isoforms 1 and 2 (BAE64158, BAE62029), *Escherichia coli* (CAH56923), *Saccharomyces cerevisiae* Sam1 and Sam2 (AAB67461, AAB64944), *Neurospora crassa* (AAC49260), *Homo sapiens* MAT1A and MAT2A (BAA08355, CAA48726), *Drosophila melanogaster* isoforms 1, 2, 3, and 4 (AAF51558, AAF51555, AAF51556, AAF51557), *Arabidopsis thaliana* isoforms 1, 2, 3, and 4 (AEE27438.1, AEE82085.1, AEC09311.1, AEE75948.1).

A ClustalW alignment of the predicted protein sequence of SasA with other filamentous fungi, yeast, bacteria, plant, human and fly SAM synthetases revealed high similarities between the different species. The identity to other Aspergilli varies between 87% and 93%. Interestingly, all *Aspergillus* species carry one SAM synthetase encoding gene, except for

Aspergillus flavus and *Aspergillus oryzae*. These organisms possess two independent isoforms with only 55% identity to each other. They form a separate group in a phylogenetic comparison (Fig. 30B), indicating that these proteins have evolved to perform a different function. Likewise, *S. cerevisiae* possesses two independent SAM synthetase encoding genes *SAM1* and *SAM2*. However, the encoded proteins show a high amino acid identity of 91% to each other. In human, the identity between the two existing isoforms MAT1A and MAT2A is 84%. In *Drosophila melanogaster* four SAM synthetase isoforms exist. Isoforms 2, 3, and 4 have identities of 93-97% to each other, and only the shorter isoform 1 differs highly with identities of 55-75% to isoforms 2, 3, and 4.

The identity of *A. nidulans* SasA to the isoforms of *D. melanogaster* is 40-62%, the identity to the human isoforms 67%, to yeast Sam1 and Sam2 74-76%, to *E. coli* MetK 54%, and to the filamentous fungus *Neurospora crassa* protein 85%. The evolutionary correlation is summarized in a phylogenetic tree (Fig. 30B). These data suggest that higher eukaryotes, such as fly and human, possess multiple copies of SAM synthetases, while fungi show variability in copy number between one and two.

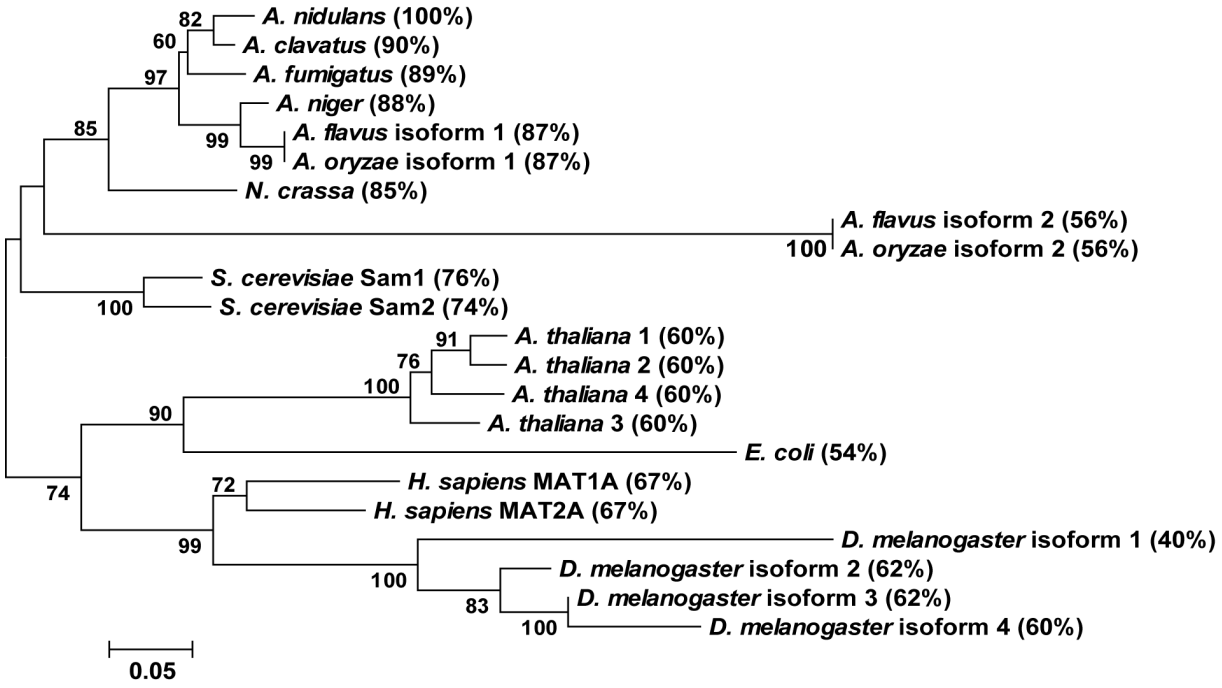

Fig. 30: Phylogenetic comparison of SAM synthetases from different organisms. The phylogenetic tree was constructed using the Neighbor-Joining method (Saitou *et al.*, 1987). The percentages of replicate trees, in which the associated taxa clustered together in the bootstrap test (1000 replicates), are shown next to the branches (Felsenstein, 1985). The tree is drawn to scale, with branch lengths in the same units as those of the evolutionary distances used to infer the phylogenetic tree. The evolutionary distances were computed using the number of differences method (Nei *et al.*, 2000) and are in the units of the number of amino acid differences per sequence. Evolutionary analyses were conducted in MEGA5 (Tamura *et al.*, 2011). Protein identities to *A. nidulans* SasA are given in parentheses and accession numbers are given in Fig. 29.

3.2.2 The *sasA* gene is highly expressed during vegetative growth

We analyzed the expression of *sasA* during different developmental stages. Northern analysis was performed with RNA extracted from vegetative, asexual and sexual cultures grown for different time periods (Fig. 31). The results show that *sasA* is strongly expressed during vegetative growth and that expression decreases immensely during development in asexual and sexual grown cultures.

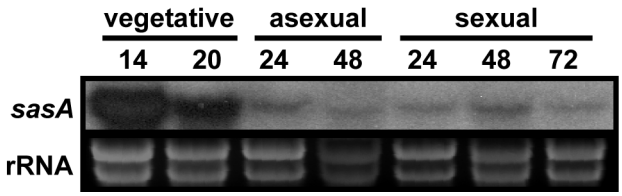

Fig. 31: Expression of *sasA* in *A. nidulans*. **A:** Northern hybridization of *sasA* during vegetative, asexual, and sexual development. Cultures were grown for 14, 20, 24, 48, and 72 hours. rRNA levels were used as loading control.

We compared the mRNA levels with the production of the SasA protein. A functional *tap*-tagged *sasA* fusion strain was constructed (Fig. 32A). Production of the tagged protein was monitored at the same stages of development as the transcripts by Western blot analysis with an anti-calmodulin antibody, recognizing the calmodulin peptide of the TAP-tag (Fig. 32B). Western results showed that SasA is strongly produced at vegetative and early developmental stages, but production ceases at later stages of asexual and sexual development.

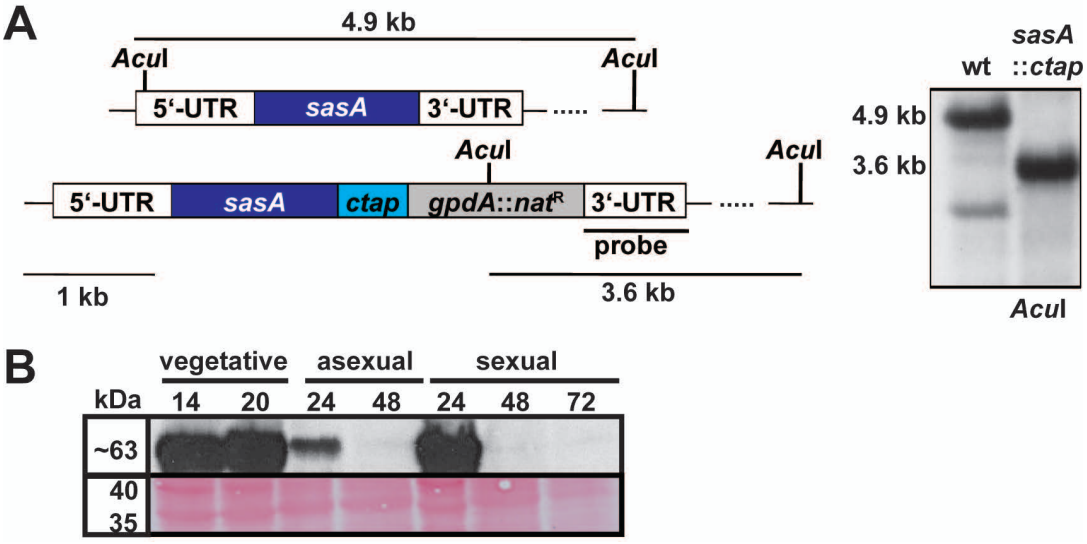

Fig. 32: TAP-tagged SasA. **A:** Restriction map and Southern hybridization of *sasA*::*ctap* strain. **B:** Western blot analysis of C-terminally TAP-tagged SasA with an anti-calmodulin antibody. Protein extracts were prepared after 14, 20, 24, 48, and 72 hours of vegetative, asexual, and sexual growth. Ponceau staining is shown as equal loading control.

3.2.3 Constitutively expressed *sasA* is essential for the viability of *A. nidulans*

SAM is one of the most commonly used enzyme substrates and the major methyl group donor in all living organisms. Therefore, the deletion of the single *sasA* gene should be lethal, except there is a second, yet not identified SAM synthetase encoding gene in the genome of *A. nidulans*, which can take over the function. We addressed whether *sasA* is essential by constructing a pyrithiamine resistance marker (*ptrA*) containing deletion cassette and integrated it into the genome of an *A. nidulans* wild type strain homologously (Fig. 33A). We obtained 18 primary transformants, which did not grow while generating single colonies.

We applied the heterokaryon rescue technique as a method which allows to determine if the gene of interest is essential (Nayak *et al.*, 2006). First, a growth test on selecting and non-selecting medium was performed (Fig. 33B). The primary transformants grew on non-selecting medium, but they did not grow on selecting medium containing pyrithiamine, indicating, the existence of a heterokaryon with a wild type *sasA* gene ($sasA^+$, $ptrA^-$) and the deletion ($sasA^-$, $ptrA^+$). Second, a diagnostic PCR was carried out using genomic DNA extracted from the heterokaryon (Fig. 33C). One primer annealing to the 5'-UTR region of the deletion cassette and one primer annealing in the genome directly behind the deletion cassette were chosen. The primer selection theoretically results in PCR products of 3.5 kb for the wild type ($sasA^+$, $ptrA^-$) and 4.2 kb for the deletion event ($sasA^-$, $ptrA^+$). The diagnostic PCR showed double bands at 3.5 and 4.2 kb for almost all clones, proving the existence of a heterokaryon. These results corroborate that the *sasA* gene is essential and its functions are indispensable for the cellular activities of *A. nidulans*.

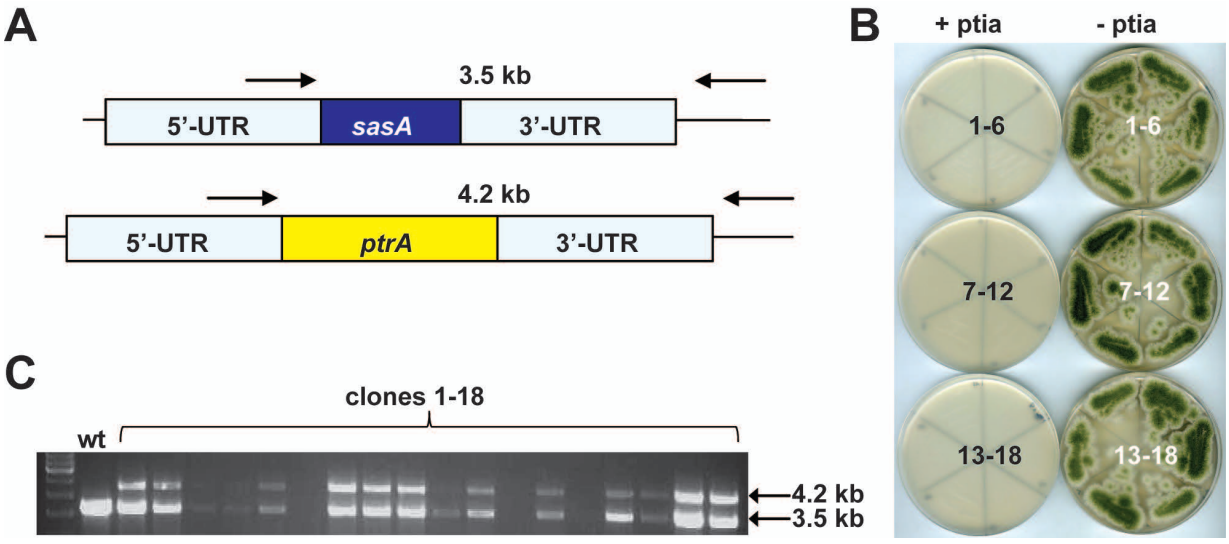

Fig. 33: Deletion of *sasA* is lethal. **A:** Construction of *sasA* deletion. *sasA* was replaced by a pyrithiamine resistance marker (*ptrA*) via homologous recombination. Arrows indicate primers used for heterokaryon rescue PCR. For wild type locus a PCR amplicon of 3.5 kb and for deletion strain locus a PCR amplicon of 4.2 kb was expected. **B:** Growth of primary transformants 1-18 was tested on selecting pyrithiamine (+ ptia) and non-selecting (- ptia) medium. **C:** Diagnostic PCR with DNA extracted from primary transformants 1-18. Primers given in Fig. 3A were used. For wild type DNA one band of 3.5 kb was detected, and for clones 1-18 DNA a double band of 3.5 kb and 4.2 kb was detected, proving the existence of a heterokaryon.

3.2.4 Overexpression of *sasA* leads to sterile microcleistothecia with pigmented Hülle cells

We then addressed whether SasA production, which is primarily observed during vegetative development and at initial stages of fungal development, has a major impact on development of *A. nidulans*. We cloned *sasA* under the inducible *niiA*/*niiD* promoter. The correct homologous integration of the cloning cassette was verified by Southern hybridization experiments (Fig. 34).

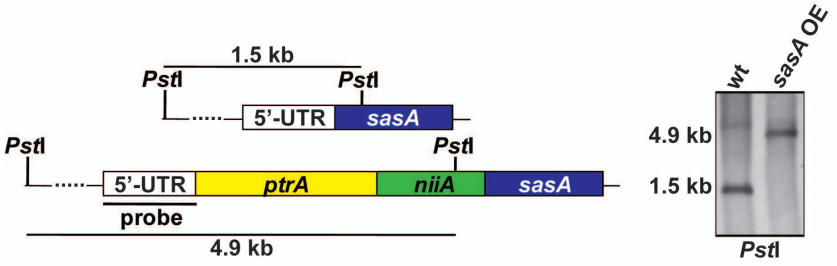

Fig. 34: Southern construct of *sasA* overexpression strain

For expression studies, wild type and *sasA* overexpressing (OE) strain were grown on different inducing and repressing media. Growth on nitrate medium induces the specific *niiA*/*niiD* transcription factor and thus *sasA* expression, whereas growth on the universal repressor ammonium reduces activity of the general nitrogen source transcription factor *areA* and therefore reduces *sasA* expression (Arst *et al.*, 1973, Punt *et al.*, 1995). Both strains were grown on inducing nitrate medium (NO_3^-), inducing and repressing proline, nitrate and ammonium medium (proline + NH_4^+ + NO_3^-), repressing proline and ammonium medium (proline + NH_4^+) and noninducing and nonrepressing proline medium. The developmental defects were analyzed during asexual and sexual growth and the results are shown in Fig. 35 and Fig. 36.

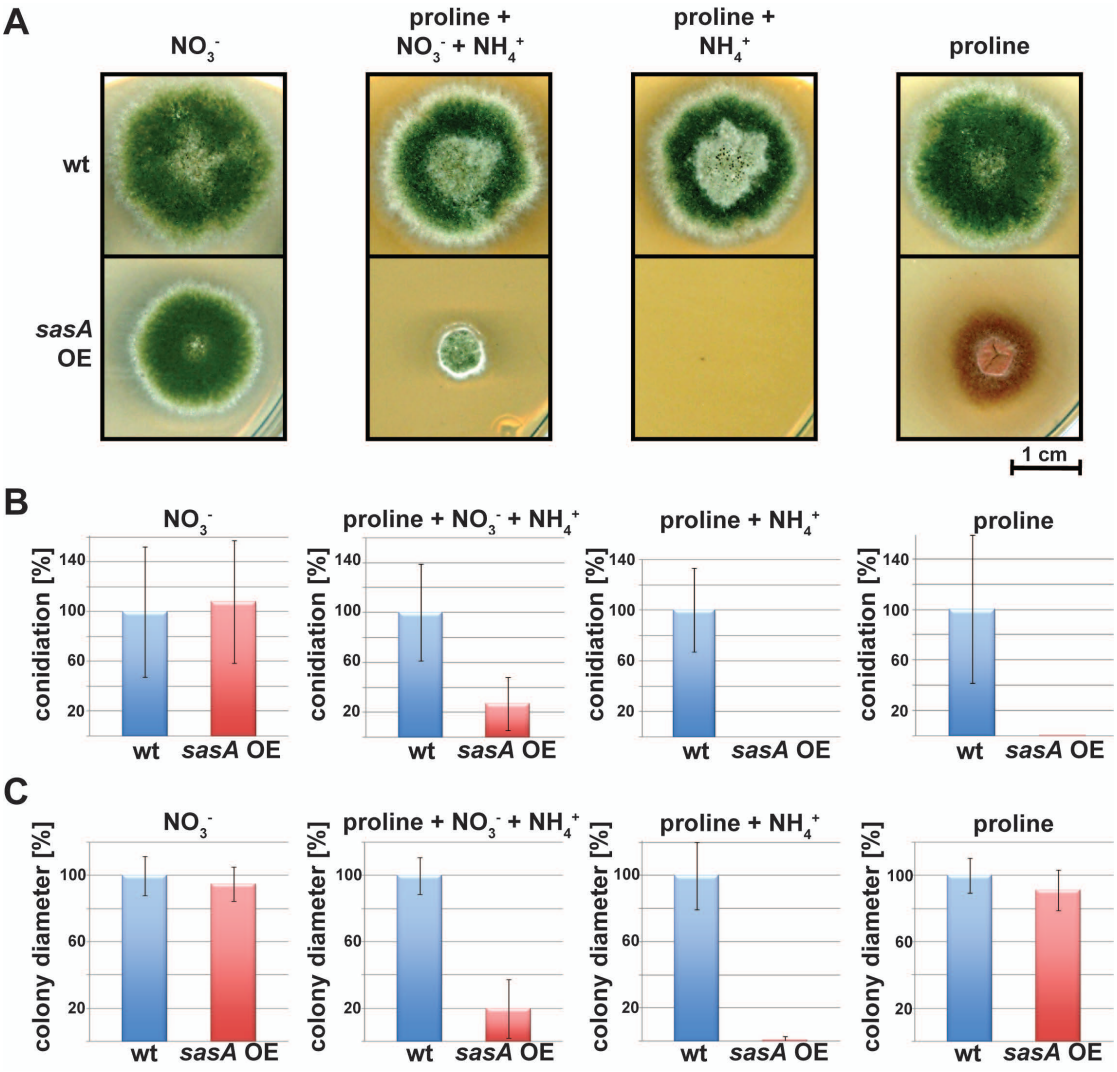

Fig. 35: Results of modified *sasA* expression in *A. nidulans* during asexual development. **A:** Growth test of *sasA* OE strain. *sasA* is under control of the inducible nitrate promoter. This promoter is induced by nitrate (NO_3^-), induced and repressed by medium containing proline, ammonium and nitrate (proline + NH_4^+ + NO_3^-), repressed by proline and ammonium (proline + NH_4^+) and noninduced and nonrepressed by proline. Strains were grown 3 days at 37°C in light for initiation of asexual development. **B:** Spore quantification of *sasA* OE compared to wild type. Wild type levels were set to 100%. **C:** Colony diameter of *sasA* OE colonies compared to wild type. Wild type diameter was set to 100%.

During asexual development, *sasA* expression had impact on conidiation and colony diameter (Fig. 35A). While under inducing conditions (NO_3^-), conidiation is rather similar to wild type, under inducing and repressing conditions (proline + NH_4^+ + NO_3^-) the amount of conidia is diminished to 25% of wild type level (Fig. 35B) and the colony diameter was reduced to 20% (Fig. 35C). As the *sasA* deletion results indicated, under repressing conditions (proline + NH_4^+) the *sasA* mutant did not grow. Under noninducing plus nonrepressing conditions (proline) the mutant had a normal colony diameter, but produced nearly no conidia and additionally synthesized red pigments.

The sexual life cycle was drastically affected by *sasA* overexpression. The mutant was not able to perform its normal sexual life cycle. Under inducing conditions (NO_3^-) the mutant strain generated very few and very small cleistothecia (microcleistotecia) with a diameter of 40-50 µm after 10 days of growth compared to normal wild type cleistothecia with a diameter of 100-200 µm (Fig. 36A and B). In addition, these microcleistothecia were sterile, lacking fertile ascospores. Concludingly, *A. nidulans* was not able to reproduce sexually when *sasA* was overexpressed.

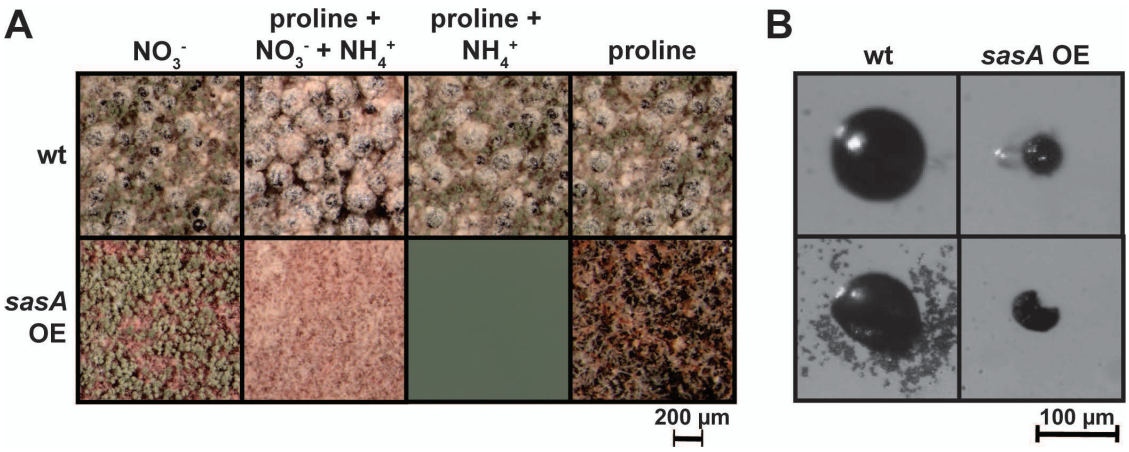

Fig. 36: Results of modified *sasA* expression in *A. nidulans* during sexual development. **A:** Phenotypes of wild type and *sasA* OE strain are shown. Strains were cultivated for 7 days at 37°C in dark under reduced oxygen level for induction of sexual development. **B:** Cleistothecia of *sasA* OE and wild type after 10 days of sexual growth.

Although only very few cleistothecia were developed, the amount of nursing Hülle cells was unaffected during sexual development. The Hülle cells which normally do not contain significant amounts of SasA (see chapter 3.2.6) were remarkably different in comparison to wild type because they accumulated a pink colored pigment. Under inducing and repressing conditions (proline + NH_4^+ + NO_3^-) and under noninducing and nonrepressing conditions (proline) no sexual structures were formed and under repressing conditions (proline + NH_4^+) the mutant did not grow. Hülle cell formation is regulated by LaeA (Sarikaya Bayram *et al.*, 2010), suggesting a possible link between LaeA and SasA activity to control accurate Hülle cell formation.

3.2.5 Overexpression of *sasA* leads to reduced production of sterigmatocystin

As overexpression of *sasA* had an impact on secondary metabolism, indicated by the red color produced on proline medium, we analyzed whether overexpression influenced the biosynthesis of the well studied aflatoxin precursor sterigmatocystin (ST). Initially, we tested expression of the genes *aflR*, encoding the specific transcription factor for ST biosynthesis, *stcU*, encoding a ketoreductase involved in ST biosynthesis, and *laeA*, encoding the master regulator for secondary metabolism, by Northern hybridization. Additionally, we tested the expression of the penicillin and terrequinone A producing *ipnA* and *tdiA*. Our results showed no significant changes in expression levels in *sasA* OE in comparison to wild type strain (Fig. 37A).

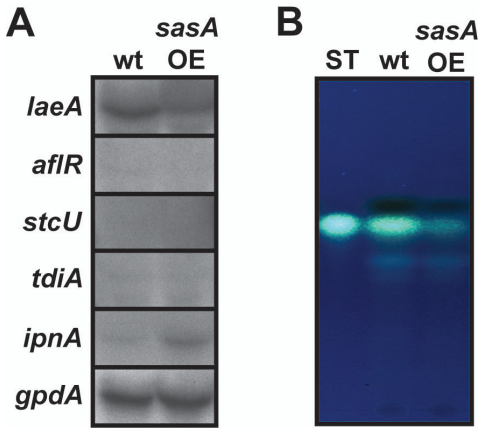

Fig. 37: Secondary metabolism in *sasA* OE strain. **A:** Northern analysis of biosynthetic genes in *sasA* overexpression strain and wild type. As probes, *laeA* (encoding a global regulator), *aflR* and *stcU* (ST biosynthesis), *tdiA* (terrequinone A biosynthesis) and *ipnA* (penicillin biosynthesis) were used. Expression of *gpdA* is shown as equal loading control. **B:** Sterigmatocystin production levels of *sasA* OE and wild type were analyzed with TLC (chloroform/acetone 4:1). Metabolites were visualized with an alcoholic aluminum chloride solution at 366 nm. Sterigmatocystin (ST) was used as standard.

We further analyzed whether there are posttranscriptional effects which might influence secondary metabolism. Therefore, we extracted the unpolar metabolites from asexual grown wild type and overexpression cultures and determined the amount of ST with thin layer chromatography (TLC, Fig. 37B). Our results showed that production of ST in *sasA* overexpression strain is significantly reduced compared to wild type, suggesting a repressive posttranscriptional effect on secondary metabolism.

Taken together, our results suggest that a correct expression of *sasA* is needed for a coordinated secondary metabolism of *A. nidulans*.

3.2.6 SasA is predominantly localized to the cytoplasm in most fungal cell types except Hülle cells

In *S. cerevisiae*, the SAM synthetases Sam1 and Sam2 are both primarily localized in the cytoplasm (Kumar *et al.*, 2002). We determined the subcellular localization of the *A. nidulans* SasA via fluorescence microscopy. Therefore, *sgfp* (synthetic green fluorescent protein) was fused to *sasA* and integrated into the genome of *A. nidulans* homologously (Fig. 38). The construct was expressed under the native promoter of *sasA*.

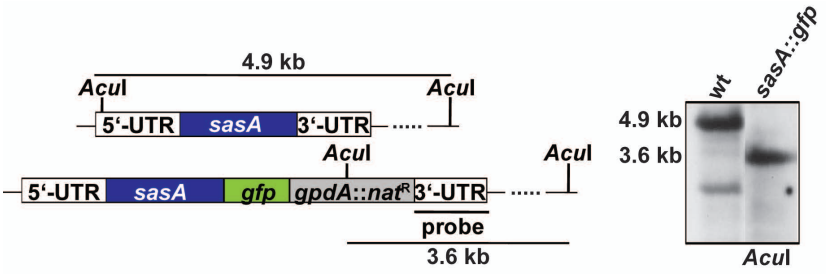

Fig. 38: Restriction map and Southern hybridization of *sasA*::*gfp* strain.

Fluorescence microscopy revealed that SasA is primarily localized in the cytoplasm (Fig. 39). SasA is not restrictively localized during asexual development to a distinct cell type but is visible in the cytoplasm of entire conidiophores including the conidiospores. During sexual development, SasA is localized to the ascospores but not to the Hülle cells, which are the nursing cells surrounding the cleistothecium (Sarikaya Bayram *et al.*, 2010). Predominant cytoplasmic localization of SasA::GFP fusion indicates that SasA functions mostly in the cytoplasm, whereas any activity in other compartments might be only due to small SasA subpopulations.

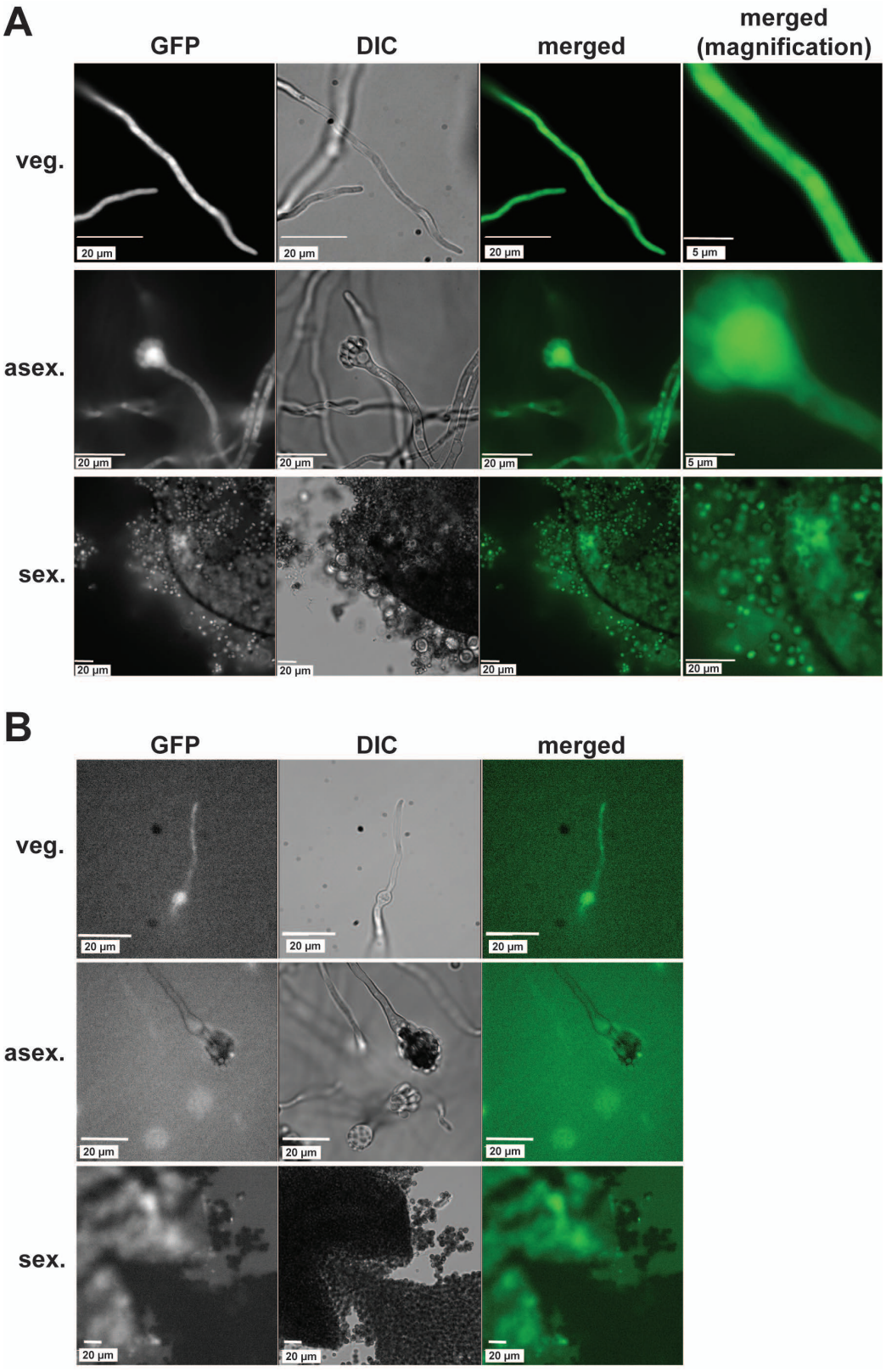

Fig. 39: Localization of C-terminally GFP-tagged SasA was determined via fluorescence microscopy. Strains were cultivated in liquid medium for vegetative growth and on solid medium with and without light for asexual and sexual development, respectively. **A:** SasA::GFP strain. SasA is localized to the cytoplasm. **B:** Wild type strain as negative control.

3.2.7 Protein interaction studies revealed involvement of SasA in methionine metabolism and fungal growth

Protein interaction studies were performed for a more comprehensive picture of SasA function in the fungal cell. The tandem affinity purification (TAP) was applied using the SasA::TAP fusion strain (Fig. 32). The protein interactions were determined in extracts obtained from vegetative, asexual, or sexual grown cultures. In addition, an untagged wild type strain was analyzed as a control at the same conditions to exclude unspecific protein bindings. The purified protein extracts were separated on an SDS polyacrylamide gel. A protein band with an expected molecular weight for SasA of approximately 43 kDa was detectable (Fig. 40).

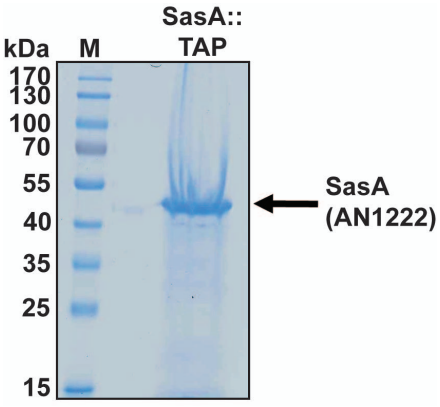

Fig. 40: C-terminally TAP tagged SasA was purified via tandem affinity purification (TAP). SasA with a size of approximately 43 kDa was detected on SDS polyacrylamide gel.

During TAP analysis 22 putative interaction partners of SasA were identified via mass spectrometry (Tab. 11 and Tab. 12, ribosomal proteins were not listed). We further divided the identified proteins into subcategories. Three proteins (AN10747, AN4443, and AN8224) are connected to metabolism of the SAM synthetase substrate methionine. A second group spans proteins, which are putatively localized to the mitochondria in eukaryotes. An aconitase and a malate dehydrogenase were identified that are involved in citrate cycle. Additionally, we found an aspartate aminotransferase, which in *S. cerevisiae* acts together with the malate dehydrogenase in malate-aspartate shuttle to transport NADH from cytoplasm into mitochondria (Easlon *et al.*, 2008). The AN8216 homologue nucleoside diphosphate kinase Ynk1 of yeast, which catalyzes the transfer of gamma phosphates from nucleoside triphosphates to nucleoside diphosphates, is also partially localized to mitochondria in yeast (Amutha *et al.*, 2003).

Tab. 11: Putative interaction partners of *Aspergillus nidulans* SasA identified with Tandem Affinity Purification (TAP). Proteins were purified from vegetative (V), asexual (A), and sexual (S) samples. Homologous proteins in *Saccharomyces cerevisiae* are given.

A. nidulans	***S. cerevisiae***	**Protein description**	**Dev.**
Methionine metabolism			
AN4443 (MetH)	Met6p	cobalamin-independent methionine synthase	A, S
AN8224	Gus1p	glutamyl-tRNA synthetase	A, S
AN10474	Arc1p	cofactor for methionyl- and glutamyl-tRNA synthetases	A, S
Putative mitochondrial proteins			
AN1993	Aat1p	aspartate aminotransferase	A, S
AN5525 (AcoA)	Aco1p	aconitase	V, S
AN6717	Mdh1p	malate dehydrogenase	V, A, S
AN8216	Ynk1p	nucleoside diphosphate kinase	V, S
Gluconeogenesis			
AN1918 (AcuF)	Pck1p	phosphoenolpyruvate carboxykinase	A, S
AN2875	Fba1p	fructose 1,6-bisphosphate aldolase	A
Fungal morphogenesis			
AN0316	Tub1p	α-tubulin	V, A
AN2047	Cmd1p	calmodulin	V
AN6150	Bud4p	GTP-binding protein	V, A
AN6542	Act1p	actin	V, A
AN7254	Cdc48p	cell division control protein 48	A, S
AN9094	Qri1p	uridin diphosphate-N-acetylglucosamine pyrophosphorylase	A, S
Stress			
AN2248	Uga1p	γ-amino-N-butyrate (GABA) transaminase	A, S
AN10202	Ssa1p	ATPase, member of heat shock protein 70 family	V, A, S
Histone			
AN3469	Htb1p/Htb2p	histone-2B	V, A
Other proteins			
AN4739	Ade1p	N-succinyl-5-aminoimidazole-4-carboxamide ribotide synthetase	S
AN5989	-	NAD-dependent epimerase/dehydratase	A, S
AN7708	-	aldo-keto reductase	A, S
AN10540	Yol057wp	dipeptidyl-peptidase III	A, S

A third group of proteins putatively interacting with SasA are involved in gluconeogenesis. Phosphoenolpyruvate carboxykinase catalyzing the GTP-dependent reaction of oxaloacetate to phosphoenolpyruvate, is a key enzyme in this reaction cascade. The fructose-bisphosphate aldolase catalyzes the conversion of fructose 1,6-bisphosphate to glyceraldehyde-3-phosphate and dihydroxyacetone-phosphate. Gluconeogenesis is an important process as it allows

organisms to grow on different carbon sources than sugar, like glycerol or ethanol (Haarasilta *et al.*, 1975).

The fourth group comprises proteins, which are involved in fungal morphogenesis. This includes cell division, growth or cell wall growth. In this group are the conserved cytoskeletal elements tubulin and actin (Pruyne *et al.*, 2000, Schatz *et al.*, 1986), and calmodulin A, which regulates many processes including response to various stress conditions, mating, budding, and actin-based processes (Cyert, 2001). The GTP-binding yeast protein Bud4 (homologous to AN6150) is involved in bud-site selection and required for axial budding pattern (Chant *et al.*, 1991, Sanders *et al.*, 1996) and Qri1 (homologous to AN9094) is important in e.g. cell wall biosynthesis (Cid *et al.*, 1995).

Two proteins are putative stress proteins, like the heat shock protein AN10202 (homologous to Ssa1p in yeast) or the GABA transaminase AN2248, which homologous protein in yeast is involved in oxidative stress response (Coleman *et al.*, 2001). We identified histone-2B as the only histone which could be an interaction partner of SasA. Four additional putative SasA interacting proteins (other proteins) could not be obviously assigned to a specific category.

Protein methylation can occur at several different amino acid residues including lysine and arginine. With a computational method (Bi-profile Bayes - Prediction of Protein Methylation Sites (BPB-PPMS)), based on Bi-profile Bayes feature extraction combined with support vector machines putative, lysine and arginine methylation sites can be predicted (Shao *et al.*, 2009). We utilized this method to predict possible methylation sites in the putative SasA interacting proteins. In Tab. 13, all proteins are listed that have a methylation probability of more than 80%. Six of the identified proteins possess at least one putative methylation site with a high score, what makes them highly likely to be SAM methylation targets. Interestingly, these six proteins are distributed into six of the seven protein categories where we found SasA interaction partners.

Taken together, the SAM synthetase SasA plays a role in a variety of vegetative reactions in the filamentous fungus *Aspergillus nidulans*, including methionine biosynthesis and other metabolic pathways in mitochondria, and stress. The observed overexpression phenotypes in development and secondary metabolism might depend on these metabolic functions as well as on the proteins essential for fungal morphogenesis. Furthermore, the histone-2B hints to an additional nuclear effect provided by SasA. SasA might be part of several protein complexes, which might include methylation targets as well as associated proteins.

Tab. 12: Peptides identified by LC-MS/MS from strain *sasA*::*ctap*. Identified proteins of *A. nidulans* (AN) by TurboSEQUEST analysis of the ESI-MS/MS2 data, protein coverage and TurboSEQUEST cross-correlation values of the identified peptides (X_{corr}) are given. M* = oxidized methionine.

	Peptide sequence	**% aa coverage**	**X_{corr}**
AN0316			
	R.TIQFVDWCPTGFK.I	2.89	3.68
	K.ETHAAVATLK.T	2.22	2.38
AN1222			
	K.IIVDTYGGWGAHGGGAFSGK.D	5,15	5.88
	R.KIIVDTYGGWGAHGGGAFSGK.D	5,41	6.19
	K.TQVTVEYAHDNGAVKPLR.V	4,64	5.91
	R.VDTVVVSAQHSDDVTTEELR.A	5,15	5.75
	K.TCNVLVAIEQQSPDIAQGLHYEEALEK.L	6,96	5.95
	K.IADQISDAILDACLAEDPLSK.V	5,41	6.68
	K.TGMIMVFGEITTQAR.L	3,87	5.63
	K.PIYFETAQNGHFTNQK.F	4,12	5.06
	R.ELDLAKPIYFETAQNGHFTNQK.F	5,67	4.93
	R.FVIGGPQGDAGLTGR.K	3,87	4.86
	K.TGMIMVFGEITTQAR.L	3,87	5.63
	K.LGAGDQGIMFGYATDETPELLPLTLVLSHK.L	7,73	5.50
	R.NDGSIPWLRPDTK.T	3,35	3.88
	K.VIPAELLDDR.T	2,58	3.15
	K.DIGYDDSEKGFDYK.T	3,61	3.60
	K.KVIPAELLDDR.T	2,84	3.65
	K.LNAAMTTAR.N	2,32	3.23
	K.TSEELVQIIR.N	2,58	4.44
	R.TVYHIQPSGR.F	2,58	3.04
	K.IADQISDAILDACLAEDPLSK.V	5,41	6.53
	R.LDYQAIIR.G	2,06	3.67
	K.SLVAAGLAR.R	2,32	3.08
	K.FSWEQPK.A	1,80	2.42
	R.NNFDLRPGVIVR.E	3,09	2.66
	R.PGVIVR.E	1,55	2.15
	K.GFDYK.T	1,29	1.45
AN1918			
	R.FGSVLENVVFDPISR.V	2.50	2.95
	K.ANAWLLNTGWVGAGATTGGK.R	3.33	3.05
AN1993			
	K.DTIGLDFEGLVEDLK.A	3.49	4.71
	K.AAAQLAYGADSPVLKEDR.L	4.19	3.80
	R.VGAFSLVCESAEEK.K	3.26	4.05
	K.AAAQLAYGADSPVLK.E	3.49	4.04
AN2047			
	K.VFDRDNNGFISAAELR.H	10.67	3.95
	K.LTDDEVDEMIR.E	7.33	4.10
	R.IDYNEFVQLMMQK.-	8.67	4.91
	K.EAFSLFDKDGDGQITTK.E	11.33	3.79
	K.MKDTDSEEEIR.E	7.33	3.93
	R.HVMTSIGEK.L	6.00	3.00
AN2248			
	R.LFLVENTAATGDYLYSGLER.L	4.01	5.12
	R.NNVLFIVDEVQTGVGATGK.F	3.81	4.95
	-.MASAFRSSLKLR.A	2.40	2.15
AN2875			
	K.GVSNDGQAASIAGGIAAAHYIR.S	6.09	4.20
	R.DQNCPVILQVSQGGAAFFAGK.G	5.82	3.97
	K.TGVIVGDDVLR.L	3.05	2.53
AN3469			
	R.AM*SILNSFVNDIFER.V	11.35	4.91
	K.QVHPDTGISTR.A	7.80	1.79

Tab. 12 continued: Peptides identified by LC-MS/MS from strain *sasA*::*ctap*.

	Peptide sequence	% aa coverage	X_{corr}
	K.ETYSSYIYK.V	6.38	1.51
	K.LAAYNKK.S	4.96	1.41
AN4443			
	K.LPLFPTTTIGSFPQTK.E	2.06	3.63
	R.NPEQLDSVIGALGPK.Q	1.94	4.70
	R.PVILGPVSFLTLAK.A	1.81	3.26
	K.EAGVEDVQIDEPVLVFDLPLK.S	2.71	4.71
	R.VIVSTSSSLLHVPHTLASEK.N	2.58	4.01
	K.AVTEGPAAVR.E	1.29	2.89
	K.DGQPAIDVPSLEMVK.W	1.94	2.63
	K.VIQVDEPALR.E	1.29	2.95
	K.PVVEFLEAK.E	1.16	2.49
	K.TSEVVVIAK.A	1.16	2.77
	K.LGSLGAQAPR.L	1.29	3.27
	K.AALSNLVQAAK.Y	1.42	2.10
	K.VELAIQK.L	0.90	2.06
	K.NLDPEVQDWFSFAVEK.T	2.06	2.46
AN4739			
	R.ESEAFPDGPIYTPSTK.A	5.32	4.50
	K.AEQGEHDENIHPDK.A	4.65	3.22
AN5525			
	K.NVFTGEYGAVPATAR.D	1.91	3.91
	R.SSVDVAVSPSSDR.L	1.66	2.49
	K.DATGIPILIK.C	1.28	2.73
	K.SIFTVTPGSEQIR.A	1.66	2.40
	R.DTYQAPPTDR.S	1.28	1.94
AN5989			
	K.IISQVDPDYVVWSAGAGGK.G	6.76	5.18
	R.NVFDNVLPTYAK.A	4.27	2.70
AN6150			
	K.AVKLIDDR.S	0.60	2.53
	R.QKHSAFSK.M	0.60	1.94
	R.RNSPVWNQSNR.S	0.82	1.03
AN6542			
	R.VAPEEHPVLLTEAPINPK.S	4.79	4.31
	K.SYELPDGQVITIGNER.F	4.26	4.92
	K.AGFAGDDAPR.A	2.66	2.88
	R.GYTFSTTAER.E	2.66	2.86
	R.TTGIVLDSGDGVTHVVPIYEGFALPHAISR.V	7.98	4.99
	K.EITALAPSSM*K.V	3.19	2.19
	R.DLTDYLMK.I	2.13	2.21
	R.DLTDYLM*KILAER.G	3.72	1.26
AN6717			
	K.GVVEPTFVESPLYK.D	4.11	4.42
	R.LFGVTTLDVVR.A	3.23	3.78
	R.FISQVQGTDPSK.E	3.52	4.60
	K.VAVLGASGGIGQPLSLLLK.L	5.57	5.66
	R.GGPGVAADISHINTNSTVK.G	5.57	5.12
	K.INPVGEVNEFEQK.L	3.81	3.88
	K.GYEPTESGLADALK.G	4.11	3.82
	R.DDLFNTNASIVR.D	3.52	3.61
	K.TRDELVHR.I	2.35	2.96
	K.VELGPNGAEK.I	2.93	4.05
	R.IQFGGDEVVK.A	2.93	1.77
AN7254			
	R.AAAPCVVFLDELDSIAK.S	2.09	3.22
	K.NSPAIIFIDEIDSIAPK.R	2.09	3.99
	R.LDTLVYVPLPDQASR.E	1.84	2.79

Tab. 12 continued: Peptides identified by LC-MS/MS from strain *sasA*::*ctap*.

	Peptide sequence	% aa coverage	X_{corr}
AN7254			
	K.RKETVLIVLADDDLDDGSAR.I	2.45	2.06
	K.QM*AQIRELVELPLR.H	1.84	1.32
AN7708			
	K.EVGDAIHESGLPR.S	4.58	3.11
	K.ANDPTLVEIAK.K	3.87	3.10
	K.ILAPAGSPEATYEK.I	4.93	2.15
AN8216			
	R.TILGATNPLASAPGTIR.G	11.04	4.21
	R.NVCHGSDSVESAK.K	8.44	3.01
	R.NVCHGSDSVESAKK.E	9.09	3.28
	R.GLVGPIISR.F	5.84	1.76
AN8224			
	K.LVEQGVVDGWSDPR.F	2.06	4.57
	R.NVQIWDFAR.M	1.32	2.69
	K.ANQAALLPILLVATSVNEAR.P	2.94	3.51
	K.GGPDSPYTQDKPK.H	1.91	3.17
	K.ELLLSFPYLNSK.E	1.76	1.04
AN9094			
	K.VAVAPDGNGGIYQALLAAGVR.E	4.15	3.78
	K.LVADNQVAVVLLAGGQGTR.L	3.75	5.87
	K.SLFQLQAER.I	1.78	3.30
	K.VADPVFIGFAASK.K	2.57	3.44
	K.GCFDIGLPSHK.S	2.17	2.46
	R.KPTEEFFQQHNYFGLDK.S	3.36	2.87
AN10202			
	K.SINPDEAVAYGAAVQAGILSGK.A	5.63	5.57
	K.SFSGTLEPVQQVLK.D	3.58	3.61
	K.NQVDEIVLVGGSTR.I	3.58	4.86
	K.LSTTEIEQMIDDAAK.F	3.84	4.46
	R.SANITISNAVGK.L	3.07	3.50
	K.LLSDFFDGK.K	2.30	2.52
AN10474			
	R.SYPAAISPDETEPDLLAVNPK.V	4.78	3.85
	K.AAAQGAGAEQTVVVGQTKPEK.A	4.78	2.88
	R.VFSLQIPDEEK.V	2.51	2.97
	R.HVDFVQNSR.V	2.05	2.43
	R.IYFEGWNDGEPEK.V	2.96	2.69
	K.GYHNIVR.H	1.59	1.88
	K.ASVADVAAYALLAPVVEK.W	4.10	2.57
AN10540			
	R.LPLDAFEALASATPETK.A	2.40	4.61
	K.QAGLYAANDTQK.K	1.69	2.49

Tab. 13: List of all SasA interacting proteins with a methylation probability of over 80% predicted by BPB-PPMS (Shao *et al.*, 2009).

A. nidulans	Protein description	Putative methylation site	Score (%)
AN8224	glutamyl-tRNA synthetase	K71	86
AN8216	nucleoside diphosphate kinase	K76, K786	89, 95
AN6150	GTP-binding protein	K1243	88
AN10202	ATPase, member of heat shock protein 70 family	R197, K380	85, 89
AN3469	histone-2B	K40	82
AN5989	NAD-dependent epimerase/dehydratase	K90	88

3.2.8 Does SasA interact with the velvet complex?

The putative methyltransferase LaeA is part of the trimeric velvet complex and coordinates sexual development and secondary metabolism. Sequence analysis showed that SasA possesses a SAM-binding motif (Bok *et al.*, 2004). For interaction studies of SasA with the velvet complex, several *tap*-tagged velvet strains were designed and tandem affinity purification was performed after different time periods of asexual and sexual development.

By using a double *tap*-tagged *veA*::*ctap*/*velB*::*ctap* strain, besides the already known interaction partners VosA (a velvet family protein) and LaeA, we could also identify the SAM synthetase SasA as putative interaction partner of VeA and VelB (Tab. 14). SasA was detected in protein extracts of sexual grown cultures after 32 hours of development. Unfortunately, SasA could only be identified in one round of purification. These findings indicate a weak or transient interaction of SasA with the velvet complex.

Tab. 14: Peptides identified by LC-MS/MS from strain *veA*::*ctap*/*velB*::*ctap*. Identified proteins of *A. nidulans* (AN) by TurboSEQUEST analysis of the ESI-MS/MS2 data, protein coverage and TurboSEQUEST cross-correlation values of the identified peptides (X_{corr}) are given. M* = oxidized methionine.

	Peptide sequence	**% aa coverage**	**X_{corr}**
AN1052 (VeA)			
	R.PSYGQPSQTTSLPPLR.H	2.97	4.93
	R.RPDQYAGSDAYANAPERPR.S	3.53	6.05
	R.STSISTNM*DPYSYPSR.R	3.16	3.89
	R.NQSISEYEPSM*GYPGSQTR.L	3.72	4.48
	R.RPSAVEYGQPIAQPYQR.P	3.16	5.1
	K.LSSPQEFLEFR.L	2.04	3.69
	K.KFPGLTTSTPISR.M	2.42	3.38
	R.LWETNSM*LSK.R	2.04	2.85
	R.TEDYDYDNER.G	1.86	3.54
	K.DATEGTQPM*PSPVPGK.L	3.16	3.62
	R.SSLLDGPDQM*AYK.R	2.60	3.71
	R.HSLEPSVNSR.S	1.86	3.01
	K.FPGLTTSTPISR.M	2.23	3.11
	R.LSAERPSYGQPSQTTSLPPLR.H	3.90	3.9
	R.AGYFIFPDLSVR.N	2.23	3.08
	R.LEVISNPFIVYSAK.K	2.60	3.6
	K.RTEDYDYDNER.G	2.04	2.26
AN0363 (VelB)			
	K.SVSDLPQSDIAEVINK.G	4.32	4.95
	K.KFPGVIESTPLSK.V	3.51	3.83
	R.IWSLQVVQQPIR.A	3.24	4.4
	R.NLIGCLSASAYR.L	3.24	4.45
	K.FPGVIESTPLSK.V	3.24	3.64
	K.GTAPILASTFSEPFQVFSAK.K	5.41	5.02
	R.LKFSFVNVGK.S	2.70	3.17
	R.LIVKDAQTQK.E	2.70	2.99
	K.FSFVNVGK.S	2.16	2.64
	K.VFANQGIK.I	2.16	2.52
	R.RPITPPPCIR.L	2.70	3.09

Tab. 14 continued: Peptides identified by LC-MS/MS from strain *veA*::*ctap*/*velB*::*ctap*.

	Peptide sequence	**% aa coverage**	**X_{corr}**
AN0363 (VelB)			
	R.AHSGHHPPPLSM*DR.I	4.05	2.62
	R.TEGIFR.L	1.62	1.61
AN0807 (LaeA)			
	R.VSESLIYAPHPTNGR.F	4.14	2.72
	R.YAVAGGPAPWNR.N	3.31	3.94
	K.QATAETM*RPIAHSSR.D	4.42	2.54
	K.QATAETMRPIAHSSR.D	4.14	2.14
	R.IQQLAADVK.S	2.49	3.21
AN1959 (VosA)			
	R.TAPRPEEYPQAAIPR.S	3.36	3.7
	K.SFPGM*AESTFLSR.S	3.14	2.67
	R.DYSYYAPVKR.Q	2.24	1.79
	R.KPVDPPPIVQIR.V	2.69	3.13
	R.SFADQGVK.L	1.79	1.56
AN1222 (SasA)			
	R.FVIGGPQGDAGLTGR.K	3.87	4.39
	R.TVYHIQPSGR.F	2.58	2.49

4 Discussion

4.1 Activation of a silent PKS gene cluster in *A. nidulans*

4.1.1 A novel approach for activation of silent gene clusters by impairment of the protein degradation machinery

Identification of silent and orphan gene clusters is of broad interest for biotechnology, including pharmaceutical or food industry (Frisvad *et al.*, 2007). Only a fraction of all presumed biosynthetic genes and their products are known and it is necessary to develop new tools for activation of silent gene clusters. We showed here the successful application of a new approach to awaken silenced biosynthetic gene clusters, which resulted in the identification of a bioactive compound that was not described in *Aspergillus nidulans* before. This approach is based on the idea that interruption of the protein degradation machinery can lead to an increased stabilization of regulators including transcriptional activators for biosynthetic gene clusters. We chose the deletion of the *csnE* gene, encoding a subunit of the COP9 signalosome (CSN complex), where we had observed metabolic changes in former studies (Busch *et al.*, 2003, Nahlik *et al.*, 2010). The multiprotein complex CSN is highly conserved in eukaryotes (Wei *et al.*, 1994) and plays a crucial role in control of ubiquitin-mediated protein degradation in the cell (Braus *et al.*, 2010). The *csnE* deletion of *A. nidulans* is not only altered in secondary metabolite production, but is also blocked in sexual development (Busch *et al.*, 2007, Nahlik *et al.*, 2010).

Previously established strategies to activate silent gene clusters can be divided into environmental approaches, often affecting several pathways of an organism, or molecular genetic approaches, targeting single or multiple pathways, respectively (see chapter 1.3). The environmental OSMAC or the 'inter-species crosstalk' approaches can activate many different silenced gene clusters in an organism. However, it can be tedious and difficult to find the specific growth conditions under a variety of parameters and organisms (Bode *et al.*, 2002, Schroeckh *et al.*, 2009, Zähner *et al.*, 1982). Molecular genetic approaches can concentrate on a single gene cluster by expressing the complete gene cluster heterologously in a different host organism (Sakai *et al.*, 2008). However, especially PKS and NRPS containing gene clusters are very large in size what makes this strategy challenging. Expression of transcription factor encoding genes, located within a cluster, by inducible promoters is a successful strategy (Bok *et al.*, 2006b), but might require that many gene clusters have to be

identified and tested in a fungus. Unfortunately, gene clusters can also contain more than one or even lack transcription factor encoding genes.

The CSN5 based approach, that is described here, activates multiple biosynthetic gene clusters in an organism. The advantage of this approach is that no deeper knowledge of possibly present gene clusters is necessary and the amount of transcription factors in the cluster is primarily non-relevant, although this method can be combined with our approach in a later stage of the analysis. Furthermore, *csn* is highly conserved among eukaryotes and can be easily identified in uncharacterized fungi.

4.1.2 The *dba* gene cluster and heterochromatin

We assume that CSN represses activation of the *dba* cluster. This could happen on different levels, like directly destabilizing the transcription factor DbaA, or by epigenetic control, influencing directly or indirectly heterochromatin structure. Previous studies showed that activation of silent gene clusters can be achieved by deleting genes involved in heterochromatin formation or modification, or by deleting members of the COMPASS complex, a transcriptional effector, regulating chromatin-mediated processes (Bok *et al.*, 2009, Shwab *et al.*, 2007). We also have some evidence that transcription of the *dba* gene cluster is repressed by heterochromatin (Fig. 21). A hypothesis to explain the phenomenon of lost pigmentation after several generations is a possible toxic effect of the *dba* gene cluster products on *A. nidulans* itself. The direct PKS product DHMBA showed no toxicity against *A. nidulans* in an agar diffusion test, but the yellow pigments might contribute to toxicity. This would also explain repression of the gene cluster in wild type. The *dba* products might be active against competitors and used as defence mechanism, but under normal conditions *dba* products are not synthesized by *A. nidulans*, because they might be self-harming. This hypothesis is emphasized by the fact that all mutant strains producing the yellow pigments (*dbaA* OE, Δ*dbaB*/*dbaA* OE, Δ*dbaC*/*dbaA* OE, Δ*dbaE*/*dbaA* OE and Δ*dbaF*/*dbaA* OE) are reduced in colony diameter and spore production. In contrast, the deletion strain of *dbaD*, encoding the transporter, released no pigments to the growth medium and consequently showed no growth defects. A possible intracellular accumulation of pigments apparently does not affect growth of the mutant.

4.1.3 Correlation between the neighbored *dba* and *ors* gene clusters

Transcriptional profiling of the *A. nidulans csnE* deletion strain had shown that many genes involved in secondary metabolism are misregulated (Nahlik *et al.*, 2010). Besides the newly identified DHMBA gene cluster *dbaA-dbaI*, controlled by the transcription factor DbaA, also the recently identified orsellinic acid gene cluster *orsA-orsE* (Schroeckh *et al.*, 2009) was partially upregulated in Δ*csnE* (Tab. 8), which was verified by UPLC TOF-MS data, showing orsellinic acid assigned to prototype 8 in 1D-SOM clustering (Fig. 24B). Interestingly, the *dba* cluster is located directly 5'-upstream of the orsellinic acid gene cluster. The *ors* gene cluster, which is silenced under standard laboratory conditions, was identified by cocultivation of *A. nidulans* with actinomycetes, which are bacterial competitors of the fungus. The physical fungal-bacterial interaction led to the transcriptional activation of several silenced gene clusters, which might contribute to defence mechanisms of the fungus. Besides the *ors* gene cluster also parts of the *dba* gene cluster were activated (Schroeckh *et al.*, 2009).

By deletion of the PKS gene *dbaI* in Δ*csnE* background, orsellinic acid production was diminished, suggesting an interaction of both gene clusters (Fig. 24B). Recently, a cooperation of the PKSs DbaI and OrsA was also hypothesized by the group of Mortensen (Nielsen *et al.*, 2011). In an OSMAC approach, they analyzed different PKS deletion strains, among them the PKS encoding *dbaI* (AN7903) and *orsA* (AN7909). Although they did not identify the product of the PKS DbaI, they showed that both PKS deletions lead to a loss of F9775-A and F9775-B production, even though both compounds could not be detected during our work.

Our data show, that our new approach awakens and enhances the expression of many different gene clusters in *A. nidulans*. 184 out of 895 metabolic marker candidates, which were upregulated in Δ*csnE* compared to wild type strain indicate the great influence of the COP9-signalosome on metabolite production (Nahlik *et al.*, 2010). Additionally, the novel gene cluster does not act independently, but might cooperate with its neighbored orsellinic acid gene cluster.

4.1.4 DHMBA is the direct PKS product

The deduced amino acid sequence of the PKS gene *dbaI* showed similarities to five conserved domains: the essential *β*-ketoacyl synthase (KS), acyl transferase (AT), and acyl carrier

protein (ACP) domains, and the optional methyl transferase (MT) and thioester reductase (R) domains (Fig. 41A). The R domain is responsible for reduction of the thioester to an aldehyde during release of the PKS product (Bailey *et al.*, 2007). In addition to these domains, also the recently identified starter unit acyl transferase (SAT) and product template (PT) domains were found in DbaI. The SAT domain with the conserved GXCXG motif is located at the N-terminal region of the protein and selects the acyl starter unit (Chiang *et al.*, 2010). The PT domain is located between the AT and ACP domain and is supposed to control the ketide chain length. These identified domains were consistent with the structure of DHMBA. DHMBA is build up from five ketide units, one additional methyl group and one aldehyde group, proposing it as the direct product of DbaI (Fig. 41B).

Experimental proof that DHMBA is the direct product of DbaI is based on deletion mutants of the genes in the cluster (Fig. 23B and Fig. 27). All deletions of the cluster except for the transcription factor *dbaA* or the polyketide synthase *dbaI* could still produce DHMBA while the cluster was activated (Fig. 24B and Fig. 28).

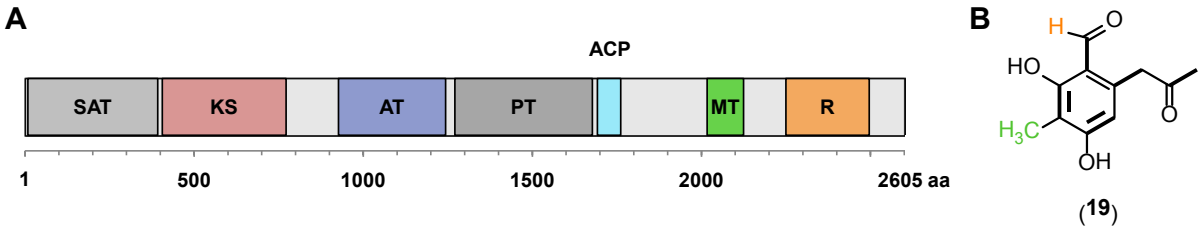

Fig. 41: Comparison of PKS domains with DHMBA structure. **A**: Schematic presentation of the polyketide synthase DbaI (AN7903) and its conserved domains. SAT = starter unit acyl transferase, KS = β-ketoacyl synthase, AT = acyl transferase, PT = product template, ACP = acyl carrier protein, MT = methyltransferase, R = thioester reductase. **B:** Chemical structure of DHMBA (**19**). Bold bonds = pentaketide skeleton, orange = hydrogen of aldehyde group produced by thioester reductase subunit of PKS, green = methyl group introduced by methyltransferase subunit of PKS.

4.1.5 A model for the biosynthesis of DHMBA

The deduced amino acid sequences of the proteins encoded by the *dba* gene cluster (plus AN7893-7895) were analyzed in silico in more detail. A BLAST (NCBI) search revealed that the amino acid sequences show similarities to proteins of the citrinin-producing cluster of the mold *Monascus purpureus* and the methylorcinaldehyde-producing cluster of the mold *Acremonium strictum* (protein identities are given in Tab. 15). The protein sequences of AN7893, DbaA and DbaE have identities between 39% and 49% to an oxygenase, a transcriptional activator and an oxidoreductase of the citrinin-producing cluster of

M. purpureus. The protein sequence of DbaI reveals 47% identity to the citrinin-producing PKS of *M. purpureus*, and 47% identity to the methylorcinaldehyde-producing PKS (MOS) of *Acremonium strictum*.

Tab. 15: Protein identities of *Aspergillus nidulans* proteins upregulated in Δ*csnE* and their homologous proteins in *Monascus purpureus* and *Acremonium strictum*. Protein identities were determined by BLAST search (NCBI).

Protein in *A. nidulans*	**Homologous protein in *M. purpureus* and *A. strictum***	**Protein identity**	**Function**
AN7893	CtnA[5]	43%	citrinin oxygenase
DbaA	CtnR[5]	39%	citrinin transcriptional activator
DbaE	CtnB[5]	49%	citrinin oxidoreductase
DbaI	citrinin PKS[5]	47%	citrinin polyketide synthase
	methylorcinaldehyde PKS[6]	47%	methylorcinaldehyde polyketide synthase

[5] Homologous protein in *M. purpureus*. [6] Homologous protein in *A. strictum*.

Methylorcinaldehyde (**21**, Fig. 42) is a tetraketide and the precursor of the pharmacologically relevant Xenovulene A that is able to displace high affinity ligands from the γ-aminobutyric acid $GABA_A$ receptor. The structures of methylorcinaldehyde and DHMBA differ only in the ligand at the 3'-position of the phenol ring.

Citrinin (**22**, Fig. 42) is a polyketide derived from several *Monascus*, *Penicillium* and *Aspergillus* species (Deruiter *et al.*, 1992, Hajjaj *et al.*, 1999, Sankawa *et al.*, 1983, Shimizu *et al.*, 2005), but has not been identified in *A. nidulans*. It exhibits antibiotic activity against Gram-positive bacteria, but, due to its nephrotoxic properties to mammalian cells, it is not used in medicine. Its biosynthesis was decrypted by ^{13}C-NMR in *Monascus ruber* (Hajjaj *et al.*, 1999). It is formed by a tetraketide precursor derived from one acetyl-CoA and three malonyl-CoA units with a subsequent addition of one acetyl-CoA to the tetraketide precursor. Formerly, it was proposed that citrinin is build up from a pentaketide precursor (one acetyl-CoA and four malonyl-CoA molecules).

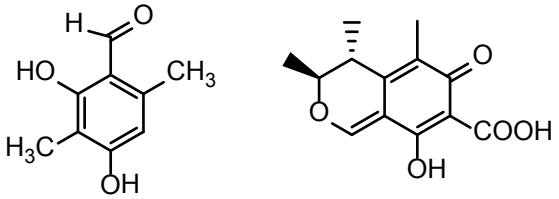

(**21**) (**22**)

Fig. 42: Chemical structures of methylorcinaldehyde (**21**) and citrinin (**22**).

A phylogenetic analysis of the PT domains of different PKSs, of which the products are already identified, was performed (Fig. 43A). The PT domain is supposed to be involved in chain length control and therefore, we expect to gain insight into the biosynthesis of DHMBA. Interestingly, the phylogenetic analysis showed that DHMBA is closely related to tetraketides, although it is build up from five ketide units. It seems that instead of the expected pentaketide precursor, DHMBA is, like citrinin, derived from a tetraketide precursor with the following addition of one acetyl-CoA (Fig. 43B). Subsequent methylation, cyclization and reductive release result in the final PKS product DHMBA.

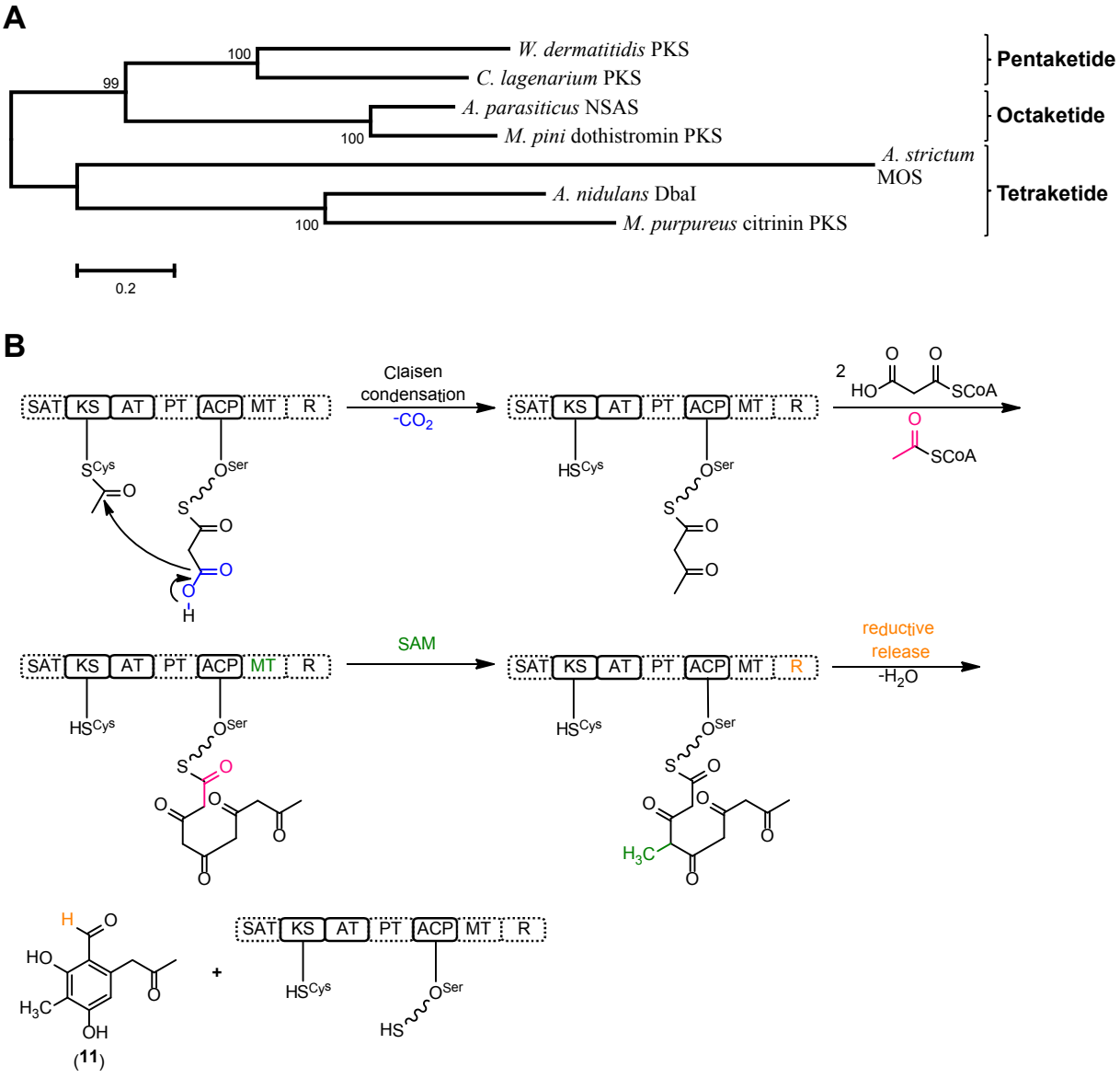

Fig. 43: Model for DHMBA biosynthesis. **A:** Phylogenetic tree of PT domains of different PKSs. GenBank Accession numbers for sequences are: *Wangiella dermatitidis* PKS (AAD31436.3), *Colletotrichum lagenarium* PKS (BAA18956.1), *A. parasiticus* norsolorinic acid synthase NSAS (3HRQ_A), *Mycosphaerella pini* dothistromin PKS (AAZ95017.1), *Acremonium strictum* MOS (CAN87161), *A. nidulans* DbaI (AN7903), *Monascus purpureus* citrinin PKS (BAD44749.1). The evolutionary history was inferred using the Neighbor-Joining method (Saitou *et al.*, 1987). The percentage of replicate trees, in which the associated taxa clustered together in the bootstrap test (1000 replicates), are shown next to the branches (Felsenstein, 1985). The tree is

drawn to scale, with branch lengths in the same units as those of the evolutionary distances used to infer the phylogenetic tree. The evolutionary distances were computed using the p-distance method (Nei *et al.*, 2000) and are in the units of the number of base differences per site. Evolutionary analyses were conducted in MEGA5 (Tamura *et al.*, 2011). **B:** Proposed biosynthesis of DHMBA (**11**). DHMBA is derived from a tetraketide, formed by one acetyl-CoA and three malonyl-CoA, with the subsequent addition of another acetyl-CoA, methylation, cyclization and reductive release.

4.1.6 Azaphilones and sinapic aldehyde

DHMBA was identified as the direct product of the PKS DbaI. But, production of this colorless compound does not explain the yellow color observed in cultures of *dbaA* overexpression strain. Deletion of *dbaH*, encoding a putative oxygenase, in overexpressing *dbaA* background led to an accumulation of DHMBA, whereas the production of the yellow pigments ceased (Fig. 28). We concluded that DHMBA might be oxidized by the oxygenase DbaH to the yellow metabolites.

DHMBA was isolated before from *S. chrysospermum* (Mitova *et al.*, 2006), but never from aspergilli. Some compounds similar to DHMBA have been isolated before from fungi, like the orsellinaldehyde (**23**, Fig. 44) isolated from *Aspergillus rugulosus* (Ballantine *et al.*, 1968), or methylorcinaldehyde (**21**, Fig. 42) from *Acremonium strictum* (Bailey *et al.*, 2007).

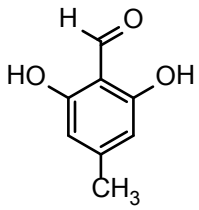

(**23**)

Fig. 44: Chemical structure of orsellinaldehyde (**23**).

DHMBA had been known as intermediate in the synthesis of azaphilones (Suzuki *et al.*, 2001). Azaphilones are a structurally diverse class of secondary metabolites. They are pigments with pyrone-quinone structures, containing a highly oxygenated bicyclic core and quaternary center, like the yellow citrinin (**22**, Fig. 42). Some of them show biological activities, like antimicrobial and antitumor activities (Dong *et al.*, 2006, Phonkerd *et al.*, 2008, Yasukawa *et al.*, 1994) and recently, the application of azaphilones as future food colorants has been proposed (Mapari *et al.*, 2010). Several azaphilones have been identified from different fungal species, like *Monascus*, *Penicillium*, *Epicoccum*, and also *Aspergillus* species (Osmanova *et al.*, 2010, Shao *et al.*, 2011). Azaphilones are biosynthetically classified as a

subgroup of polyketides, but a comprehensive knowledge of the biosynthetic pathway is not yet available. Many azaphilones are synthesized from precursors similar to DHMBA, variably substituted at the 3'-position. According to their biosynthesis, we suggest the following model (Fig. 45) for the biosynthesis of the putative azaphilone 8-hydroxy-3,7-dimethyl-6H-2-benzopyran-6-one (**24**, Fig. 45) from the DHMBA precursor (**19**, Fig. 45). We propose 8-hydroxy-3,7-dimethyl-6H-2-benzopyran-6-one (**24**, Fig. 45) as one of the pigments contributing to the color in *dbaA* OE and Δ*csnE* strains.

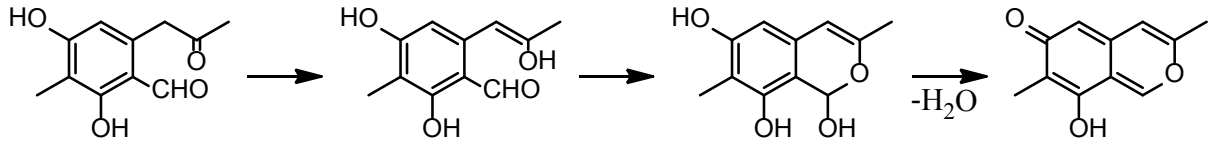

(**19**) (**24**)

Fig. 45: Model for the proposed biosynthesis of the azaphilone 8-hydroxy-3,7-dimethyl-6H-2-benzopyran-6-one (**24**) derived from DHMBA (**19**).

Interestingly, Yang *et al*. isolated a metabolite (**25**, Fig. 46A) synthesized from an azaphilone and orsellinic acid by an *Aspergillus* sp. culture (Yang *et al.*, 2009). We already suggested a cooperation between the *dba* and the *ors* gene cluster in chapter 4.1.3. According to this, a putative metabolite synthesized from DHMBA and orsellinic acid could be **26** (Fig. 46B).

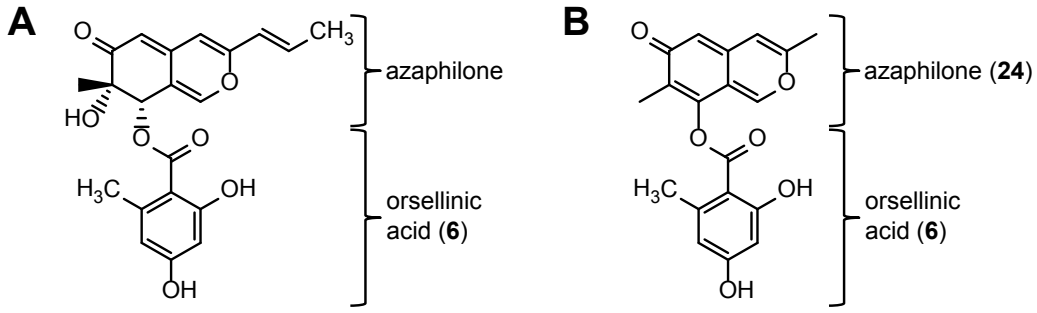

(**25**) (**26**)

Fig. 46: Metabolites derived from orsellinic acid and azaphilones. **A:** Chemical structure of Sch 1385568 (**25**) produced by *Aspergillus* sp. (Yang *et al.*, 2009). **B:** Proposed chemical structure for a metabolite (**26**) putatively synthesized from orsellinic acid (**6**) and 8-hydroxy-3,7-dimethyl-6H-2-benzopyran-6-one (**24**).

The *dbaA* overexpression strain is characterized by yellow pigments released to the growth medium. Besides the colorless DHMBA, we could identify masses of 21 metabolites by UPLC-TOF-MS analysis, which are not present in wild type, seven of them with UV maxima between 350 and 400 nm, indicating a yellow color. Interestingly, DHMBA with the sum

formula $C_{11}H_{12}O_4$ is an isomer of sinapic aldehyde, which is part of the lignin biosynthesis pathway in plants. By database comparison, several masses of our 21 metabolites correlate with masses of the sinapic aldehyde pathway. In Fig. 47, a proposed biosynthetic pathway similar to that of sinapic aldehyde is depicted. The aldehyde DHMBA ($C_{11}H_{12}O_4$, **19**, Fig. 47) can be oxidized to the carboxylic acid $C_{11}H_{12}O_5$ (**27**, Fig. 47), which in turn can be reduced to an alcohol $C_{11}H_{14}O_4$ (**28**, Fig. 47). Furthermore, a CoA-activated DHMBA can undergo a reaction with three malonyl-CoA moieties and build a lactone ($C_{17}H_{16}O_7$, **29**, Fig. 47) or a chalcone ($C_{17}H_{16}O_7$, **30**, Fig. 47), respectively (Sinlapadech *et al.*, 2007).

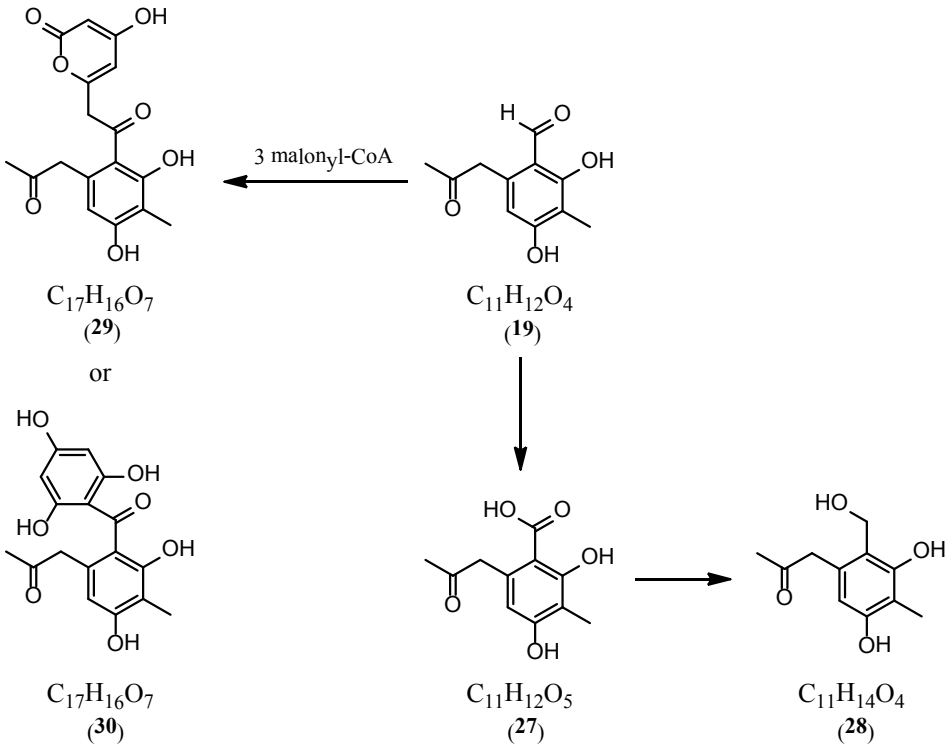

Fig. 47: Proposed biosynthetic pathway of DHMBA (**19**) modifications, similar to the pathway of its isomer sinapic aldehyde. DHMBA (**19**) can be oxidized to the carboxylic acid $C_{11}H_{12}O_5$ (**27**), which in turn can be reduced to an alcohol $C_{11}H_{14}O_4$ (**28**). A CoA-activated DHMBA can undergo a reaction with three malonyl-CoA moieties and build a lactone $C_{17}H_{16}O_7$ (**29**) or a chalcone $C_{17}H_{16}O_7$ (**30**), respectively.

4.1.7 The oxygenase DbaH and sexual development

Deletion of *dbaH* in *dbaA* overexpression background led to an accumulation of DHMBA and a loss of yellow pigment production. Besides these metabolic changes, also the developmental phenotype was altered. The mutant produced very few cleistothecia, which were delayed in pigmentation. A correlation between PKS gene cluster expression and sexual development has been recognized before in *Neurospora crassa* and *Sordaria macrospora* (Nowrousian, 2009). In both organisms, the deletion mutant of the oxygenase encoding *fbm1* (fruiting body

maturation 1), which is member of a PKS gene cluster, also showed fewer and delayed fruiting body formation. Although the *dbaH* and *fbm1* sequences show no similarities, they might play a similar role in the respective organism.

4.1.8 The diindole DHPDI and a possible cluster crosstalk

The follow-up experiments of the comparison of the *dbaA* OE mutant and wild type resulted in a second compound isolated from wild type *A. nidulans*, which was identified as 3,3-(2,3-dihydroxypropyl)diindole (DHPDI). It is known to be produced by *Balansia epichloë* and *Oceanibulbus indolifex* (Porter *et al.*, 1977, Schröder, 2001, Wagner-Dobler *et al.*, 2004), but like DHMBA, DHPDI has not been described in an *Aspergillus* species until now. Interestingly, this nitrogen containing metabolite, probably build up from tryptophan, is not produced anymore when *dbaA* is overexpressed. This suggests a possible role of DbaA as regulator for more than only one gene cluster. A recently published study showed, that transcription factors do not exclusively regulate the gene cluster they are embedded in, but they are also able to navigate the cross-talk between gene clusters located even on different chromosomes (Bergmann *et al.*, 2010). Bergman *et al.* identified a novel NRPS gene cluster. Its regulator ScpR (secondary metabolism cross-pathway regulator) activated transcription of the NRPS genes *inpA* and *inpB* on chromosome II and, additionally, the expression of the asperfuranone gene cluster on chromosome VIII. Here, DbaA might additionally regulate expression of an indole producing gene cluster or, instead of DbaA, the cluster product DHMBA itself takes over the regulatory role of turning-on an indole gene cluster. Additionally, we identified masses of 21 metabolites in the *dbaA* overexpressing strain, among them three nitrogen containing compounds, emphasizing our hypothesis of inter-cluster crosstalk. In Δ*csnE* we observed a reduced production of the aflatoxin precursor ST (Nahlik *et al.*, 2010), whereas *dbaA* overexpression did not affect ST production (Fig. 19), implying independence of *dbaA* from the well-studied ST gene cluster.

4.2 Characterization of the SAM synthetase in *A. nidulans*

SAM synthetases are highly conserved proteins as they catalyze the synthesis of the major methyl group donor SAM. The number of SAM synthetases in an organism can vary between one and multiple isoforms. In the filamentous fungus *Aspergillus nidulans* one SAM synthetase encoding gene, that was named *sasA*, was identified. Its deduced amino acid

sequence possesses two known conserved motifs and shows high similarities to SAM synthetases from other organisms. A phylogenetic analysis revealed highest similarities to SAM synthetases of other filamentous fungi. Interestingly, *A. flavus* and *A. oryzae* possess two isoforms of SAM synthetases with only 55% amino acid identity. Also *S. cerevisiae* has two isoforms but with a high identity of 91%. It will be interesting to analyze this phenomenon in the future.

4.2.1 Expression of *sasA* in the *csnE* deletion strain

During transcriptomic and proteomic analysis of the COP9 impaired *csnE* deletion strain, also expression levels of *sasA* transcript and its encoded protein were analyzed (Nahlik *et al.*, 2010). Deletion of *csnE* significantly increased the SAM synthetase mRNA and protein levels. SasA is involved in the biosynthesis of cysteine, which is a precursor for the antioxidant glutathione. As Δ*csnE* is hypersensitive to oxidative stress, an enriched amount of glutathione might be needed for protection against damaging reactive oxygen species.

4.2.2 SAM synthetase encoding genes are essential

We could provide evidence that the single SAM synthetase gene of *A. nidulans* is essential. This is not surprising as SAM synthetases catalyze the reaction from methionine to SAM and this methyl donor is essential for numerous reactions in the cell. The deletion of *sam1* in *Schizosaccharomyces pombe* was also lethal, as it carries only one SAM synthetase encoding gene (Hilti *et al.*, 2000). In organisms with two SAM synthetase encoding genes, like *S. cerevisiae*, the deletion of one gene can be compensated by the other gene and both genes need to be deleted to achieve lethality (Cherest *et al.*, 1978).

4.2.3 SAM synthetases and development

In the filamentous fungus *A. nidulans* we could show an impact of *sasA* overexpression on development and secondary metabolism. This is in contrast to the filamentous fungus *Neurospora crassa* where overexpression of the SAM synthetase encoding gene *eth-1* led to no phenotypical changes in growth rate or morphogenesis (Mautino *et al.*, 1996). In the yeast *Schizosaccharomyces pombe*, underexpression of *sam1* resulted in reduced growth, mating and sporulation, while overexpression led to methionine sensitive growth, which was partially

abolished by the addition of adenine (Hilti *et al.*, 2000). Expression effects of SAM synthetase encoding genes have also been examined in other kingdoms. Overexpression and suppression of the plant *Arabidopsis thaliana sam1* in tobacco led to developmental defects, as yellow leaves, reduced plant height, necrotic lesions and stunted plants (Boerjan *et al.*, 1994). Additionally, the secondary metabolism was influenced. During overexpression, the nicotine and nornicotine biosynthesis was enhanced (Belbahri *et al.*, 2000), while during repression, the plants produced the volatile methanethiol, resulting in a disagreeable odor (Boerjan *et al.*, 1994). An influence of SAM synthetase gene expression levels on development was also observed in *Bacillus subtilis*. Mutants overexpressing this gene showed increased spontaneous sporulation (Ochi *et al.*, 1982). In *E. coli* underexpression of the SAM synthetase encoding gene *metK* resulted in an abnormal cell division. The septal ring formation was blocked, resulting in the formation of filaments (Newman *et al.*, 1998, Wang *et al.*, 2005). A possible explanation for missing overexpression phenotypes in some organisms is that the SAM synthetases in *E. coli* (Markham *et al.*, 1983), *Trypanosoma brucei* (Yarlett *et al.*, 1993), *S. cerevisiae* (Thomas *et al.*, 1991), human and rat liver (Cabrero *et al.*, 1988, Corrales *et al.*, 1991, Corrales *et al.*, 1992, Duce *et al.*, 1988) are negatively regulated by its product SAM, in order to maintain normal SAM concentrations in the cell. But this is not the case in *A. nidulans* and *S. pombe* (Hilti *et al.*, 2000, Pieniazek *et al.*, 1973). Exogenously added methionine induced *sasA* expression in *A. nidulans* and drastically increased the intracellular SAM levels in *S. pombe*. Therefore, the impact of SAM synthetases on growth, morphogenesis and secondary metabolism might not be specific for *A. nidulans*, but reflects a much more general cellular feature.

4.2.4 SAM synthetases and protein complexes

Methyltransferases transport the methyl group of SAM to its target substrate. The tandem affinity purification (TAP) method allows to identify large relatively stable protein complexes (Bayram *et al.*, 2008, Gavin *et al.*, 2002), whereas the yeast-two-hybrid assay shows binary interactions which might be transient. Therefore several proteins found to act within the same metabolic pathway or during the same developmental stage by TAP might be part of a larger complex. In *S. cerevisiae,* the glutamyl-tRNA synthetase Gus1 forms a complex with the methionyl-tRNA synthetase Mes1 and the cofactor Arc1, corroborating our results (Deinert *et al.*, 2001, Galani *et al.*, 2001). SAM synthetases catalyze the reaction from methionine to SAM. This is consistent with the co-purification of SasA with proteins involved in methionine

metabolism, which might act in a complex together. The interaction partners we found for SasA might be composed of methylation targets (candidates are described in Tab. 13) and associated proteins.

Fluorescence microscopy showed that SasA is primarily localized to the cytoplasm, whereas mitochondrial or nuclear subpopulations are significantly less pronounced. Similarly, the *S. cerevisiae* SAM synthetases are primarily cytoplasmic. A yeast mitochondrial carrier protein Sam5 transports SAM from cytoplasm to mitochondria, where it is needed for biotin biosynthesis (Marobbio *et al.*, 2003). We found mitochondrial proteins, which are involved in citrate cycle, and proteins, which act in malate-aspartate shuttle, as putative SasA interaction partners. The interaction of these proteins with SasA might occur outside of the mitochondria or might reflect small mitochondrial SasA subpopulations.

SasA is highly produced during vegetative and early developmental growth at mRNA and protein levels. The identified interaction partners suggest multiple cellular roles of SasA. Early stages of development require changes in morphogenesis and an increased cell division rate. The corresponding co-purified SasA interaction partners and the developmental overexpression phenotypes, including colony diameter, spore production and viability, suggest a function of SasA during fungal morphogenesis. Some of these functions might be at least partially conserved, because the yeast homologue Sam1 also recruits proteins required for morphogenesis like the aconitase Aco1 and α-tubulin Tub1 (Gavin *et al.*, 2006), and additionally the cobalamin-independent methionine synthetase Met6 (Malkowski *et al.*, 2007) and the heat shock protein Ssa1 (Gong *et al.*, 2009). Furthermore, Aco1 was found to interact with calmodulin Cmd1 (Krogan *et al.*, 2006), which interacts with actin Act1 (Collins *et al.*, 2007) and the nucleoside diphosphate kinase Ynk1 (Ho *et al.*, 2002), supporting the idea of co-interactions with Sam1 in accordance with our results.

4.2.5 SAM-dependent methyltransferases

SAM-dependent methyltransferases were not co-purified with SasA by TAP. This is presumably the consequence of weak or transient interactions of SasA with methyltransferases. Similarly, a yeast proteome study also did not reveal any methyltransferases as interaction partners of SAM synthetases (Gavin *et al.*, 2006). The putative methyltransferase LaeA possesses a conserved SAM binding motif, which is typical for arginine and histone methyltransferases (Bok *et al.*, 2004). LaeA is known as a global regulator of secondary metabolism and as a part of the trimeric velvet complex, coordinating

sexual development and secondary metabolism (Bayram *et al.*, 2008). We cannot exclude a direct interaction between SasA and LaeA, which might not be stable enough to detect with the TAP protocol. Another possibility is an indirect link between LaeA and SasA provided by the VelB-VeA heterodimer. TAP-tagged VelB or TAP-tagged VeA did not recruit SasA (Bayram *et al.*, 2008), but a strain where both velvet domain proteins were TAP-tagged could recruit SasA (Tab. 14), suggesting a possible weak or transient interaction between SasA and the velvet protein complex. This is supported by the *sasA* overexpression and the *laeA* deletion phenotype, which both result in defects in the coordination of secondary metabolism and development. It is tempting to speculate that overexpression of *sasA* leads to dysfunction of sexual reproduction due to multiple effects, including defects in the described complexes involved in cell division and morphogenesis. Overproduction of SasA might also lead to dysfunction of LaeA, which might act antagonistically to methylation on histone-2B. Therefore, not only development is disrupted, but also LaeA dependent secondary metabolite production might be impaired. Histone-3 trimethylation at lysine 9 had been found to be associated with the repression of secondary metabolism clusters in *A. nidulans* and LaeA is involved in reversal of this heterochromatin signature inside the cluster (Reyes-Dominguez *et al.*, 2010). We found an interaction of SasA with histone-2B. This is consistent with recent findings by Wu *et al.* (Wu *et al.*, 2011) that histone-2B can stimulate histone methyltransferase activity when modified at lysine 34 by ubiquitin. An interesting possibility would be, that LaeA is not only involved in modulating histone-3 signature, but also in an epigenetic control including histone-2B.

4.3 Conclusions

Despite the recent progress in development of different strategies, identification of silent secondary metabolite producing gene clusters still remains challenging. The new approach based on interrupting the protein degradation system establishes a new possibility to uncover hidden secondary metabolites in a broader manner. For the model *A. nidulans* as a paradigm of a secondary metabolite producing filamentous fungus, we could show that deletion of *CSN5/csnE* results in the activation of several clusters, which led to the identification of two new metabolites so far unknown to be produced by aspergilli. A summarizing model of the already identified actions of the previously orphaned gene cluster is shown in Fig. 48.

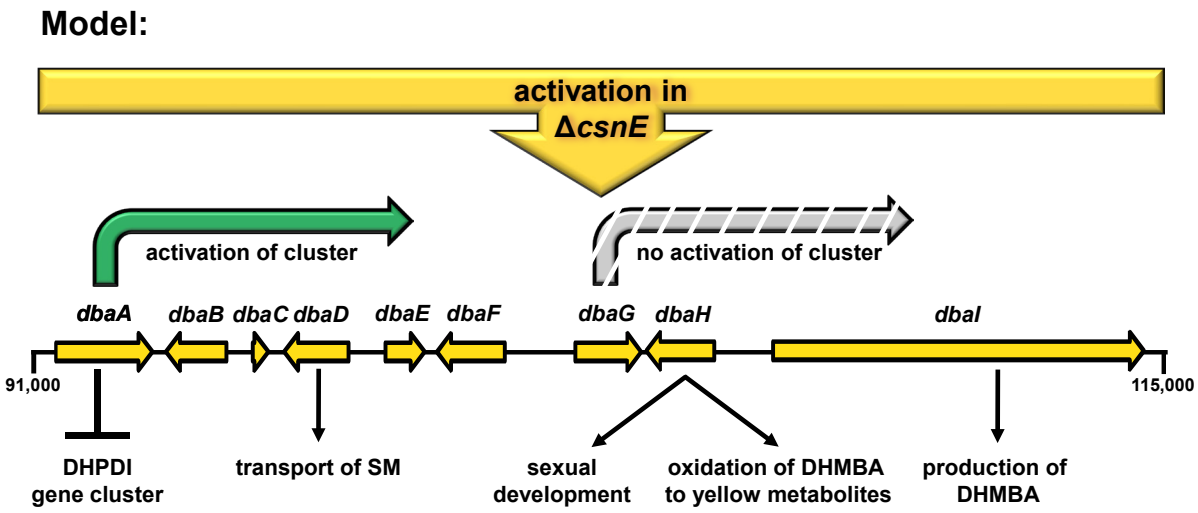

Fig. 48: Model, summarizing the actions of the novel PKS gene cluster.

The *dba* gene cluster *dbaA-dbaI* comprises eight genes, including the PKS gene *dbaI*. The specific activator of the cluster was identified as $Zn(II)_2Cys_6$-domain containing DbaA. Induced expression of *dbaA* activated expression of the complete gene cluster and interestingly, repressed a diindole DHPDI producing gene cluster, suggesting a gene cluster cross-talk. The function of the second putative transcription factor DbaG was not yet identified, although we suspect that it is involved in repressive regulation of the gene cluster. The PKS DbaI synthesizes the benzaldehyde derivative DHMBA and oxidation of DHMBA by the putative oxygenase DbaH presumably leads to the production of the yellow metabolites, which might be azaphilones. The produced metabolites are released to the growth medium by the putative transporter DbaD. Deletion of the putative oxygenase encoding *dbaH*, results in delayed fruiting body formation, suggesting an additional role in sexual development.

As shown in this study, the application of a *csn* mutant impaired in protein degradation is a highly promising approach to identify new bioactive secondary metabolites from already established model organisms as well as from new species. The CSN complex is highly conserved in eukaryotes and can be easily identified in uncharacterized species. In the future, it will be interesting to see which other secondary metabolites will be identified by this new approach from other fungi or even lower plants like algae, which also promise to have a high potential for bioactive molecules urgently required to combat multidrug-resistant microbes.

Comprehension of the regulation of gene expression is an important step in analysis of secondary metabolism. Gene expression is partially regulated by heterochromatin formation

in which SAM-dependent methylation is a crucial process. Additionally, histone methylation by methyltransferases had been proposed as control mechanism for fungal development and secondary metabolism. This function had been suggested for the global regulator of secondary metabolism, LaeA. In this study, the first comprehensive analysis of the SAM synthetase SasA of the filamentous fungus *Aspergillus nidulans* was performed. The results provide an insight into the complex network in which SasA acts (Fig. 49). As the major methyl group donor it is involved in a variety of reactions. Therefore, a precise balance of SasA levels is necessary to enable normal fungal morphogenesis, development and secondary metabolism. By generation of different *sasA* mutants and protein interaction studies, an involvement of SasA in methionine metabolism and other metabolic pathways, stress response, fungal morphogenesis and secondary metabolism was detected. Furthermore, the putative interaction of SasA to histone-2B supports a SasA mediated epigenetic link to gene expression by methylation. SasA might be part of several protein complexes, which might include methylation targets as well as associated proteins.

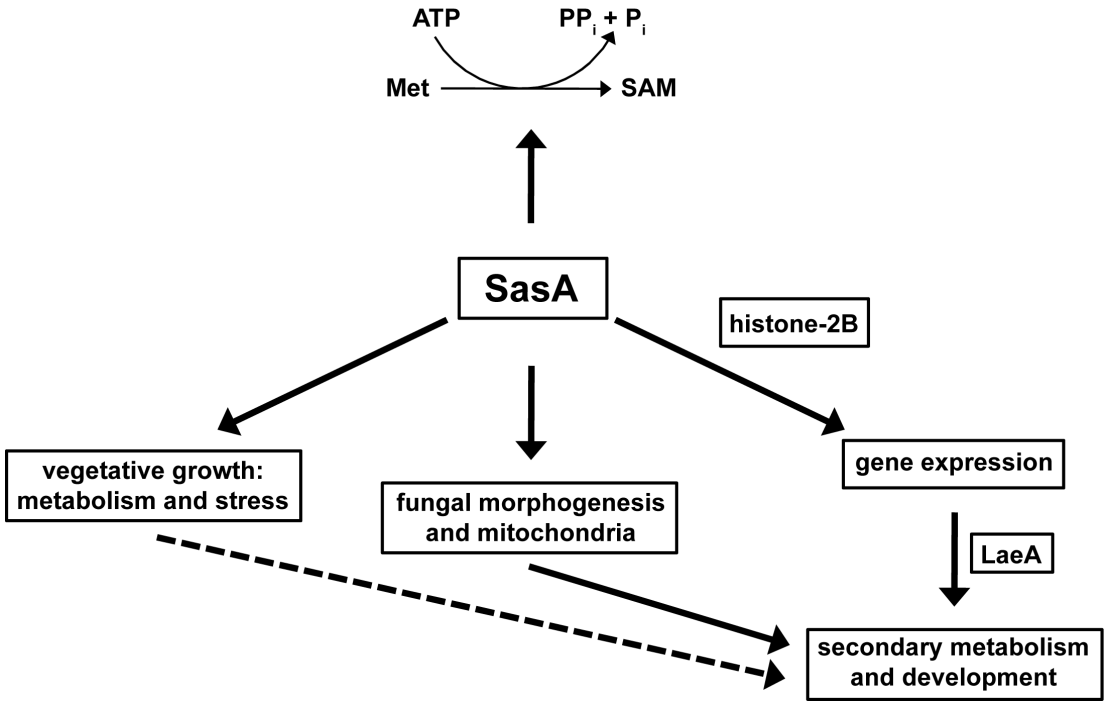

Fig. 49: Proposed model for SasA actions in *Aspergillus nidulans*. SasA catalyzes the biosynthesis of SAM from methionine (Met) and ATP. Expression of *sasA* has impact on metabolism and stress response during vegetative growth, on fungal morphogenesis including spore production, colony diameter and sexual fruiting body formation, and on mitochondrial processes. Additionally, it might be involved in coordination of development and secondary metabolism by regulating gene expression.

5 References

Adams, T. H., Wieser, J. K., Yu, J. H. (1998) Asexual sporulation in *Aspergillus nidulans*. *Microbiol Mol Biol Rev* **62**: 35-54.

Amutha, B., Pain, D. (2003) Nucleoside diphosphate kinase of *Saccharomyces cerevisiae*, Ynk1p: localization to the mitochondrial intermembrane space. *Biochem J* **370**: 805-815.

Aramayo, R., Timberlake, W. E. (1990) Sequence and molecular structure of the *Aspergillus nidulans yA* (laccase I) gene. *Nucleic Acids Res* **18**: 3415.

Arst, H. N., Jr., Cove, D. J. (1973) Nitrogen metabolite repression in *Aspergillus nidulans*. *Mol Gen Genet* **126**: 111-141.

Bailey, A. M., Cox, R. J., Harley, K., Lazarus, C. M., Simpson, T. J., Skellam, E. (2007) Characterisation of 3-methylorcinaldehyde synthase (MOS) in *Acremonium strictum*: first observation of a reductive release mechanism during polyketide biosynthesis. *Chem Commun (Camb)*: 4053-4055.

Ballantine, J. A., Hassal, C. H., Jones, B. D. (1968) The biosynthesis of phenols-XVII. Some phenolic metabolites of mutant strains of *Aspergillus rugulosus*. *Phytochemistry* **7**: 1529-1534.

Barratt, R. W., Johnson, G. B., Ogata, W. N. (1965) Wild-type and mutant stocks of *Aspergillus nidulans*. *Genetics* **52**: 233-246.

Bayram, O., Krappmann, S., Ni, M., Bok, J. W., Helmstaedt, K., Valerius, O*., et al.* (2008) VelB/VeA/LaeA complex coordinates light signal with fungal development and secondary metabolism. *Science* **320**: 1504-1506.

Bayram, O., Sari, F., Braus, G. H., Irniger, S. (2009) The protein kinase ImeB is required for light-mediated inhibition of sexual development and for mycotoxin production in *Aspergillus nidulans*. *Mol Microbiol* **71**: 1278-1295.

Bayram, O., Braus, G. H. (2011) Coordination of secondary metabolism and development in fungi: the velvet family of regulatory proteins. *FEMS Microbiol Rev*.

Belbahri, L., Chevalier, L., Bensaddek, L., Gillet, F., Fliniaux, M. A., Boerjan, W*., et al.* (2000) Different expression of an S-adenosylmethionine synthetase gene in transgenic tobacco callus modifies alkaloid biosynthesis. *Biotechnol Bioeng* **69**: 11-20.

Bennett, J. W. (1995) From molecular genetics and secondary metabolism to molecular metabolites and secondary genetics. *Can J Bot* **73**: 917-924.

Bergmann, S., Funk, A. N., Scherlach, K., Schroeckh, V., Shelest, E., Horn, U.*, et al.* (2010) Activation of a silent fungal polyketide biosynthesis pathway through regulatory cross talk with a cryptic nonribosomal peptide synthetase gene cluster. *Appl Environ Microbiol* **76**: 8143-8149.

Bjork, G. R., Ericson, J. U., Gustafsson, C. E., Hagervall, T. G., Jonsson, Y. H., Wikstrom, P. M. (1987) Transfer RNA modification. *Annu Rev Biochem* **56**: 263-287.

Bode, H. B., Bethe, B., Hofs, R., Zeeck, A. (2002) Big effects from small changes: possible ways to explore nature's chemical diversity. *Chembiochem* **3**: 619-627.

Boerjan, W., Bauw, G., Van Montagu, M., Inze, D. (1994) Distinct phenotypes generated by overexpression and suppression of S-adenosyl-L-methionine synthetase reveal developmental patterns of gene silencing in tobacco. *Plant Cell* **6**: 1401-1414.

Bok, J. W., Keller, N. P. (2004) LaeA, a regulator of secondary metabolism in *Aspergillus* spp. *Eukaryot Cell* **3**: 527-535.

Bok, J. W., Noordermeer, D., Kale, S. P., Keller, N. P. (2006a) Secondary metabolic gene cluster silencing in *Aspergillus nidulans*. *Mol Microbiol* **61**: 1636-1645.

Bok, J. W., Hoffmeister, D., Maggio-Hall, L. A., Murillo, R., Glasner, J. D., Keller, N. P. (2006b) Genomic mining for *Aspergillus* natural products. *Chem Biol* **13**: 31-37.

Bok, J. W., Chiang, Y. M., Szewczyk, E., Reyes-Dominguez, Y., Davidson, A. D., Sanchez, J. F.*, et al.* (2009) Chromatin-level regulation of biosynthetic gene clusters. *Nat Chem Biol* **5**: 462-464.

Bowman, W. H., Tabor, C. W., Tabor, H. (1973) Spermidine biosynthesis. Purification and properties of propylamine transferase from *Escherichia coli*. *J Biol Chem* **248**: 2480-2486.

Brakhage, A., Schroeckh, V. (2011) Fungal secondary metabolites - strategies to activate silent gene clusters. *Fungal Genet Biol* **48**: 15-22.

Braus, G. H., Krappmann, S., Eckert, S. E. (2002) Sexual development in ascomycetes: fruit body formation of *Aspergillus nidulans*. In: *Molecular biology of fungal development.* Osiewacz, H. D. (ed). New York, Basel: Marcel Dekker, Inc., pp. 215-244.

Braus, G. H., Irniger, S., Bayram, O. (2010) Fungal development and the COP9 signalosome. *Curr Opin Microbiol* **13**: 672-676.

Brodhun, F., Gobel, C., Hornung, E., Feussner, I. (2009a) Identification of PpoA from *Aspergillus nidulans* as a fusion protein of a fatty acid heme dioxygenase/peroxidase and a cytochrome P450. *J Biol Chem* **284**: 11792-11805.

Brodhun, F., Schneider, S., Goebel, C., Hornung, E., Feussner, I. (2009b) PpoC from *Aspergillus nidulans* is a fusion protein with one active heme. *Biochem J* **425**: 553-565.

Brown, D. W., Yu, J. H., Kelkar, H. S., Fernandes, M., Nesbitt, T. C., Keller, N. P.*, et al.* (1996) Twenty-five coregulated transcripts define a sterigmatocystin gene cluster in *Aspergillus nidulans*. *Proc Natl Acad Sci U S A* **93**: 1418-1422.

Brown, T., Mackey, K. (1997) Analysis of RNA by Northern and slot blot hybridization. In: *Current Protocols in Molecular Biology.* Ausubel, F. M., Brent, R., Kingston, R. E., Moore, D. D., Seidmann, J. G. and Smith, K. (eds). New York: John Wiley and Sons, pp. 4.9.1-4.9.16.

Busch, S., Eckert, S. E., Krappmann, S., Braus, G. H. (2003) The COP9 signalosome is an essential regulator of development in the filamentous fungus *Aspergillus nidulans*. *Mol Microbiol* **49**: 717-730.

Busch, S., Schwier, E. U., Nahlik, K., Bayram, O., Helmstaedt, K., Draht, O. W.*, et al.* (2007) An eight-subunit COP9 signalosome with an intact JAMM motif is required for fungal fruit body formation. *Proc Natl Acad Sci U S A* **104**: 8089-8094.

Cabrero, C., Duce, A. M., Ortiz, P., Alemany, S., Mato, J. M. (1988) Specific loss of the high-molecular-weight form of S-adenosyl-L-methionine synthetase in human liver cirrhosis. *Hepatology* **8**: 1530-1534.

Calvo, A. M., Wilson, R. A., Bok, J. W., Keller, N. P. (2002) Relationship between secondary metabolism and fungal development. *Microbiol Mol Biol Rev* **66**: 447-459, table of contents.

Catoni, G. L. (1953) S-Adenosylmethionine; a new intermediate formed enzymatically from L-methionine and adenosinetriphosphate. *J Biol Chem* **204**: 403-416.

Champe, S. P., Nagle, D. L., Yager, L. N. (1994) Sexual sporulation. *Prog Ind Microbiol* **29**: 429-454.

Chang, P. K., Ehrlich, K. C., Yu, J., Bhatnagar, D., Cleveland, T. E. (1995) Increased expression of *Aspergillus parasiticus aflR*, encoding a sequence-specific DNA-binding protein, relieves nitrate inhibition of aflatoxin biosynthesis. *Appl Environ Microbiol* **61**: 2372-2377.

Chant, J., Herskowitz, I. (1991) Genetic control of bud site selection in yeast by a set of gene products that constitute a morphogenetic pathway. *Cell* **65**: 1203-1212.

Cherest, H., Surdin-Kerjan, Y. (1978) S-adenosyl methionine requiring mutants in *Saccharomyces cerevisiae*: evidences for the existence of two methionine adenosyl transferases. *Mol Gen Genet* **163**: 153-167.

Chiang, P. K., Gordon, R. K., Tal, J., Zeng, G. C., Doctor, B. P., Pardhasaradhi, K.*, et al.* (1996) S-Adenosylmethionine and methylation. *FASEB J* **10**: 471-480.

Chiang, Y. M., Oakley, B. R., Keller, N. P., Wang, C. C. (2010) Unraveling polyketide synthesis in members of the genus *Aspergillus*. *Appl Microbiol Biotechnol* **86**: 1719-1736.

Cid, V. J., Duran, A., del Rey, F., Snyder, M. P., Nombela, C., Sanchez, M. (1995) Molecular basis of cell integrity and morphogenesis in *Saccharomyces cerevisiae*. *Microbiol Rev* **59**: 345-386.

Clutterbuck, A. J. (1974) *Aspergillus nidulans.* In: *Handbook of Genetics.* King, R. C. (ed). New York: Plenum, pp. 447-510.

Coleman, S. T., Fang, T. K., Rovinsky, S. A., Turano, F. J., Moye-Rowley, W. S. (2001) Expression of a glutamate decarboxylase homologue is required for normal oxidative stress tolerance in *Saccharomyces cerevisiae*. *J Biol Chem* **276**: 244-250.

Collins, S. R., Kemmeren, P., Zhao, X. C., Greenblatt, J. F., Spencer, F., Holstege, F. C.*, et al.* (2007) Toward a comprehensive atlas of the physical interactome of *Saccharomyces cerevisiae*. *Mol Cell Proteomics* **6**: 439-450.

Cooper, M. A., Shlaes, D. (2011) Fix the antibiotics pipeline. *Nature* **472**: 32.

Corbino, K. A., Barrick, J. E., Lim, J., Welz, R., Tucker, B. J., Puskarz, I.*, et al.* (2005) Evidence for a second class of S-adenosylmethionine riboswitches and other regulatory RNA motifs in alpha-proteobacteria. *Genome Biol* **6**: R70.

Corrales, F., Ochoa, P., Rivas, C., Martin-Lomas, M., Mato, J. M., Pajares, M. A. (1991) Inhibition of glutathione synthesis in the liver leads to S-adenosyl-L-methionine synthetase reduction. *Hepatology* **14**: 528-533.

Corrales, F., Gimenez, A., Alvarez, L., Caballeria, J., Pajares, M. A., Andreu, H.*, et al.* (1992) S-adenosylmethionine treatment prevents carbon tetrachloride-induced S-adenosylmethionine synthetase inactivation and attenuates liver injury. *Hepatology* **16**: 1022-1027.

Cyert, M. S. (2001) Genetic analysis of calmodulin and its targets in *Saccharomyces cerevisiae*. *Annu Rev Genet* **35**: 647-672.

Deinert, K., Fasiolo, F., Hurt, E. C., Simos, G. (2001) Arc1p organizes the yeast aminoacyl-tRNA synthetase complex and stabilizes its interaction with the cognate tRNAs. *J Biol Chem* **276**: 6000-6008.

Deng, X. W., Dubiel, W., Wei, N., Hofmann, K., Mundt, K. (2000) Unified nomenclature for the COP9 signalosome and its subunits: an essential regulator of development. *Trends Genet* **16**: 289.

Deruiter, J., Jacyno, J. M., Davis, R. A., Cutler, H. G. (1992) Studies on aldose reductase inhibitors from fungi. I. Citrinin and related benzopyran derivatives. *J Enzyme Inhib* **6**: 201-210.

Dong, J., Zhou, Y., Li, R., Zhou, W., Li, L., Zhu, Y*., et al.* (2006) New nematicidal azaphilones from the aquatic fungus *Pseudohalonectria adversaria* YMF1.01019. *FEMS Microbiol Lett* **264**: 65-69.

Dowzer, C. E., Kelly, J. M. (1989) Cloning of the *creA* gene from *Aspergillus nidulans*: a gene involved in carbon catabolite repression. *Curr Genet* **15**: 457-459.

Duce, A. M., Ortiz, P., Cabrero, C., Mato, J. M. (1988) S-adenosyl-L-methionine synthetase and phospholipid methyltransferase are inhibited in human cirrhosis. *Hepatology* **8**: 65-68.

Easlon, E., Tsang, F., Skinner, C., Wang, C., Lin, S. J. (2008) The malate-aspartate NADH shuttle components are novel metabolic longevity regulators required for calorie restriction-mediated life span extension in yeast. *Genes Dev* **22**: 931-944.

Eckert, S. E., Kubler, E., Hoffmann, B., Braus, G. H. (2000) The tryptophan synthase-encoding *trpB* gene of *Aspergillus nidulans* is regulated by the cross-pathway control system. *Mol Gen Genet* **263**: 867-876.

Ehrlich, K. C., Montalbano, B. G., Bhatnagar, D., Cleveland, T. E. (1998) Alteration of different domains in AFLR affects aflatoxin pathway metabolism in *Aspergillus parasiticus* transformants. *Fungal Genet Biol* **23**: 279-287.

Eng, J. K., Mccormack, A. L., Yates, J. R. (1994) An approach to correlate tandem mass-spectral data of peptides with amino-acid-sequences in a protein database. *J Am Soc Mass Spectr* **5**: 976-989.

Esser, K. (1982) Cryptogams : cyanobacteria, algae, fungi, lichens : textbook and practical guide. In. Cambridge ; New York: Cambridge University Press, pp. xi, 610 p.

Feinberg, A. P., Vogelstein, B. (1983) A technique for radiolabeling DNA restriction endonuclease fragments to high specific activity. *Anal Biochem* **132**: 6-13.

Felsenstein, J. (1985) Confidence limits on phylogenies: An approach using the bootstrap. *Evolution* **39**: 783-791.

Fernandes, M., Keller, N. P., Adams, T. H. (1998) Sequence-specific binding by *Aspergillus nidulans* AflR, a C6 zinc cluster protein regulating mycotoxin biosynthesis. *Mol Microbiol* **28**: 1355-1365.

Freilich, S., Oron, E., Kapp, Y., Nevo-Caspi, Y., Orgad, S., Segal, D.*, et al.* (1999) The COP9 signalosome is essential for development of *Drosophila melanogaster*. *Curr Biol* **9**: 1187-1190.

Frisvad, J. C., Larsen, T. O., de Vries, R., Meijer, M., Houbraken, J., Cabanes, F. J.*, et al.* (2007) Secondary metabolite profiling, growth profiles and other tools for species recognition and important *Aspergillus* mycotoxins. *Stud Mycol* **59**: 31-37.

Galagan, J. E., Calvo, S. E., Cuomo, C., Ma, L. J., Wortman, J. R., Batzoglou, S.*, et al.* (2005) Sequencing of *Aspergillus nidulans* and comparative analysis with *A. fumigatus* and *A. oryzae*. *Nature* **438**: 1105-1115.

Galani, K., Grosshans, H., Deinert, K., Hurt, E. C., Simos, G. (2001) The intracellular location of two aminoacyl-tRNA synthetases depends on complex formation with Arc1p. *EMBO J* **20**: 6889-6898.

Gavin, A. C., Bosche, M., Krause, R., Grandi, P., Marzioch, M., Bauer, A.*, et al.* (2002) Functional organization of the yeast proteome by systematic analysis of protein complexes. *Nature* **415**: 141-147.

Gavin, A. C., Aloy, P., Grandi, P., Krause, R., Boesche, M., Marzioch, M.*, et al.* (2006) Proteome survey reveals modularity of the yeast cell machinery. *Nature* **440**: 631-636.

Gong, Y., Kakihara, Y., Krogan, N., Greenblatt, J., Emili, A., Zhang, Z.*, et al.* (2009) An atlas of chaperone-protein interactions in *Saccharomyces cerevisiae*: implications to protein folding pathways in the cell. *Mol Syst Biol* **5**: 275.

Guzman-de-Pena, D., Ruiz-Herrera, J. (1997) Relationship between aflatoxin biosynthesis and sporulation in *Aspergillus parasiticus*. *Fungal Genet Biol* **21**: 198-205.

Guzman-de-Pena, D., Aguirre, J., Ruiz-Herrera, J. (1998) Correlation between the regulation of sterigmatocystin biosynthesis and asexual and sexual sporulation in *Emericella nidulans*. *Antonie Van Leeuwenhoek* **73**: 199-205.

Haarasilta, S., Oura, E. (1975) On the activity and regulation of anaplerotic and gluconeogenetic enzymes during the growth process of baker's yeast. The biphasic growth. *Eur J Biochem* **52**: 1-7.

Hajjaj, H., Klaebe, A., Loret, M. O., Goma, G., Blanc, P. J., Francois, J. (1999) Biosynthetic pathway of citrinin in the filamentous fungus *Monascus ruber* as revealed by 13C nuclear magnetic resonance. *Appl Environ Microbiol* **65**: 311-314.

Hanahan, D., Jessee, J., Bloom, F. R. (1991) Plasmid transformation of *Escherichia coli* and other bacteria. *Methods Enzymol* **204**: 63-113.

He, Q., Cheng, P., Liu, Y. (2005) The COP9 signalosome regulates the *Neurospora* circadian clock by controlling the stability of the SCFFWD-1 complex. *Genes Dev* **19**: 1518-1531.

Hertweck, C. (2009) Hidden biosynthetic treasures brought to light. *Nat Chem Biol* **5**: 450-452.

Hicks, J. K., Yu, J. H., Keller, N. P., Adams, T. H. (1997) *Aspergillus* sporulation and mycotoxin production both require inactivation of the FadA G alpha protein-dependent signaling pathway. *EMBO J* **16**: 4916-4923.

Hilti, N., Graub, R., Jorg, M., Arnold, P., Schweingruber, A. M., Schweingruber, M. E. (2000) Gene *sam1* encoding adenosylmethionine synthetase: effects of its expression in the fission yeast *Schizosaccharomyces pombe*. *Yeast* **16**: 1-10.

Ho, Y., Gruhler, A., Heilbut, A., Bader, G. D., Moore, L., Adams, S. L*., et al.* (2002) Systematic identification of protein complexes in *Saccharomyces cerevisiae* by mass spectrometry. *Nature* **415**: 180-183.

Inoue, H., Nojima, H., Okayama, H. (1990) High efficiency transformation of *Escherichia coli* with plasmids. *Gene* **96**: 23-28.

Kaefer, E. (1965) Origins of translocations in *Aspergillus nidulans*. *Genetics* **52**: 217-232.

Kaever, A., Lingner, T., Feussner, K., Gobel, C., Feussner, I., Meinicke, P. (2009) MarVis: a tool for clustering and visualization of metabolic biomarkers. *BMC Bioinformatics* **10**: 92.

Keller, N. P., Hohn, T. M. (1997) Metabolic pathway gene clusters in filamentous fungi. *Fungal Genet Biol* **21**: 17-29.

Keller, N. P., Turner, G., Bennett, J. W. (2005) Fungal secondary metabolism - from biochemistry to genomics. *Nat Rev Microbiol* **3**: 937-947.

Kolar, M., Punt, P. J., van den Hondel, C. A., Schwab, H. (1988) Transformation of *Penicillium chrysogenum* using dominant selection markers and expression of an *Escherichia coli lacZ* fusion gene. *Gene* **62**: 127-134.

Krogan, N. J., Cagney, G., Yu, H., Zhong, G., Guo, X., Ignatchenko, A.*, et al.* (2006) Global landscape of protein complexes in the yeast *Saccharomyces cerevisiae*. *Nature* **440**: 637-643.

Kumar, A., Agarwal, S., Heyman, J. A., Matson, S., Heidtman, M., Piccirillo, S.*, et al.* (2002) Subcellular localization of the yeast proteome. *Genes Dev* **16**: 707-719.

Lee, B. N., Adams, T. H. (1994a) The *Aspergillus nidulans fluG* gene is required for production of an extracellular developmental signal and is related to prokaryotic glutamine synthetase I. *Genes Dev* **8**: 641-651.

Lee, B. N., Adams, T. H. (1994b) Overexpression of *flbA*, an early regulator of *Aspergillus* asexual sporulation, leads to activation of *brlA* and premature initiation of development. *Mol Microbiol* **14**: 323-334.

Lengeler, K. B., Davidson, R. C., D'Souza, C., Harashima, T., Shen, W. C., Wang, P.*, et al.* (2000) Signal transduction cascades regulating fungal development and virulence. *Microbiol Mol Biol Rev* **64**: 746-785.

Lingens, F., Göbel, W. (1967) Zur Biosynthese des Tryptophans in *Saccharomyces cerevisiae*. *Biochim. Biophys. Acta* **148**: 70-83.

Link, A. J., Eng, J., Schieltz, D. M., Carmack, E., Mize, G. J., Morris, D. R.*, et al.* (1999) Direct analysis of protein complexes using mass spectrometry. *Nat Biotechnol* **17**: 676-682.

Loenen, W. A. (2006) S-adenosylmethionine: jack of all trades and master of everything? *Biochem Soc Trans* **34**: 330-333.

MacPherson, S., Larochelle, M., Turcotte, B. (2006) A fungal family of transcriptional regulators: the zinc cluster proteins. *Microbiol Mol Biol Rev* **70**: 583-604.

Malkowski, M. G., Quartley, E., Friedman, A. E., Babulski, J., Kon, Y., Wolfley, J.*, et al.* (2007) Blocking S-adenosylmethionine synthesis in yeast allows selenomethionine incorporation and multiwavelength anomalous dispersion phasing. *Proc Natl Acad Sci U S A* **104**: 6678-6683.

Mapari, S. A., Thrane, U., Meyer, A. S. (2010) Fungal polyketide azaphilone pigments as future natural food colorants? *Trends Biotechnol* **28**: 300-307.

Markham, G. D., Hafner, E. W., Tabor, C. W., Tabor, H. (1983) S-adenosylmethionine synthetase (methionine adenosyltransferase) (*Escherichia coli*). *Methods Enzymol* **94**: 219-222.

Marobbio, C. M., Agrimi, G., Lasorsa, F. M., Palmieri, F. (2003) Identification and functional reconstitution of yeast mitochondrial carrier for S-adenosylmethionine. *EMBO J* **22**: 5975-5982.

Mato, J. M., Alvarez, L., Ortiz, P., Pajares, M. A. (1997) S-adenosylmethionine synthesis: molecular mechanisms and clinical implications. *Pharmacol Ther* **73**: 265-280.

Mautino, M. R., Barra, J. L., Rosa, A. L. (1996) *eth-1*, the *Neurospora crassa* locus encoding S-adenosylmethionine synthetase: molecular cloning, sequence analysis and in vivo overexpression. *Genetics* **142**: 789-800.

Mayorga, M. E., Timberlake, W. E. (1992) The developmentally regulated *Aspergillus nidulans wA* gene encodes a polypeptide homologous to polyketide and fatty acid synthases. *Mol Gen Genet* **235**: 205-212.

Maytal-Kivity, V., Pick, E., Piran, R., Hofmann, K., Glickman, M. H. (2003) The COP9 signalosome-like complex in *S. cerevisiae* and links to other PCI complexes. *Int J Biochem Cell Biol* **35**: 706-715.

McDaniel, B. A., Grundy, F. J., Henkin, T. M. (2005) A tertiary structural element in S box leader RNAs is required for S-adenosylmethionine-directed transcription termination. *Mol Microbiol* **57**: 1008-1021.

Meinicke, P., Lingner, T., Kaever, A., Feussner, K., Gobel, C., Feussner, I.*, et al.* (2008) Metabolite-based clustering and visualization of mass spectrometry data using one-dimensional self-organizing maps. *Algorithms Mol Biol* **3**: 9.

Minto, R. E., Townsend, C. A. (1997) Enzymology and molecular biology of aflatoxin biosynthesis. *Chem Rev* **97**: 2537-2556.

Mitova, M. I., Stuart, B. G., Cao, G. H., Blunt, J. W., Cole, A. L., Munro, M. H. (2006) Chrysosporide, a cyclic pentapeptide from a New Zealand sample of the fungus *Sepedonium chrysospermum*. *J Nat Prod* **69**: 1481-1484.

Mudd, S. H., Cantoni, G. L. (1958) Activation of methionine for transmethylation. III. The methionine-activating enzyme of Bakers' yeast. *J Biol Chem* **231**: 481-492.

Mundt, K. E., Porte, J., Murray, J. M., Brikos, C., Christensen, P. U., Caspari, T.*, et al.* (1999) The COP9/signalosome complex is conserved in fission yeast and has a role in S phase. *Curr Biol* **9**: 1427-1430.

Nahlik, K., Dumkow, M., Bayram, O., Helmstaedt, K., Busch, S., Valerius, O.*, et al.* (2010) The COP9 signalosome mediates transcriptional and metabolic response to hormones, oxidative stress protection and cell wall rearrangement during fungal development. *Mol Microbiol* **78**: 964-979.

Nathan, C. (2004) Antibiotics at the crossroads. *Nature* **431**: 899-902.

Nayak, T., Szewczyk, E., Oakley, C. E., Osmani, A., Ukil, L., Murray, S. L.*, et al.* (2006) A versatile and efficient gene-targeting system for *Aspergillus nidulans*. *Genetics* **172**: 1557-1566.

Nei, M., Kumar, S. (2000) Molecular Evolution and Phylogenetics. In. New York: Oxford University Press, pp.

Newman, E. B., Budman, L. I., Chan, E. C., Greene, R. C., Lin, R. T., Woldringh, C. L.*, et al.* (1998) Lack of S-adenosylmethionine results in a cell division defect in *Escherichia coli*. *J Bacteriol* **180**: 3614-3619.

Nielsen, M. L., Nielsen, J. B., Rank, C., Klejnstrup, M. L., Holm, D. K., Brogaard, K. H.*, et al.* (2011) A genome-wide polyketide synthase deletion library uncovers novel genetic links to polyketides and meroterpenoids in *Aspergillus nidulans*. *FEMS Microbiol Lett* **321**: 157-166.

Nowrousian, M. (2009) A novel polyketide biosynthesis gene cluster is involved in fruiting body morphogenesis in the filamentous fungi *Sordaria macrospora* and *Neurospora crassa*. *Curr Genet* **55**: 185-198.

Ochi, K., Freese, E. (1982) A decrease in S-adenosylmethionine synthetase activity increases the probability of spontaneous sporulation. *J Bacteriol* **152**: 400-410.

Ochi, K., Okamoto, S., Tozawa, Y., Inaoka, T., Hosaka, T., Xu, J.*, et al.* (2004) Ribosome engineering and secondary metabolite production. *Adv Appl Microbiol* **56**: 155-184.

Osmanova, N., Schultze, W., Ayoub, N. (2010) Azaphilones: a class of fungal metabolites with diverse biological activities. *Phytochem Rev* **9**: 315-342.

Pajares, M. A., Corrales, F. J., Ochoa, P., Mato, J. M. (1991) The role of cysteine-150 in the structure and activity of rat liver S-adenosyl-L-methionine synthetase. *Biochem J* **274 (Pt 1)**: 225-229.

Phonkerd, N., Kanokmedhakul, S., Kanokmedhakul, K., Soytong, K., Prabpai, S., Kongsearee, P. (2008) Bis-spiro-azaphilones and azaphilones from the fungi *Chaetomium cochliodes* VTh01 and *C. cochliodes* CTh05. *Tetrahedron* **64**: 9636-9645.

Pieniazek, N. J., Kowalska, I. M., Stepien, P. P. (1973) Deficiency in methionine adenosyltransferase resulting in limited repressibility of methionine biosynthetic enzymes in *Aspergillus nidulans*. *Mol Gen Genet* **126**: 367-374.

Pimm, S. L., Russell, G. J., Gittleman, J. L., Brooks, T. M. (1995) The future of biodiversity. *Science* **269**: 347-350.

Poeggeler, S., Nowrousian, M., Kueck, U. (2006) Fruiting-body development in ascomycetes. In: *Mycota.* Kues, U. and Fischer, R. (eds). Berlin, Heidelberg, New York: Springer, pp. 325-355.

Pontecorvo, G., Roper, J. A., Hemmons, L. M., Macdonald, K. D., Bufton, A. W. (1953) The genetics of *Aspergillus nidulans*. *Adv Genet* **5**: 141-238.

Porter, J. K., Bacon, C. W., Robbins, J. D., Himmelsbach, D. S., Higman, H. C. (1977) Indole alkaloids from *Balansia epichloe* (Weese). *J Agr Food Chem* **25**: 88-93.

Pruyne, D., Bretscher, A. (2000) Polarization of cell growth in yeast. *J Cell Sci* **113 (Pt 4)**: 571-585.

Punt, P. J., van den Hondel, C. A. (1992) Transformation of filamentous fungi based on hygromycin B and phleomycin resistance markers. *Methods Enzymol* **216**: 447-457.

Punt, P. J., Strauss, J., Smit, R., Kinghorn, J. R., van den Hondel, C. A., Scazzocchio, C. (1995) The intergenic region between the divergently transcribed *niiA* and *niaD* genes of *Aspergillus nidulans* contains multiple NirA binding sites which act bidirectionally. *Mol Cell Biol* **15**: 5688-5699.

Reyes-Dominguez, Y., Bok, J. W., Berger, H., Shwab, E. K., Basheer, A., Gallmetzer, A.*, et al.* (2010) Heterochromatic marks are associated with the repression of secondary metabolism clusters in *Aspergillus nidulans*. *Mol Microbiol* **76**: 1376-1386.

Saitou, N., Nei, M. (1987) The neighbor-joining method: a new method for reconstructing phylogenetic trees. *Mol Biol Evol* **4**: 406-425.

Sakai, K., Kinoshita, H., Shimizu, T., Nihira, T. (2008) Construction of a citrinin gene cluster expression system in heterologous *Aspergillus oryzae*. *J Biosci Bioeng* **106**: 466-472.

Sanchez, J. F., Chiang, Y. M., Szewczyk, E., Davidson, A. D., Ahuja, M., Elizabeth Oakley, C.*, et al.* (2010) Molecular genetic analysis of the orsellinic acid/F9775 gene cluster of *Aspergillus nidulans*. *Mol Biosyst* **6**: 587-593.

Sanchez, J. F., Entwistle, R., Hung, J. H., Yaegashi, J., Jain, S., Chiang, Y. M.*, et al.* (2011) Genome-based deletion analysis reveals the prenyl xanthone biosynthesis pathway in *Aspergillus nidulans*. *J Am Chem Soc*.

Sanders, S. L., Herskowitz, I. (1996) The BUD4 protein of yeast, required for axial budding, is localized to the mother/BUD neck in a cell cycle-dependent manner. *J Cell Biol* **134**: 413-427.

Sankawa, U., Ebizuka, Y., Noguchi, H., Isikawa, Y., Kitaghawa, S., Yamamoto, Y.*, et al.* (1983) Biosynthesis of natural-products.13. Biosynthesis of citrinin in *Aspergillus*

terreus - Incorporation studies with [2-C-13,2-H-2(3)], [1-C-13,O-18(2)] and [1-C-13,O-17]-acetate. *Tetrahedron* **39**: 3583-3591.

Sarikaya Bayram, O., Bayram, O., Valerius, O., Park, H. S., Irniger, S., Gerke, J.*, et al.* (2010) LaeA control of velvet family regulatory proteins for light-dependent development and fungal cell-type specificity. *PLoS Genet* **6**: e1001226.

Schatz, P. J., Solomon, F., Botstein, D. (1986) Genetically essential and nonessential alpha-tubulin genes specify functionally interchangeable proteins. *Mol Cell Biol* **6**: 3722-3733.

Schröder, D. (2001) Untersuchungen zum Sekundärmetabolismus arktischer und antarktischer Meereisbakterien. *Dissertation*.

Schroeckh, V., Scherlach, K., Nutzmann, H. W., Shelest, E., Schmidt-Heck, W., Schuemann, J.*, et al.* (2009) Intimate bacterial-fungal interaction triggers biosynthesis of archetypal polyketides in *Aspergillus nidulans*. *Proc Natl Acad Sci U S A* **106**: 14558-14563.

Seeger, M., Kraft, R., Ferrell, K., Bech-Otschir, D., Dumdey, R., Schade, R.*, et al.* (1998) A novel protein complex involved in signal transduction possessing similarities to 26S proteasome subunits. *FASEB J* **12**: 469-478.

Shao, C. L., Wang, C. Y., Wei, M. Y., Gu, Y. C., She, Z. G., Qian, P. Y.*, et al.* (2011) Aspergilones A and B, two benzylazaphilones with an unprecedented carbon skeleton from the gorgonian-derived fungus *Aspergillus* sp. *Bioorg Med Chem Lett* **21**: 690-693.

Shao, J., Xu, D., Tsai, S. N., Wang, Y., Ngai, S. M. (2009) Computational identification of protein methylation sites through bi-profile Bayes feature extraction. *PLoS One* **4**: e4920.

Sharon, M., Mao, H., Boeri Erba, E., Stephens, E., Zheng, N., Robinson, C. V. (2009) Symmetrical modularity of the COP9 signalosome complex suggests its multifunctionality. *Structure* **17**: 31-40.

Shelest, E. (2008) Transcription factors in fungi. *FEMS Microbiol Lett* **286**: 145-151.

Shevchenko, A., Wilm, M., Vorm, O., Mann, M. (1996) Mass spectrometric sequencing of proteins silver-stained polyacrylamide gels. *Anal Chem* **68**: 850-858.

Shimizu, K., Keller, N. P. (2001) Genetic involvement of a cAMP-dependent protein kinase in a G protein signaling pathway regulating morphological and chemical transitions in *Aspergillus nidulans*. *Genetics* **157**: 591-600.

Shimizu, K., Hicks, J. K., Huang, T. P., Keller, N. P. (2003) Pka, Ras and RGS protein interactions regulate activity of AflR, a Zn(II)2Cys6 transcription factor in *Aspergillus nidulans*. *Genetics* **165**: 1095-1104.

Shimizu, T., Kinoshita, H., Ishihara, S., Sakai, K., Nagai, S., Nihira, T. (2005) Polyketide synthase gene responsible for citrinin biosynthesis in *Monascus purpureus*. *Appl Environ Microbiol* **71**: 3453-3457.

Shwab, E. K., Bok, J. W., Tribus, M., Galehr, J., Graessle, S., Keller, N. P. (2007) Histone deacetylase activity regulates chemical diversity in *Aspergillus*. *Eukaryot Cell* **6**: 1656-1664.

Sinlapadech, T., Stout, J., Ruegger, M. O., Deak, M., Chapple, C. (2007) The hyper-fluorescent trichome phenotype of the *brt1* mutant of *Arabidopsis* is the result of a defect in a sinapic acid:UDPG glucosyltranferase. *The Plant Journal* **49**: 655-668.

Sonjak, S., Frisvad, J. C., Gunde-Cimerman, N. (2005) Comparison of secondary metabolite production by *Penicillium crustosum* strains, isolated from Arctic and other various ecological niches. *FEMS Microbiol Ecol* **53**: 51-60.

Strauss, J., Reyes-Dominguez, Y. (2011) Regulation of secondary metabolism by chromatin structure and epigenetic codes. *Fungal Genet Biol* **48**: 62-69.

Suzuki, T., Okada, C., Arai, K., Awaji, A., Shimizu, T., Tanemura, K.*, et al.* (2001) Synthesis of 7-acetyloxy-3,7-dimethyl-7,8-dihydro-6H-isochromene-6,8-dione and its analogues. *J Heterocycl Chem* **38**: 1409-1418.

Tabor, C. W., Tabor, H. (1984) Methionine adenosyltransferase (S-adenosylmethionine synthetase) and S-adenosylmethionine decarboxylase. *Adv Enzymol Relat Areas Mol Biol* **56**: 251-282.

Takano, Y., Kikuchi, T., Kubo, Y., Hamer, J. E., Mise, K., Furusawa, I. (2000) The *Colletotrichum lagenarium* MAP kinase gene CMK1 regulates diverse aspects of fungal pathogenesis. *Mol Plant Microbe Interact* **13**: 374-383.

Takusagawa, F., Kamitori, S., Misaki, S., Markham, G. D. (1996a) Crystal structure of S-adenosylmethionine synthetase. *J Biol Chem* **271**: 136-147.

Takusagawa, F., Kamitori, S., Markham, G. D. (1996b) Structure and function of S-adenosylmethionine synthetase: crystal structures of S-adenosylmethionine synthetase with ADP, BrADP, and PPi at 28 angstroms resolution. *Biochemistry* **35**: 2586-2596.

Tamura, K., Peterson, D., Peterson, N., Stecher, G., Nei, M., Kumar, S. (2011) MEGA5: Molecular Evolutionary Genetics Analysis using maximum likelihood, evolutionary distance, and maximum parsimony methods. *Mol Biol Evol* **28**: 2731-2739.

Thomas, D., Surdin-Kerjan, Y. (1991) The synthesis of the two S-adenosyl-methionine synthetases is differently regulated in *Saccharomyces cerevisiae*. *Mol Gen Genet* **226**: 224-232.

Tilburn, J., Sarkar, S., Widdick, D. A., Espeso, E. A., Orejas, M., Mungroo, J.*, et al.* (1995) The *Aspergillus* PacC zinc finger transcription factor mediates regulation of both acid- and alkaline-expressed genes by ambient pH. *EMBO J* **14**: 779-790.

Timberlake, W. E. (1990) Molecular genetics of *Aspergillus* development. *Annu Rev Genet* **24**: 5-36.

Tsai, H. F., Chang, Y. C., Washburn, R. G., Wheeler, M. H., Kwon-Chung, K. J. (1998) The developmentally regulated *alb1* gene of *Aspergillus fumigatus*: its role in modulation of conidial morphology and virulence. *J Bacteriol* **180**: 3031-3038.

Tsitsigiannis, D. I., Zarnowski, R., Keller, N. P. (2004) The lipid body protein, PpoA, coordinates sexual and asexual sporulation in *Aspergillus nidulans*. *J Biol Chem* **279**: 11344-11353.

Udwary, D. W., Merski, M., Townsend, C. A. (2002) A method for prediction of the locations of linker regions within large multifunctional proteins, and application to a type I polyketide synthase. *J Mol Biol* **323**: 585-598.

Vogel, H. J. (1956) A convenient growth medium for *Neurospora*. *Microb. Genet. Bull.* **13**: 42.

Vogt, N., Seiler, S. (2008) The RHO1-specific GTPase-activating protein LRG1 regulates polar tip growth in parallel to Ndr kinase signaling in *Neurospora*. *Mol Biol Cell* **19**: 4554-4569.

Wagner-Dobler, I., Rheims, H., Felske, A., El-Ghezal, A., Flade-Schroder, D., Laatsch, H.*, et al.* (2004) *Oceanibulbus indolifex* gen. nov., sp. nov., a North Sea alphaproteobacterium that produces bioactive metabolites. *Int J Syst Evol Microbiol* **54**: 1177-1184.

Wang, S., Arends, S. J., Weiss, D. S., Newman, E. B. (2005) A deficiency in S-adenosylmethionine synthetase interrupts assembly of the septal ring in *Escherichia coli* K-12. *Mol Microbiol* **58**: 791-799.

Watanabe, A., Fujii, I., Sankawa, U., Mayorga, M. E., Timberlake, W. E., Ebizuka, Y. (1999) Re-identification of *Aspergillus nidulans wA* gene to code for a polyketide synthase of naphthopyrone. *Tetrahedron Letters* **40**: 91-94.

Watson, I. R., Irwin, M. S. (2006) Ubiquitin and ubiquitin-like modifications of the p53 family. *Neoplasia* **8**: 655-666.

Wei, N., Chamovitz, D. A., Deng, X. W. (1994) *Arabidopsis* COP9 is a component of a novel signaling complex mediating light control of development. *Cell* **78**: 117-124.

Wei, N., Deng, X. W. (2003) The COP9 signalosome. *Annu Rev Cell Dev Biol* **19**: 261-286.

Wei, N., Serino, G., Deng, X. W. (2008) The COP9 signalosome: more than a protease. *Trends Biochem Sci* **33**: 592-600.

Wilson, Z. E., Brimble, M. A. (2009) Molecules derived from the extremes of life. *Nat Prod Rep* **26**: 44-71.

Winkler, W. C., Breaker, R. R. (2005) Regulation of bacterial gene expression by riboswitches. *Annu Rev Microbiol* **59**: 487-517.

Wolf, J. C., Mirocha, C. J. (1973) Regulation of sexual reproduction in *Gibberella zeae* (*Fusarium roxeum* "graminearum") by F-2 (Zearalenone). *Can J Microbiol* **19**: 725-734.

Woodcock, D. M., Crowther, P. J., Doherty, J., Jefferson, S., DeCruz, E., Noyer-Weidner, M.*, et al.* (1989) Quantitative evaluation of *Escherichia coli* host strains for tolerance to cytosine methylation in plasmid and phage recombinants. *Nucleic Acids Res* **17**: 3469-3478.

Wu, L., Zee, B. M., Wang, Y., Garcia, B. A., Dou, Y. (2011) The RING finger protein MSL2 in the MOF complex is an E3 ubiquitin ligase for H2B K34 and is involved in crosstalk with H3 K4 and K79 methylation. *Mol Cell* **43**: 132-144.

Yang, S. W., Chan, T. M., Terracciano, J., Loebenberg, D., Patel, M., Gullo, V.*, et al.* (2009) Sch 1385568, a new azaphilone from *Aspergillus* sp. *J Antibiot (Tokyo)* **62**: 401-403.

Yarlett, N., Garofalo, J., Goldberg, B., Ciminelli, M. A., Ruggiero, V., Sufrin, J. R.*, et al.* (1993) S-adenosylmethionine synthetase in bloodstream *Trypanosoma brucei*. *Biochim Biophys Acta* **1181**: 68-76.

Yasukawa, K., Takahashi, M., Natori, S., Kawai, K., Yamazaki, M., Takeuchi, M.*, et al.* (1994) Azaphilones inhibit tumor promotion by 12-O-tetradecanoylphorbol-13-acetate in two-stage carcinogenesis in mice. *Oncology* **51**: 108-112.

Yu, J., Chang, P. K., Ehrlich, K. C., Cary, J. W., Bhatnagar, D., Cleveland, T. E.*, et al.* (2004) Clustered pathway genes in aflatoxin biosynthesis. *Appl Environ Microbiol* **70**: 1253-1262.

Yu, J. H., Butchko, R. A., Fernandes, M., Keller, N. P., Leonard, T. J., Adams, T. H. (1996a) Conservation of structure and function of the aflatoxin regulatory gene *aflR* from *Aspergillus nidulans* and *A. flavus*. *Curr Genet* **29**: 549-555.

Yu, J. H., Wieser, J., Adams, T. H. (1996b) The *Aspergillus* FlbA RGS domain protein antagonizes G protein signaling to block proliferation and allow development. *EMBO J* **15**: 5184-5190.

Zähner, H., Drautz, H., Weber, W. (1982) Novel approaches to metabolite screening. In: *Bioactive Microbial Products: Search and Discovery.* Bu'lock, J. D., Nisbet, L. J. and Winstanley, D. J. (eds). New York: Academic Press, pp. 51-70.

Acknowledgements

First, I would like to thank Prof. Dr. Gerhard Braus for giving me the opportunity to conduct my research in his department. I appreciate his supervision and support of my work and the optimal working conditions he provided.

I thank Prof. Dr. Axel Zeeck for accepting to co-examine this thesis.

Especially, I want to thank Dr. Özgür Bayram for introducing me into *Aspergillus* techniques and for many fruitful discussions and a lot of ideas and help during my work.

I would like to thank BioViotica Naturstoffe GmbH for providing equipment for isolation and identification of secondary metabolites. A special thanks to Prof. Dr. A. Zeeck, Hans-Peter Kroll and Verena Brandenburg for scientific and technical advices during my work there.

I appreciate the experimental support of Dr. Krystyna Nahlik and Marc Dumkow in the initial phase of the project and of my bachelor and practical students Sarah Henze, Anne Wilkening and Diana Fritzlar, who contributed to this work.

I would like to thank Dr. Oliver Valerius for protein identifications by mass spectrometry, and Dr. Kirstin Feussner, Prof. Dr. Ivo Feussner and Pia Meyer for metabolic fingerprinting by UPLC TOF-MS. Additional thanks to Manuel Landesfeind and Alexander Kaever for providing bioinformatic tools. I thank PD Dr. Michael Hoppert for providing *Escherichia coli*, *Bacillus subtilis*, and *Micrococcus luteus* strains, Prof. Dr. Stefanie Pöggeler for *Sordaria macrospora* strain, Dr. Petra Neumann-Staubitz for *Staphylococcus aureus* and *Salmonella enteric serovar typhimurium* strains, and PD Dr. Stephan Seiler for *Neurospora crassa* strain.

For proof-reading, I want to thank Dr. Özgür Bayram, Bastian Jöhnk, Clara Hoppenau and Dr. Harald Kusch.

Thanks to all present and former members of the group, especially to my lab members Bastian Jöhnk, Özlem Sarikaya-Bayram, Verena Große, and Dr. Satoshi Suzuki for their help and a friendly atmosphere. Additional thanks to Heidi Northemann, Nicole Scheiter, Andrea Wäge, and the "Werkstatt-team" Olaf Waase, Patrick Regin, and Gerd Birke.

Finally, I would like to thank Dominik Schneider for his endless support, encouragement and love during the last years.